

NICKEL(II) SALEN COMPLEXES WITH AN ALKANETHIOL SIDE
CHAIN AND THEIR SELF-ASSEMBLY ON GOLD

THESIS

Presented to the Graduate Council of
Texas State University-San Marcos
in Partial Fulfillment
of the Requirements

for the Degree

Master of SCIENCE

by

Drew K. Brown, B.S.

San Marcos, Texas
August 2012

NICKEL(II) SALEN COMPLEXES WITH AN ALKANETHIOL SIDE
CHAIN AND THEIR SELF-ASSEMBLY ON GOLD

Committee Members Approved:

Chang Ji, Chair

Benjamin Martin

Walter Rudzinski

Approved:

J. Michael Willoughby
Dean of the Graduate College

COPYRIGHT

by

Drew Kristopher Brown

2012

FAIR USE AND AUTHOR'S PERMISSION STATEMENT

Fair Use

This work is protected by the Copyright Laws of the United States (Public Law 94-553, section 107). Consistent with fair use as defined in the Copyright Laws, brief quotations from this material are allowed with proper acknowledgment. Use of this material for financial gain without the author's express written permission is not allowed.

Duplication Permission

As the copyright holder of this work I, Drew Kristopher Brown, authorize duplication of this work, in whole or in part, for educational or scholarly purposes only.

In Loving Memory of my sister, Sara Brown,

and grandmother, Wanda Barnes.

ACKNOWLEDGEMENTS

This thesis is dedicated to the numerous family members and friends that passed away during my last few years at Texas State University-San Marcos. There are simply too many to list. So many of you all left too close together, some too young, and some without warning. I am not going to forget any of you. This is especially dedicated to both my grandmother and to my only sister Sara.

Also, I would like to thank my mother, grandfather, and my brothers, Dennis, Samuel, Thomas, and Jonathan, for their support as well as my advisor, Dr. Chang Ji, for his guidance and patience with me. Finally, I would like to thank the Department of Chemistry & Biochemistry along with my committee and other faculty, including Dan Millikin, who helped me along the way.

This manuscript was submitted on March 19, 2012.

TABLE OF CONTENTS

	Page
ACKNOWLEDGMENTS	vi
LIST OF FIGURES	x
ABSTRACT	xiii
CHAPTER	
1. INTRODUCTION	1
1.1. Metal Salen Complexes—an Overview	1
1.1.1. Brief history	1
1.1.2. Electrochemical reduction of organic halides	4
1.1.3. Modification of electrodes with metal salen complexes	6
1.1.4. Electrochemically prepared electroactive polymers	7
1.1.5. Metal salen-based films <i>via</i> chemical adsorption	8
1.2. SAMs—an Overview	9
1.2.1. Methods for preparing monolayers	10
1.2.2. Chemisorption of organosulfurs	10
1.2.3. Direct self-assembly	12
1.2.4. Linker molecule approach	13

1.2.5. Properties of Au-alkylthiolate.....	14
1.3. Summary for Literature Review	16
2. ALKANETHIOL EXPERIMENTAL AND SYNTHESIS	18
2.1. Synthetic Routes	18
2.2. Experimental Method.....	21
2.2.1. Reagents	21
2.2.2. Cells, electrodes, and instrumentation	22
2.2.3. Separation and identification of products	23
2.3. Synthesis of 5-(6-Sulfhydrylhexyl)salicylaldehyde.....	23
2.3.1. Synthesis of 6-bromo-1-(4-methoxyphenyl)-1-hexanone (1).....	23
2.3.2. Synthesis of 1-(6-bromohexyl)-4-methoxybenzene (2).....	24
2.3.3. Synthesis of 4-(6-bromohexyl)phenol (3).....	25
2.3.4. Synthesis of 5-(6-bromohexyl)salicylaldehyde (4).....	26
2.3.5. Synthesis of 5-(6-sulfhydrylhexyl)salicylaldehyde (5).....	28
2.4. Synthesis of 5-(8-Sulfhydryloctyl)salicylaldehyde.....	29
2.4.1. Synthesis of 8-bromooctanoyl chloride (6).....	29
2.4.2. Synthesis of 8-bromo-1-(4-methoxyphenyl)-1-octanone (7).....	29
2.4.3. Synthesis of 1-(8-bromooctyl)-4-methoxybenzene (8).....	30
2.4.4. Synthesis of 4-(8-bromooctyl)phenol (9).....	30
2.4.5. Synthesis of 5-(8-bromooctyl)salicylaldehyde (10).....	30
2.4.6. Synthesis of 5-(8-sulfhydryloctyl)salicylaldehyde (11).....	31
2.5. Synthesis of Ni(II) Salen Catalysts with n=6 and n=8.....	32
2.5.1. Synthesis of <i>N,N'</i> -bis(salicylidene)ethylenediamine with n=6 (12a) or n=8 (12b).....	32

2.5.2. Synthesis of alkanethiol modified Ni(II) salen mixture with n=6 (13a) or n=8 (13b).....	32
2.6. Preparation of SAMs and Cyclic Voltammetry	33
2.6.1. Preparation of bare Au electrode	33
2.6.2. Cyclic voltammetry of Ni(II) salen and salicylaldehyde in DMF.....	33
2.6.3. Coating the bare Au electrode with 5-(ω - sulfhydrylalkyl)salicylaldehydes	34
2.6.4. Coating the bare Au electrode with alkanethiol modified Ni(II) salen with n=6 or 8.....	34
2.6.5. Cyclic voltammetry analysis.....	34
3. RESULTS AND DISCUSSION	36
3.1. CVs of Ferrocene, Nickel(II) Salen, and Salicylaldehyde at a Gold Electrode	36
3.2. Self-Assembled Monolayers on Gold.....	36
3.2.1. 5-(6-Sulfhydrylhexyl)salicylaldehyde and 5-(8- sulfhydroctyl)salicylaldehyde on gold.....	36
3.2.2. [Nickel(II)salen] C_n SH films	42
3.2.3. Final remarks	53
3.3. Future Research	54
3.3.1. Proposed changes to methodology for [nickel(II)salen] C_n S-Au film development	54
3.3.2. [Metal salen] disulfides.....	55
3.3.3. Proposed synthesis for new “bulky” salen and salophen ligands	56
SUPPLEMENTAL MATERIAL.....	60
REFERENCES	94

LIST OF FIGURES

Figure	Page
1. <i>N,N'</i> -bis(salicylidene)ethylenediamine	2
2. Several examples of metal Schiff base complexes	3
3. The Jacobsen's catalyst, a Mn(III) Schiff base complex.....	3
4. Reduction of 1,6-dibromohexane with nickel(II) salen	5
5. Dinickel Schiff base complex (Ni ₂ (II)L)	5
6. Electrochemical oxidation using carbon paste electrodes (CPE) modified with metal Schiff base complexes.....	6
7. Electrochemical polymerization of metal salen.....	8
8. Alkylthiolate monolayer on a gold surface.....	10
9. Formation of SAMs on gold involving chemisorption.....	11
10. Nickel(II) pentaazamacrocyclic complex on gold	12
11. Thio(phenylacetylene) _n substituted metal salen and metal salophen complexes functionalized with unsymmetrical alkyl sulfides on gold	13
12. Co(II) phthalocyanine-modified gold electrodes	14
13. Self-assembly of thiol and disulfides	15
14. CVs of thiols and disulfides on gold.....	16
15. Synthesis of 5-(6-sulfhydrylhexyl)salicylaldehyde	18
16. Synthesis of 5-(8-sulfhydryloctyl)salicylaldehyde	19
17. Synthesis of the nickel(II) salens with an alkanethiol side chain	20

18. CV of ferrocene in DMF.....	37
19. CV of nickel(II) salen in DMF.....	37
20. CV of salicylaldehyde in DMF (1)	38
21. CV of salicylaldehyde in DMF (2)	38
22. CVs of the desorption of 5-(ω -sulfhydrylalkyl)salicylaldehydes on gold (first scans).....	40
23. CVs of the desorption of 5-(6-sulfhydrylhexyl)salicylaldehyde on gold	40
24. CVs of the desorption of 5-(8-sulfhydryloctyl)salicylaldehyde on gold	41
25. CV of the desorption of 5-(8-sulfhydryloctyl)salicylaldehyde on gold (first scan/expanded scan window).....	41
26. CV for a gold electrode after submerged in DMF containing nickel(II) salen.....	43
27. CVs of the electrochemical chain polymerization of a [nickel(II)salen]C ₆ S- Au film	43
28. CVs of the electrochemical chain polymerization of a [nickel(II)salen]C ₈ S- Au film	44
29. CVs of the electrochemical chain polymerization of [nickel(II)salen]C _n S- Au films vs. nickel(II) salen in DMF	44
30. Electrochemical chain polymerization of a [nickel(II)salen]C _n S- Au film in DMF	45
31. CV of the reduction of poly[nickel(II)salen]C ₆ S-Au film	46
32. CV of the reduction of poly[nickel(II)salen]C ₈ S-Au film	46
33. CVs of the reduction of poly[nickel(II)salen]C _n S-Au films	47
34. CVs of ferrocene in DMF before and after desorption of poly[nickel(II)salen]C ₆ S- Au film	47
35. CVs of ferrocene in DMF before and after desorption of poly[nickel(II)salen]C ₈ S- Au film	48
36. CVs of ferrocene in DMF before desorption of poly[nickel(II)salen]C _n S- Au films	48

37. CVs of the desorption of poly[nickel(II)salen]C ₆ S-Au film in DMF	51
38. CVs of the desorption of poly[nickel(II)salen]C ₈ S-Au film in DMF	51
39. CV of the desorption of poly[nickel(II)salen]C ₆ S-Au film in DMF (first scan/expanded scan window).....	52
40. CVs of the desorption of poly[nickel(II)salen]C _n S-Au films in DMF	52
41. CVs of the reduction of poly[nickel(II)salen]C ₆ S-Au film before and after treatment with 0.012 M HCl	53
42. Proposed synthesis of salen ligand on gold using disulfides	56
43. <i>p</i> -Acylthio(phenylacetylene) _n -substituted chiral salen ligands (n=1 and 2)	57
44. Several examples of syntheses of free amines from the condensation reaction of various diamines and salicylaldehydes	58
45. Proposed synthesis of salophen ligand with a single alkanethiol side chain	59

ABSTRACT

NICKEL(II) SALEN COMPLEXES WITH AN ALKANETHIOL SIDE CHAIN AND THEIR SELF-ASSEMBLY ON GOLD

by

Drew K. Brown, B.S.

Texas State University-San Marcos

August 2012

SUPERVISING PROFESSOR: CHANG JI

5-(6-Sulfhydrylhexyl)salicylaldehyde and 5-(8-sulfhydroctyl)salicylaldehyde were synthesized, self-assembled on gold, and analyzed using cyclic voltammetry (CV). The 5-(ω -sulfhydrylalkyl)salicylaldehydes were also used to synthesize two nickel(II) salens with an alkanethiol side chain *via* the condensation reaction and the metal ion was coordinated into the ligand using nickel(II) acetate in solution. These nickel(II) salen complexes were self-assembled on gold from DMF that was saturated with a mixture of approximately 10% [nickel(II)salen](CH₂)_nSH (n=6 or 8) and 90% nickel(II) salen. It was found that the chemisorbed nickel(II) salen films may undergo electrochemical chain polymerization in DMF containing 0.05 M

tetramethylammonium tetrafluoroborate (TMABF₄) to form poly[nickel(II)salen]-(CH₂)_nS-Au film. The redox reversibility of ferrocene in cyclic voltammetry was affected by the polymerized films on gold electrode. The film was fairly stable under acidic conditions. Future research was discussed to further investigate [nickel(II)salen]C_nS-Au films through the synthesis of disulfide precursors as well as a 1:1 condensation reaction to generate pure salen or salophen ligands for self-assembly.

CHAPTER 1. INTRODUCTION

In 1983, Allara and Nuzzo synthesized gold-alkylthiolate monolayers through the adsorption of di-*n*-alkyl disulfides on zerovalent gold.¹ Since then, self-assembled monolayers, SAMs, have been extensively studied for numerous applications in catalysis,² chemical and biosensor technology,^{3,4} corrosion resistant films,⁵ and electrochemistry.⁶ SAMs have also attracted a lot of interests because they are ideal for the understanding of many interactions, particularly the intermolecular forces in densely packed alkyl chains. Many interfacial properties can be affected simply by changing the functionality of the tail group in SAMs.⁷⁻¹⁴ Metal Schiff base complexes, which are widely used in catalysis, have been attached as a terminal group using thiol linkers or directly to gold surface for potential technological applications (see section 1.2). The most studied metal complexes on gold are chromophoric, electroactive, and fluorescent.¹⁵ However, there are few reports about metal salen or salophen complexes with terminal thiols chemisorbed on gold. The next a few sections will summarize the previous research in metal salen complexes and SAMs, and why two new nickel(II) salen complexes similar to **1** in Figure 2 have been synthesized and studied in this work.

1.1. Metal Salen Complexes—an Overview

1.1.1. Brief history.— Schiff bases and their metal complexes are important

compounds in the advancement of coordination chemistry and catalysis. Since the nineteenth century, Schiff bases and their metal complexes have been studied extensively. In 1864, Hugo Schiff discovered azomethine (Schiff base) from the reversible reaction of an active carbonyl compound with a primary amine.¹⁶ Mechanistically, a carbinolamine intermediate is formed and then dehydrated to a stable imine.¹⁷ These imines bear a hydrocarbonyl group bound to a nitrogen atom with a chemically important lone pair of electrons. The general formula is $R_1R_2C=NR_3$ where typically R_1 is an aryl, R_2 is a hydrogen, and R_3 is an aryl or alkyl.¹⁷ In 1869, Schiff published the preparation of several complexes using phenyl and aryl amines with salicylaldehyde, which is now an established condensation reaction.¹⁸ Soon after, Delépine synthesized similar ligands using salicylaldehyde with methylamine or benzyl amine to coordinate the metal with dissolved metal acetates.¹⁹ These initial studies resulted in the development of over 2500 salen-type complexes over the next century.²⁰

Many Schiff bases are great ligands due to the free lone pair of electrons on the imine. Other functional groups on the molecule such as hydroxyls²¹ and sulfides²² can also contribute a pair of electrons. These ligand structures are usually very diverse with

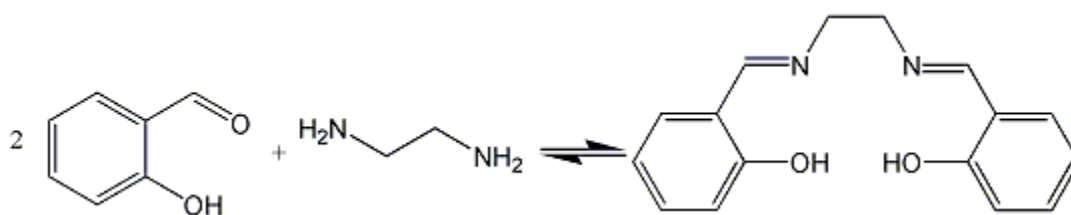


Figure 1. *N,N'*-bis(salicylidene)ethylenediamine. Synthesis of SalenH₂. From ref. 21.

the binding pockets for many metals and some metalloids involving nitrogen and oxygen atoms. The most common symmetrical Schiff base ligand is a bifunctional tetradentate ligand as shown in Figure 1, which has been extended to other ligand structures (Figure

2).^{21,23} It can be prepared conveniently by the condensation of salicylaldehyde and ethylenediamine with good yields.²¹ Further reaction with metal acetate will give metal salens, which are commonly used in catalysis. Other metal Schiff base complexes could be prepared by a similar synthetic protocol. As a famous example, the Jacobsen's

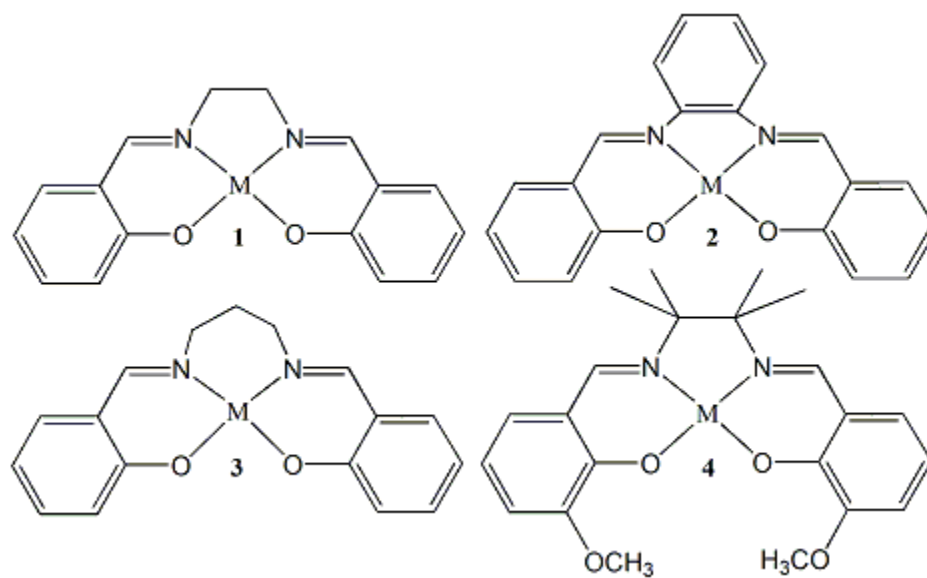


Figure 2. Several examples of metal Schiff base complexes. M(salen) **1**, M(salphen) **2**, M(salpn) **3**, and M(3-MeOsaltMe) **4**. From ref. 23.

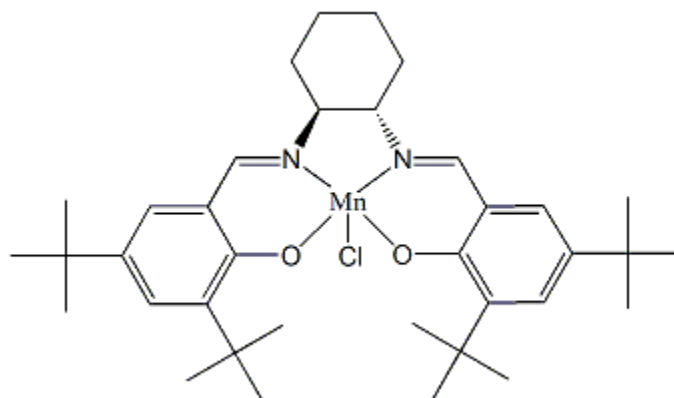


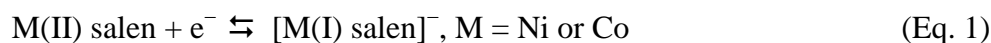
Figure 3. The Jacobsen's catalyst, a Mn(III) Schiff base complex. It was first used in enantioselective epoxidation of unfunctionalized alkenes. From ref. 24.

catalyst (Figure 3) was synthesized in the early 1990s and successfully used in enantioselective epoxidation of unfunctionalized alkenes.²⁴ The discussion will focus on

the use of metal(II) salen for the electrochemical reduction of organic halides in the following.

1.1.2. Electrochemical reduction of organic halides.— Many organic halides, which come primarily from industrial sources, have been recognized as persistent organic pollutants (POPs). They can have a long term adverse effect on animal and human health due to bioaccumulation in tissue, biomagnification in food chains, and their high toxicity. Consequently, there has been a need to detect and remove these organic halides from the environment.

In homogeneous electrochemical reductions, M(II) salen (where M = cobalt or nickel) has been used as a catalyst to reduce many organic halides in dimethylformamide (DMF) or acetonitrile.²⁵ For nickel(II) and cobalt(II) salens, both undergo a reversible



one-electron reduction (Eq. 1) to produce the corresponding metal(I) salens, which can then attack organic halides through a nucleophilic process to generate different products. Under these conditions, the potential for metal(I) salen mediated reduction of organic halides shifts more positive, the cathodic current increases, and the anodic current disappears (Figure 4).²⁶ The various detailed mechanisms have been studied and described.^{27,28} In summary, the organic halide will typically undergo carbon-halogen bond cleavage and a carbanion (R^-) or radical ($\text{R}\cdot$) will be produced. Alkanes and dimers are usually formed as the final products. However, the radical intermediates can also undergo further reactions including disproportionation,²⁶ intramolecular cyclization,²⁹ ring expansion,³⁰ and abstraction of hydrogen atoms from the solvent or electrolyte.²⁶ As

a result, the electrochemical reduction of organic halides using metal(II) salens can be very useful for the synthesis of various compounds.

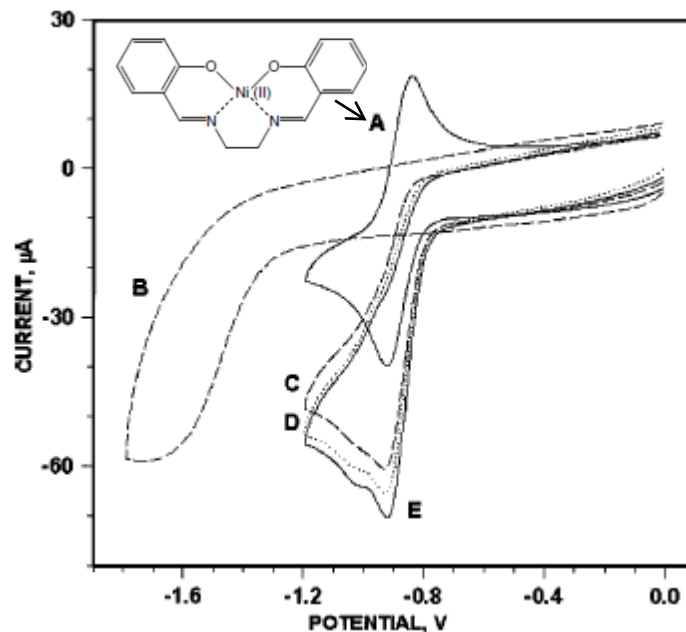


Figure 4. Reduction of 1,6-dibromohexane with nickel(II) salen. Cyclic voltammograms recorded with a glassy carbon electrode (area = 0.077 cm²) at 100 mV/s in DMF containing 0.10 M TMABF₄ and (A) 2.0 mM nickel(II) salen (structure shown); (B) 1.0 mM 1,6-dibromohexane; (C) 2.0 mM nickel(II) salen and 1.0 mM 1,6-dibromohexane; (D) 2.0 mM nickel(II) salen and 2.0 mM 1,6-dibromohexane; and (E) 2.0 mM nickel(II) salen and 4.0 mM 1,6-dibromohexane. Curves A, C, D, and E were scanned from 0 to -1.2 to 0 V; curve B was scanned from 0 to -1.8 to 0 V. From ref 28.

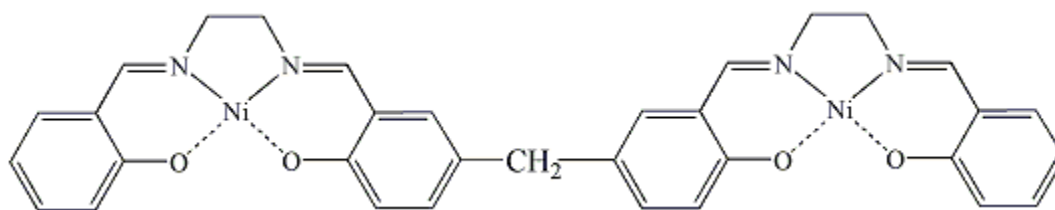


Figure 5. Dinickel Schiff base complex (Ni₂(II)L). An illustration of a dinickel Schiff base complex which has been used to reduce organic halides. From ref. 26.

For example, nickel(II) salen and a dinickel Schiff base complex (Ni₂(II)L) containing two salen units were both used to electrochemically reduce bromooctanes at reticulated glassy carbon electrodes in DMF containing 0.050 M tetramethylammonium tetrafluoroborate (TMABF₄) by bulk electrolysis.²⁶ The reduction of 1-bromooctane

produced octane, n-hexadecane, various amides, and other products while 2-bromooctane produced octane, 7,8-dimethyltetradecane, 6-ethyl-7-methyltridecane, N,N-2-trimethyloctanamide, and other products.

1.1.3. Modification of electrodes with metal salen complexes.— Carbon paste electrodes (CPE) modified with metal Schiff base complexes have been used for electrochemical oxidation and reduction of various compounds. Modified CPEs are prepared simply by mixing catalysts with graphite powder followed by assembling the electrode. Cobalt(II)-4-methylsalophan (CoMSal) modified CPE has been shown to electrochemically oxidize ascorbic acid and cysteine,³¹ while oxovanadium(IV) salen modified CPE have been used to oxidize cysteine and reduce hydrogen peroxide.³² Figure 6 shows that by using the CoMSal-modified CPE, ascorbic acid is more easily oxidized at a less positive potential, and cysteine is only detectable with the modified CPE. The increase in oxidative currents improves the sensitivity of the electrode, which also offers

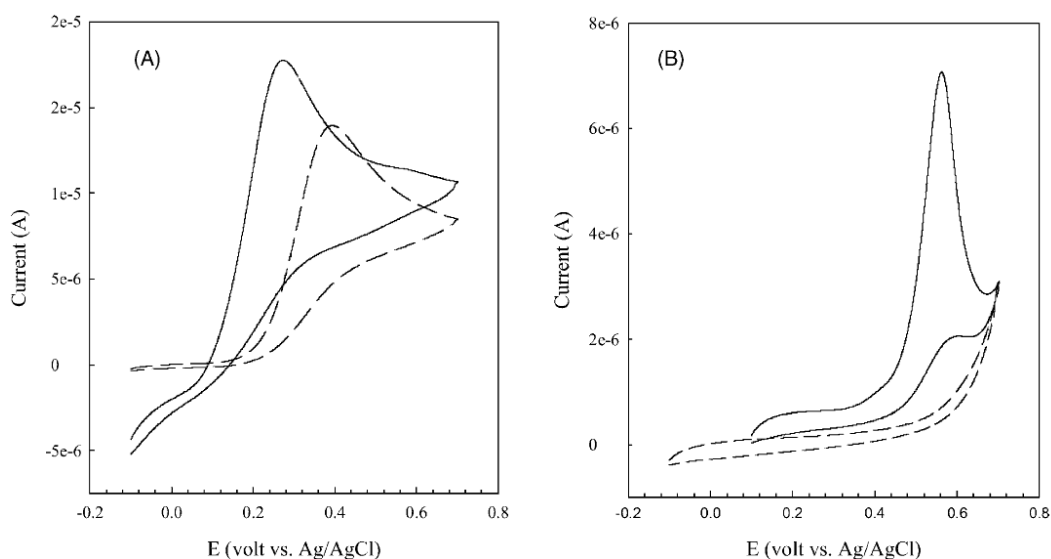


Figure 6. Electrochemical oxidation using carbon paste electrode (CPE) modified with metal Schiff base complexes. Cyclic voltammograms of 1 mM (A) ascorbic acid and (B) cysteine at the surface of unmodified CPE (dashed lines) and CoMSal-modified CPE (solid line) in 0.1 M acetate buffer solution with pH 5.0. Sweep rate was 100 mV/s. From ref. 31.

good selectivity.³¹ Nevertheless, CPEs modified with metal Schiff base complexes have primarily focused on electrochemical oxidation, and the catalysts are not chemically bound to the electrode surface. It has been reported that metal salen complexes can also undergo electrochemical polymerization directly on the electrode surface.²³ The polymer-modified electrodes can potentially be excellent electrocatalysts or sensors (for oxidation or reduction).³³

1.1.4. Electrochemically prepared electroactive polymers.— Electroactive polymers have been used as electrocatalysts and chemical sensors.¹⁷ Electrodes modified with metal salen complexes have been prepared *via* oxidative electrochemical polymerization of the monomers on the bare electrode surface where the thickness of the film can be controlled to give excellent membrane properties.³⁴ Typically, constant-potential electrolysis (at +1.4 V vs. SCE) and cyclic voltammetry (several cycles from 0 to +1.4 to 0 V vs. SCE) are used to prepare these electrodes in aprotic organic solvents such as acetonitrile, acetone, and dichloromethane.^{17,35-40} Despite extensive investigations, the mechanism of polymerization remains controversial, and two reaction mechanisms have been proposed to describe the polymerization of metal salens (Figure 7). The first electrochemically polymerized substituted metal salen complexes were synthesized by Murray and co-workers using nickel, cobalt, and manganese metal centers.³⁵ Later on, three nickel salen complexes substituted with methyl groups were used to investigate the mechanism of polymerization by cyclic voltammetry.^{36,37} Indirectly, it was determined that nickel salen complexes can electrochemically polymerize *via* oxidation in polar aprotic solvents as C-C bonds are generated between the phenyl rings of each monomer only if the para positions are not inhibited.^{36,37} These

initial studies led to the development of several new polymer films and the first mechanism (Figure 7A) for metal salen polymerization. However, despite the strong evidence for linear polymerization, another mechanism (Figure 7B) was suggested later that poly[metal salen] films have a stacked structure through the investigation of planar and non-planar salen complexes.^{38,39} Both models have been used to explain the structure of poly[metal salen] films. More interestingly, poly[nickel(II)salen] films have also been employed to reduce organic halides.⁴⁰

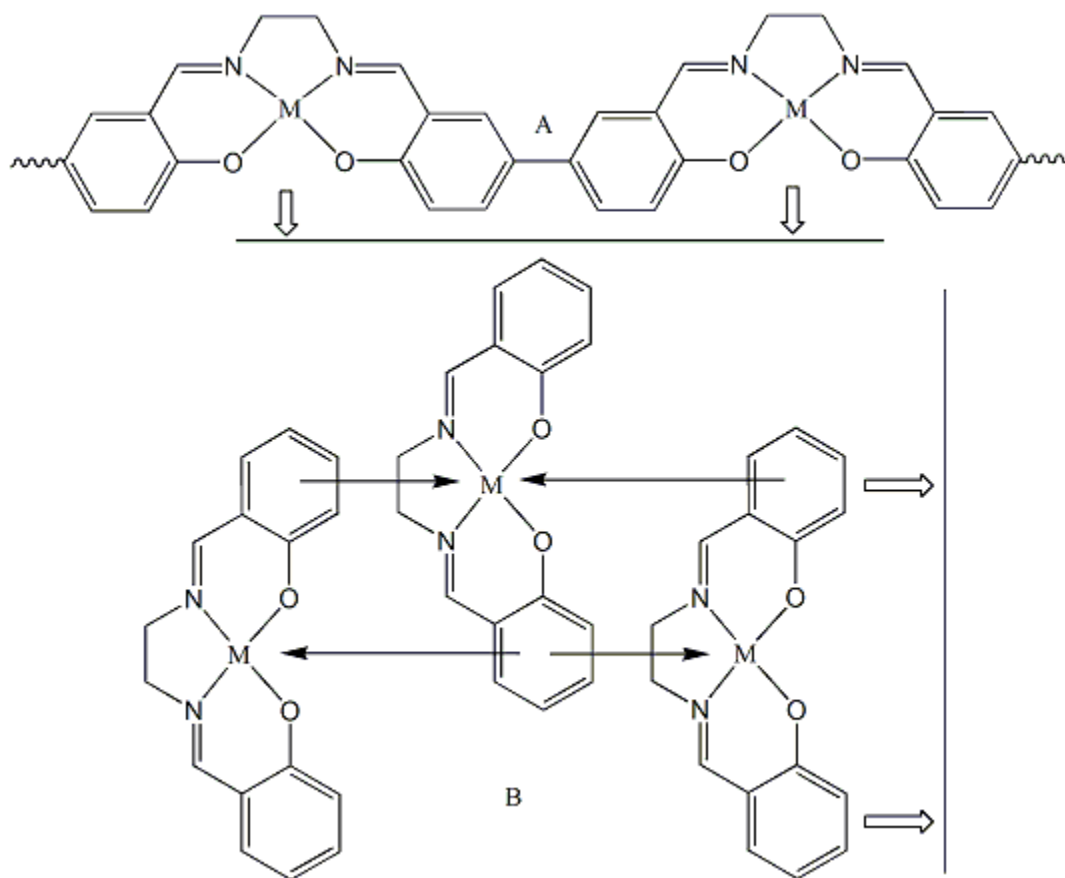


Figure 7. Electrochemical polymerization of metal salen. (A) chain polymerization and (B) stack polymerization. The white arrows indicate metal surface of electrode. From refs. 36-40.

1.1.5. Metal salen-based films via chemical adsorption.— Most previous research with metal salen-coated electrodes has primarily focused on physical adsorption

through oxidative electrochemical polymerization or modified CPE electrodes, rather than chemical adsorption on electrode surface to form monolayers. Furthermore, very little research has been carried out to study direct self-assembly of metal salens or salophens on gold using thiol or disulfide substituents. Chemical adsorption on a gold surface has been mainly focused on other metal complexes. A study using six “bulky” thio(phenylacetylene) substituted metal(III) salens was the first and possibly the only publication that shows the assembly of metal salens on gold from pre-immobilized ligands with the corresponding cyclic voltammetric response after metal coordination.⁴¹ It will be intriguing to study nickel(II) salen films directly self-assembled on gold through an alkanethiol side chain to examine if (a) polymerization can occur, and (b) if it can be used in catalysis particularly for the reduction of organic halides. The next section will elaborate more on the chemical adsorption of metal Schiff base complexes by discussing an overview of self-assembled monolayers, particularly the gold-alkylthiolate monolayers.

1.2. SAMs—an Overview

Many organic compounds can form SAMs on solid surfaces. SAMs are usually formed *via* spontaneous adsorption of molecules on a particular metal substrate to produce a dense monolayer, which becomes very ordered and homogeneously oriented with various tail group functionality (Figure 8).⁴² The most often used metal surface is gold because it is resistant to corrosion under many conditions,¹⁴ does not easily form surface oxides like silver⁴³ and copper,⁴⁴ and is thus more easily reproduced. SiO₂ has also been commonly used as a substrate for surface modification in electronic or chromatographic applications.⁴⁵ It is not surprising that studies involving alkylsilane

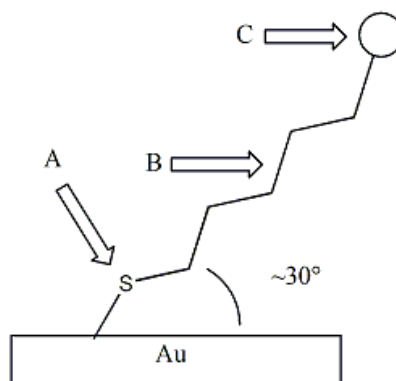


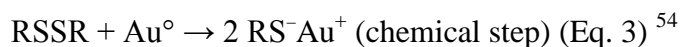
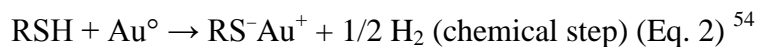
Figure 8. Alkylthiolate monolayer on a gold surface. A is the terminal sulfur, B is the spacer group, and C is the tail group.

monolayers on various substrates and gold-alkylthiolate monolayers prevail in the literature.

1.2.1. Methods for preparing monolayers.— SAMs are usually prepared by two well-understood methods: the Langmuir-Blodgett (LB) technique using surfactant molecules or the chemisorption of organosilanes or organosulfurs.⁴⁶ Although the LB technique is very useful in developing multilayer films, it is restricted to molecules that can form films on water.⁴⁷ This limits its use with metal Schiff base complexes which are more soluble in organic media. Moreover, LB films are not stable with temperature change⁴⁸ and do not covalently bond to the substrate surface.⁴⁹ These drawbacks make chemisorption a more favorable alternative for immobilizing metal Schiff base complexes on a metal surface.

1.2.2. Chemisorption of organosulfurs.— Organosulfur compounds, specifically thiols or disulfides, have been found to spontaneously self-assemble onto the surface of transition metal substrates.^{1,50-53} A stable gold-alkylthiolate monolayer can be quickly formed simply by contacting an alkanethiol or alkanedisulfide solution with the gold (Eqs. 2 and 3).⁵⁴ These monolayers have strong gold-sulfur interactions and

intermolecular forces in the alkyl chains to make a robust, thermodynamically stable film. The alkyl chains typically have an approximate 30° tilted axis.⁵⁵ Most gold-alkylthiolate



films are very stable, and the tail group can undergo further reactions to build larger molecules in a stepwise fashion. These features have been exploited extensively.⁵⁶⁻⁶²

The formation of gold-alkylthiolate SAM films containing metal complexes usually involves chemisorption either by direct self-assembly or by a linker molecule

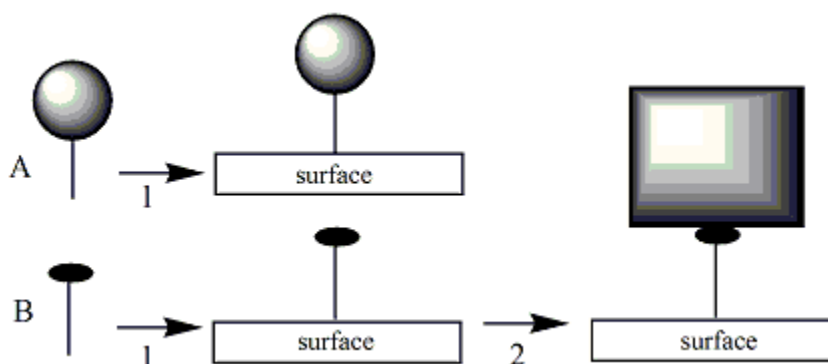


Figure 9. Formation of SAMs on gold involving chemisorption. Usually involves direct self-assembly (A) or assembly using a thiol linker molecule (B).

(Figure 9). These films have been used for electrochemical purposes.⁶³⁻⁶⁵ For direct self-assembly, the adsorbant molecule is synthesized with proper functionality prior to the development of the SAMs (see 1.2.3). While for the linker molecule protocol, the process involves adsorption of a molecule on the gold surface followed by further reaction of the adsorbant molecule with the metal complex *via* various procedures (see 1.2.4).^{62,66,67}

1.2.3. Direct self-assembly.— Several metal Schiff base complexes have been assembled directly onto gold using a sulfur functionality.^{63,67-72} Nickel(II) pentaazamacrocyclic complex, an efficient electrocatalyst, has been immobilized on gold using a disulfide derivative.⁷³ Figure 10A shows the typical cyclic voltammograms of the metal complexes bound to a gold electrode surface at various scan rates. The symmetrical reversible redox peaks (Ni(II)-Ni(III)) can be observed at +0.55 V vs. Ag/AgCl, suggesting fast electron-transfer kinetics. Additionally, the peak shape is independent of scan rate, which is characteristic for surface bound metal complexes.

Similarly, chiral Co(III), Fe(III), and Mn(III) salen complexes have been prepared using pre-immobilized ligands on gold with the reaction of metal chlorides (Figure 11A).⁴¹ Specifically, thio(phenylacetylene)_n substituted ligands (n=1 and n =2) were self-assembled onto gold electrodes. It has been observed that the longer thio(phenylacetylene) spacer would give better surface coverage, and the CVs show

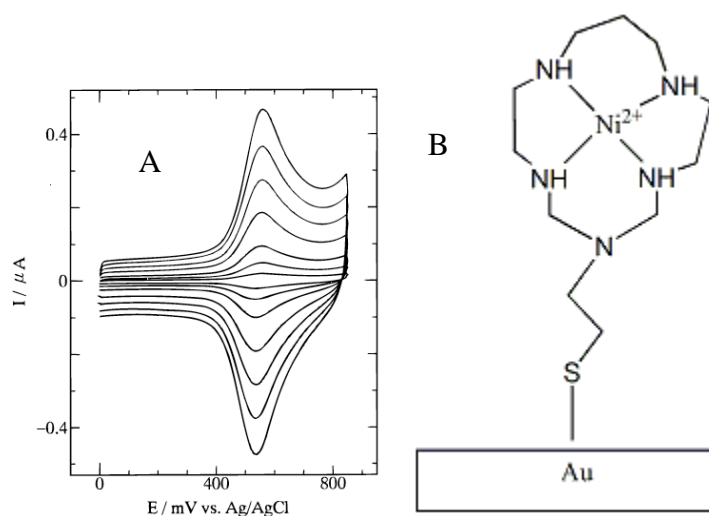


Figure 10. Nickel(II) pentaazamacrocyclic complex on gold. (a) CVs of the Au electrode modified by dipping in a methanol solution of 0.5 mM nickel(II) pentaazamacrocyclic complex (a disulfide derivative) for 36 hours. The CVs were recorded in aqueous 0.1 M Na₂SO₄ (pH 2). Potential scan rates of 500, 400, 300, 200, 100, 50, and 20 mV/s. (b) An illustration of nickel(II) pentaazamacrocyclic complex modified gold electrode. From ref. 73.

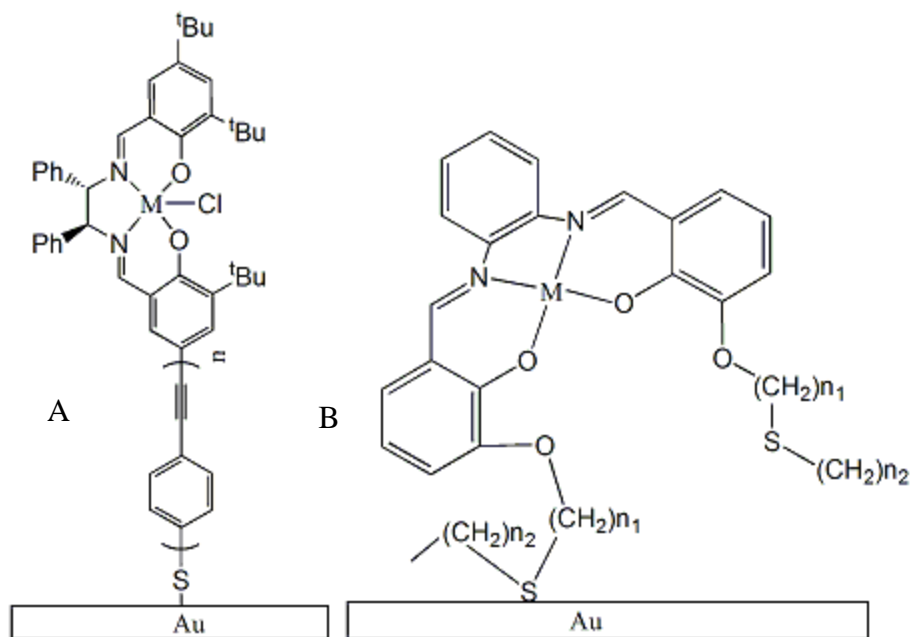


Figure 11. Thio(phenylacetylene)_n substituted metal salen and metal salophen complexes functionalized with unsymmetrical alkyl sulfides on gold. An illustration of (a) thio(phenylacetylene)_n substituted metal salens [$n=1$ and $n=2$ where $M=\text{Co(III)}$, Fe(III) , and Mn(III)] and (b) metal salophen complexes functionalized with unsymmetrical alkyl sulfides self-assembled onto gold [$M=\text{Co(II)}$ where $n_1=11$, $n_2=10$, Cu(II) where $n_1=11$, $n_2=10$, and Ni(II) where $n_1=2$ or 11 , $n_2=1$ or 10]. From refs. 41 and 74.

quasi-symmetrical (M(III)-M(II)) reversible redox waves similar to Figure 10A. Co(II), Cu(II), and Ni(II) salophen complexes functionalized with unsymmetrical alkyl sulfides have also been illustrated to self-assemble on gold electrodes, which were studied by time-of-flight secondary-ion mass spectroscopy (TOF-SIMS), X-ray photoelectron spectroscopy (XPS), and grazing-angle Fourier transform infrared spectroscopy (FT-IRS) techniques (Figure 11).⁷⁴ However, the results suggested these SAMs involve disorder, liquid-like alkyl chains.

1.2.4. Linker molecule approach.— Many metal complexes have been self-assembled onto gold using thiols as linker molecules and surface modifiers.⁵⁷⁻⁶¹ 4-Pyridinethiol (PT) and 4-aminothiophenol (ATP) have been widely employed as linkers that bind on gold. For example, Co(II) and Fe(II) porphyrins have been assembled onto

gold using PT and ATP linker molecules that can be further attached to the metal in the complex center.⁶⁰ Two substituted Co(II) salen complexes coordinated with a PT linker molecule for surface modification have also been reported.⁷⁵

Gold surfaces modified with metal complexes using the linker molecule approach have been used as electrochemical sensors. For example, Co(II) phthalocyanine modified gold electrodes (Figure 12) were used to detect L-cysteine.⁶² In this particular case, 2-mercaptoethanol was used as the linker molecule to bind the metal complex through a phenyl acid chloride functionality. The surface was studied by various electrochemical methods.

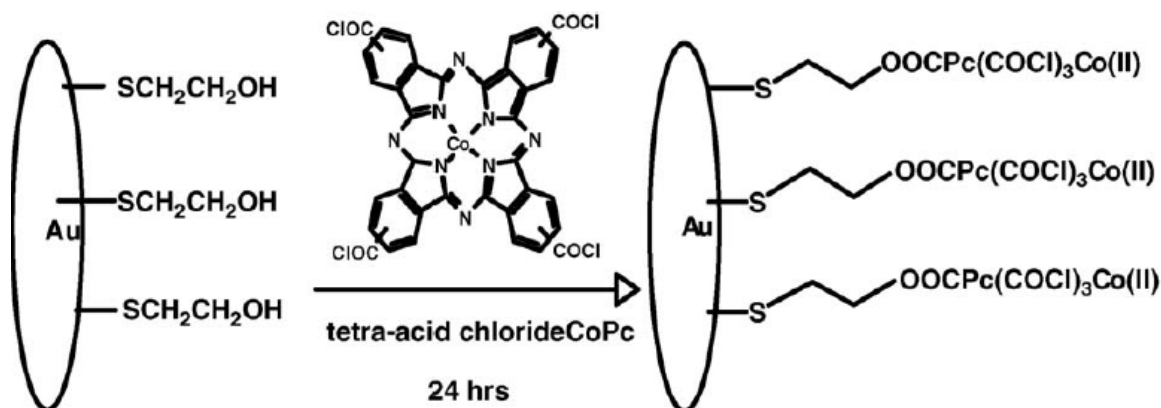


Figure 12. Co(II) phthalocyanine-modified gold electrodes. These were developed using 2-mercaptoethanol as a linker molecule. From ref. 62.

1.2.5. Properties of Au-alkylthiolate.— The self-assembly of alkanethiols on a gold surface is a fast adsorption process and SAMs grow by first-order Langmuir adsorption kinetics.⁷⁶ The rate of formation of the layer and its structure is dependent upon several parameters: concentration of adsorbate, purity of adsorbate, immersion time, concentration of oxygen in solution, cleanliness of substrate, solvent, temperature, and the alkanethiol chain length (or more generally the adsorbate's structure).⁷⁷ Scanning

tunneling microscopy has shown that a phase transition occurs on the gold surface for the formation of a densely packed alkanethiol SAM.⁷⁸ The gold and thiol head group interaction, the tail group interaction, and the dispersion forces between each alkyl chain also affect the molecular packing of the monolayer. Usually, a longer alkanethiol chain generates dense crystalline-like structures on the gold surface where the conformation of the alkyl chain is trans. As the alkyl chain is shortened, the packing is less dense, more disordered, and the surface coverage deteriorates.⁷⁹⁻⁸⁰

It has been reported that alkanethiols and alkyl disulfides form identical Au-alkylthiolate monolayers (Figure 13) which give a characteristic cyclic voltammetric response (Figure 14).^{54,81-82} The reductively desorbed thiolate can either oxidatively re-adsorb onto the surface or oxidatively dimerize to disulfides at more positive potentials.^{54,83} The dimerization occurs at oxidizing potentials, as the oxidation peaks can be observed in the CVs (Figure 14B). The cyclic voltammograms of thiophenol and diphenyl disulfide on gold are similar as they both undergo an irreversible reduction followed by an irreversible oxidation.⁵⁴ The thiol coating undergoes an irreversible one-electron reduction (Eq. 3) whereas the disulfide coating undergoes an irreversible two-

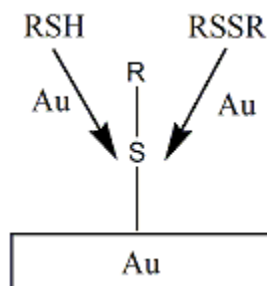


Figure 13. Self-assembly of thiol and disulfides. Widely accepted reaction scheme for the reaction of alkanethiols and alkyl disulfides with the gold surface in the process of monolayer formation. Thiols and disulfides give rise to identical monolayers. From ref. 81.

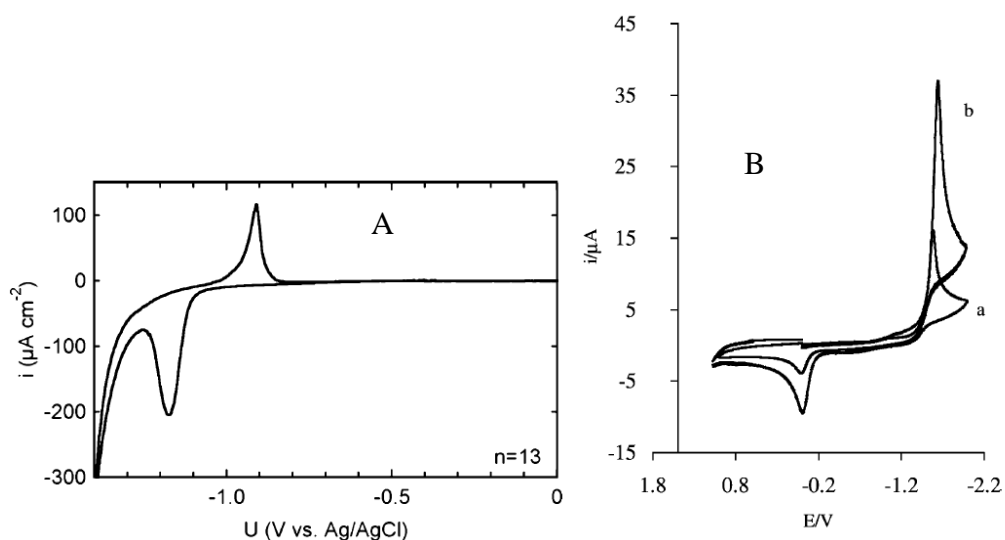


Figure 14. CVs of thiols and disulfides on gold. (A) Cyclic voltammogram for a tetradecanethiol monolayer on annealed polycrystalline gold in KOH. The scan rate was 100 mV/s. (B) Cyclic voltammograms of the a) diphenyl disulfide and b) thiophenol, $v = 100$ mV/s, $C = 4 \times 10^{-4}$ M on gold electrode in acetonitrile containing 0.05 M TBAClO₃. Irreversible reductions at -1.60 and -1.97 V and irreversible oxidations at approximately 0 V vs. SCE. From refs. 82 and 54.

electron reduction (Eq. 4).⁵⁴ Both films become damaged as smaller reductive currents are observed upon repeated sweeps (not shown). An irreversible two-electron oxidation takes place to produce the disulfide (Eq. 5) with no re-adsorption of thiolate seen in either case.⁵⁴

1.3. Summary for Literature Review

It is an attractive strategy to prepare gold electrodes surface-modified with highly organized SAM films of redox catalysts that can be used as analytical sensors. As previously mentioned, several metal complexes have been immobilized on planar gold or

used to modify CPEs for electrochemical studies. However, these investigations primarily focused on the oxidation behavior of the surface-confined catalysts. The detection of halogenated compounds *via* electrocatalytic reduction using gold electrodes surface-modified with thiol derivatives of redox species have rarely been examined, mostly due to the desorption of thiolate monolayers from the Au electrode surface at -1.3 to -1.7 V *vs.* SCE.⁵¹ Consequently, more positive reduction potentials for the affixed catalysts are required in order to utilize surface-modified gold electrodes for the detection of organic halides.

The electrochemical behavior of metal salens chemisorbed onto gold has not been studied extensively. Most previous studies prepared metal salen-modified electrodes by (a) premixing the catalyst into a CPE, (b) oxidative polymerization of monomer units onto bare electrodes, or (c) using linker molecules self-assembled onto gold to immobilize the metal salen derivatives. There have been no electrochemical studies of metal salen (**1**) chemisorbed on gold through an alkanethiol chain. It is intriguing to find out whether the immobilized complexes can be polymerized and used for redox catalysis, especially for catalytic reduction of organic halides. In this study, two nickel(II) salen complexes with different alkanethiol side chain lengths were prepared for self-assembly on gold to form the robust SAMs *via* chemical adsorption. The corresponding electrochemical properties of the modified Au electrode were carefully examined by cyclic voltammetry.

CHAPTER 2. ALKANETHIOL EXPERIMENTAL AND SYNTHESIS

2.1. Synthetic Routes.— The preparation of 5-(ω -sulfhydrylalkyl)salicyl-

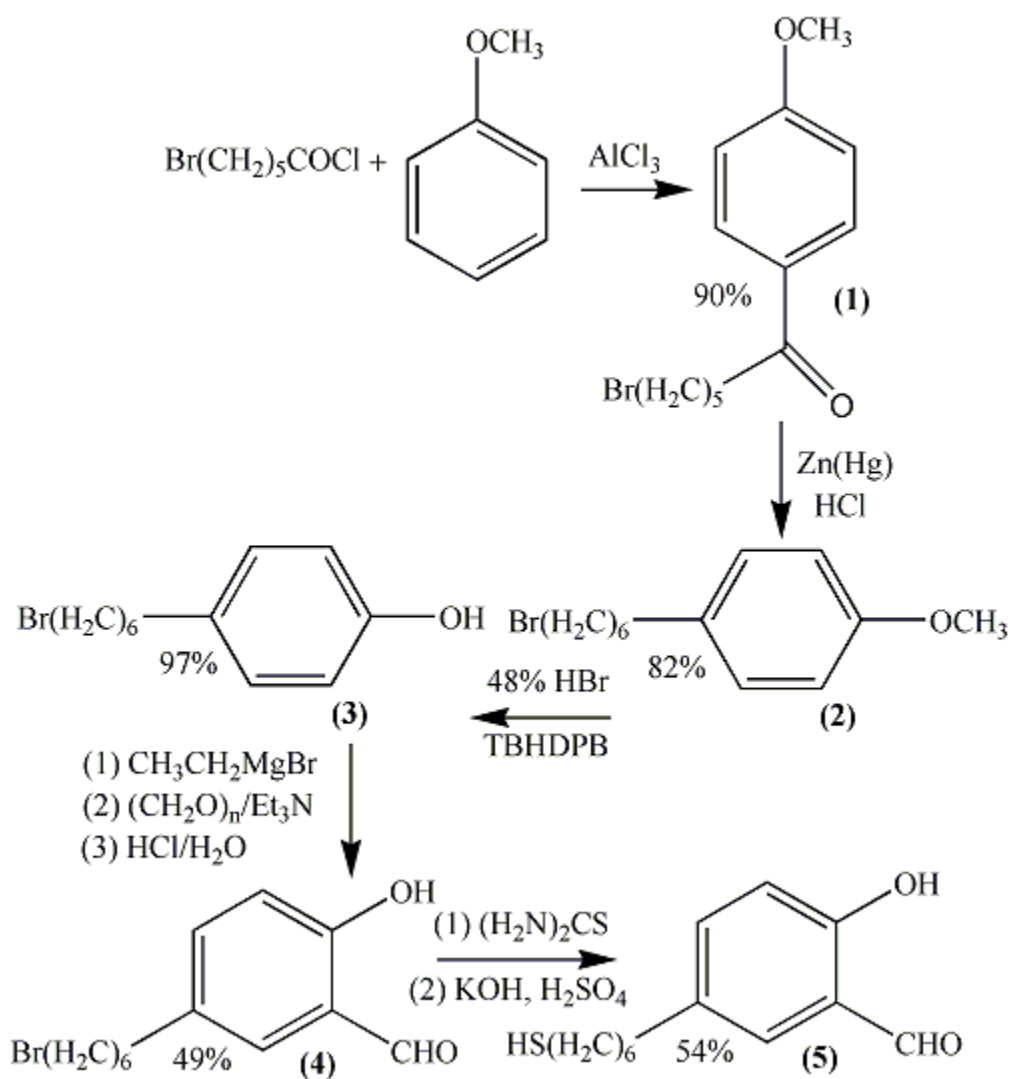


Figure 15. Synthesis of 5-(6-sulfhydrylhexyl)salicylaldehyde.

aldehydes was previously published.^{84,85} Figure 15 illustrates the synthetic route used to obtain 5-(6-sulphydrylhexyl)salicylaldehyde. 4-(6-Bromohexyl)phenol, **3**, was prepared in three steps *via* Friedel–Crafts acylation of anisole with 6-bromohexanoyl chloride,⁸⁶ followed by a Clemmensen reduction to selectively reduce the carbonyl group,⁸⁶ and finally conversion of the methoxy group to phenol in 48% HBr using (n-hexadecyl)tri-n-

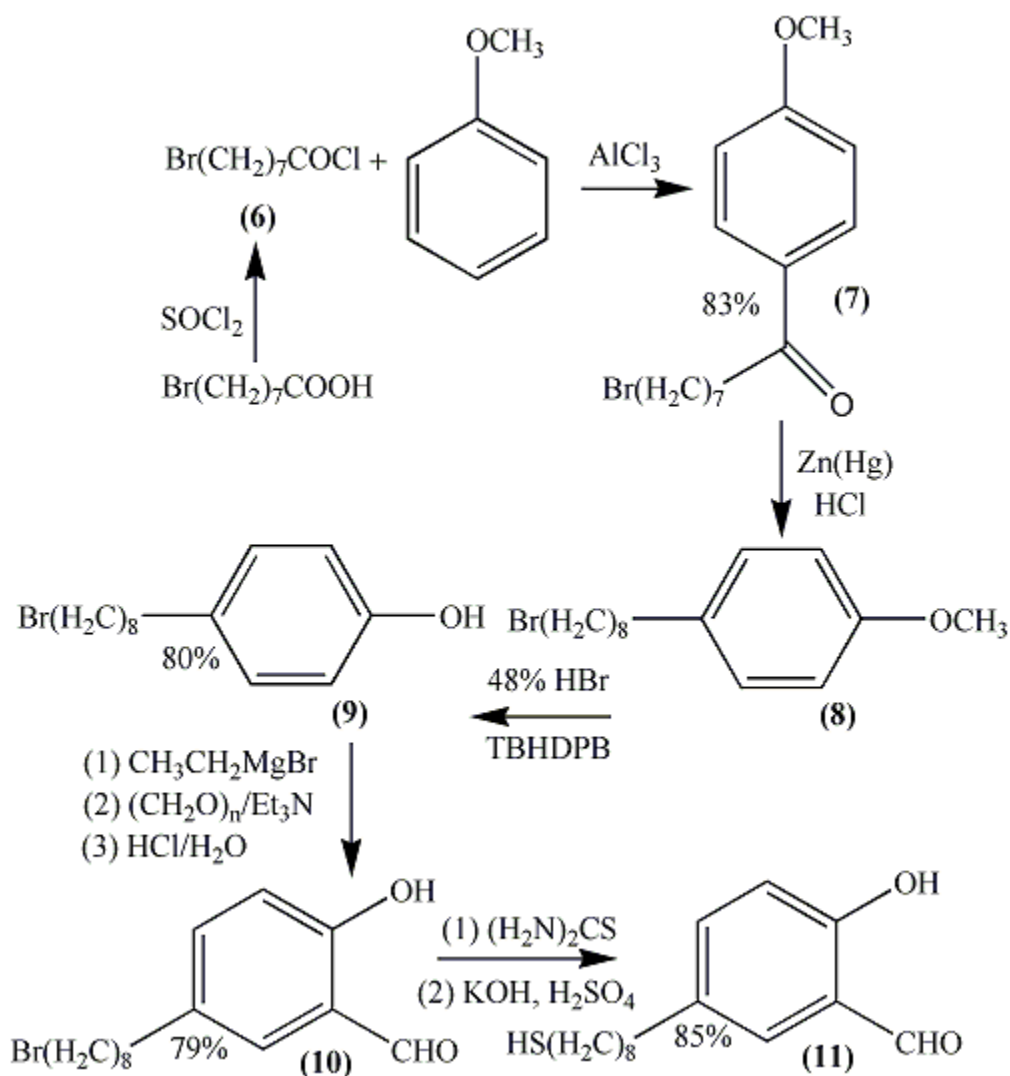


Figure 16. Synthesis of 5-(8-sulphydryloctyl)salicylaldehyde.

butylphosphonium bromide as a catalyst.⁸⁷ Treatment of the aryloxymagnesium bromide, freshly prepared from **3** and ethylmagnesium bromide, with paraformaldehyde and triethylamine gave 5-(6-bromohexyl)salicylaldehyde, **4**.⁸⁸ The product was purified by column chromatography (5% ethyl acetate–95% hexanes using silica gel) and crystallized in absolute alcohol. Finally, **4** was converted to **5** using thiourea to obtain the isothiuronium salt which was hydrolyzed using aqueous KOH and sulfuric acid.⁸⁹ The preparation of 5-(8-sulphydroctyl)salicylaldehyde, **11**, follows a similar synthetic route

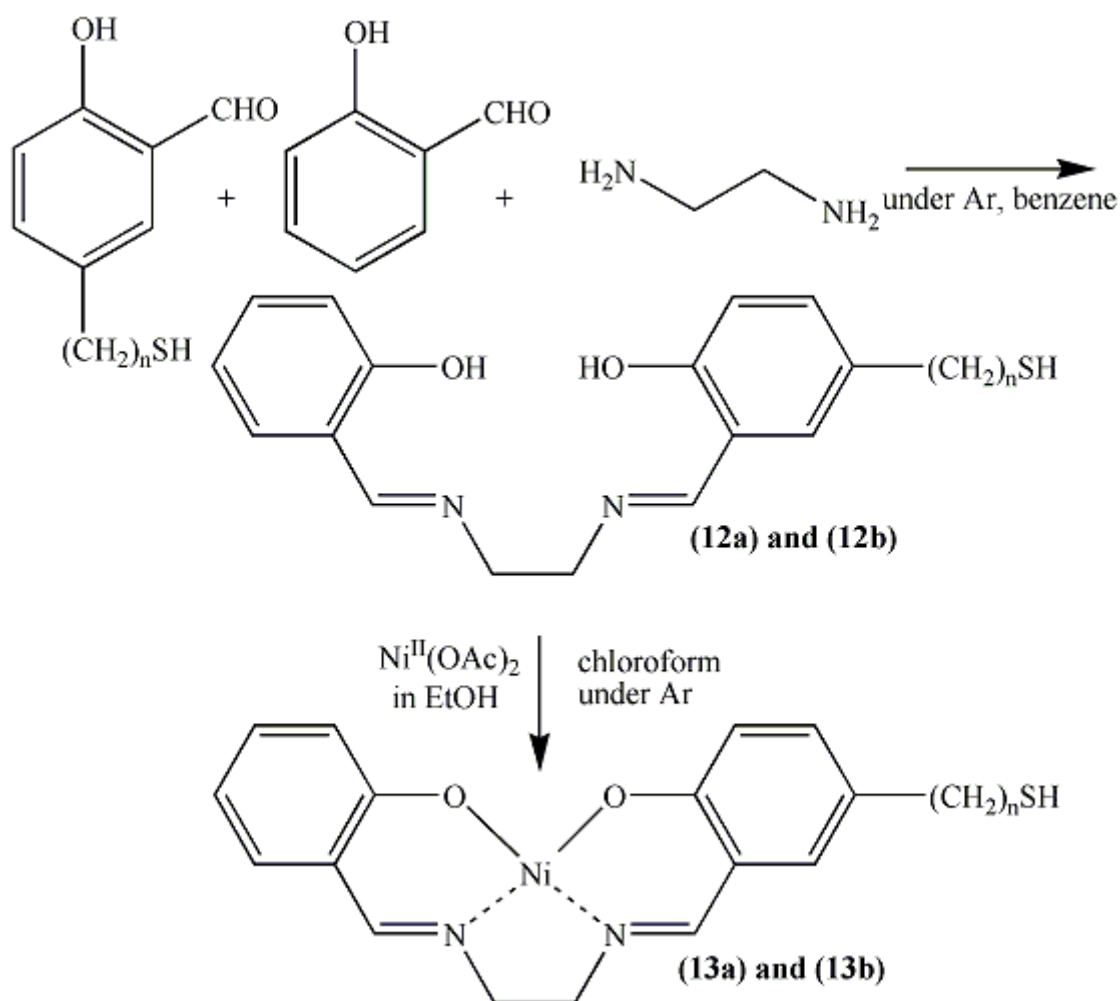


Figure 17. Synthesis of the nickel(II) salens with an alkanethiol side chain. Scheme 3 where **a** and **b** symbolize $n=6$ and $n=8$, respectively. Excess nickel(II) salen is also synthesized.

as shown in Figure 16. First, 8-bromooctanoic acid was quantitatively converted to 8-bromooctanoyl chloride, **6**, using thionyl chloride⁹⁰ prior to a Friedel–Crafts acylation with anisole. The preparation of modified nickel(II) salen catalysts, **13a** and **13b**, was achieved by mixing 5:9:1 molar ratios of ethylenediamine, salicylaldehyde, and either **5** or **11** followed by treatment with excess nickel(II) acetate.^{41,91} The product mixture containing approximately 10% **13a** or **13b** and 90% nickel(II) salen was used to saturate DMF. That solution was then employed to self-assemble **13a** or **13b** on gold electrodes.

2.2. Experimental Method

2.2.1. Reagents.— The following chemicals were purchased and used as received: 6-bromohexanoyl chloride (Alfa Aesar, 97%), anisole (Alfa Aesar, 99%), magnesium sulfate (Fisher), hexanes (Fisher, 99.9%), hexanes (Mallinckrodt, 98.5%), hexane (B& J Brand, 99.9% of C6 isomers), ethyl acetate (Fisher, 99.9%), acetone (Mallinckrodt, 99.5%), silica gel (EMD, 60-200 mesh), zinc (Aldrich, 99.8%), HgCl₂ (Alfa Aesar, 99+%), concentrated HCl (Fisher, 37.5% assay), 48% HBr, (n-hexadecyl)tri-n-butylphosphonium bromide (Alfa Aesar, 98%), sodium bicarbonate (Spectrum, 99.7-100.3%), absolute alcohol (Mallinckrodt, 94-96% methanol and ethanol), thiourea (Alfa Aesar, 99%), KOH (VMR, min 85%), concentrated H₂SO₄ (Fisher, 96.1% w/w), 8-bromooctanoic acid (Alfa Aesar, 97%), thionyl chloride (Aldrich, 99%), salicylaldehyde (Alfa Aesar, 99%), ethylenediamine (Alfa Aesar, 99%), acetonitrile (Fisher, 99.9%), chloroform (Fisher, 99.9%), nickel(II) acetate (Alfa Aesar, 98%), dimethylformamide (Fisher, 99.9%), ferrocene (bis(cyclopentadienyl)iron, Alfa Aesar, 99%), and nickel(II) salen (*N,N'*-bis(salicylidene)ethylenediaminonickel(II), Aldrich, 98%). TMABF₄ (tetramethylammonium tetrafluoroborate, Aldrich, 97%), used as a supporting electrolyte,

was stored in a vacuum oven at 60°C before use. All deaeration procedures were carried out with Praxair zero-grade or Air Gas zero-grade argon.

Dichloromethane (99.8%, EM Science), unless used for extraction purpose, was dried with anhydrous aluminum chloride (Alfa Aesar, Reagent Grade) prior to use. Benzene (Alfa Aesar, 99.5%), was continuously refluxed over anhydrous calcium chloride (Fisher, Pellets, 4-20 mesh, for desiccators) under Praxair zero-grade or Air Gas zero-grade argon or nitrogen to remove water. Anhydrous diethyl ether (J.T. Baker, 99.9%) and tetrahydrofuran (EM Science, 99.95%), were continuously refluxed over sodium (Aldrich, 99%) under Praxair zero-grade or Air Gas zero-grade argon or nitrogen to remove water. 4Å Molecular sieves (Aldrich, 8-12 mesh) were used to dry bromoethane (Alfa Aesar, 98%), triethylamine (Aldrich, 99%), and deuterated chloroform (Alfa Aesar, 99.8% (isotopic), containing 0.03% v/v TMS). Magnesium (EM Science, 99.5%) and paraformaldehyde powder (Alfa Aesar, 95%) were dried at 100°C for at least one hour prior to use.

2.2.2. Cells, electrodes, and instrumentation.— In this paper, the electrochemical cell used was a glass cell (CHI222) with a cell top (CHI221) including a platinum wire as the counter electrode. The working electrode used was a 2 mm diameter gold working electrode (CHI101P). All potentials were quoted with respect to SCE but measured using a non-aqueous pseudo reference electrode. All electrodes were purchased from CH Instruments and cyclic voltammetry (CV) experiments were carried out with a CH Instruments model 620B electrochemical analyzer using a CHI200(B) Faraday Cage.

2.2.3. Separation and identification of products.— All synthesized crude products were characterized with the aid of an Agilent Technologies model 6890N gas chromatograph (GC) equipped with a flame ionization detector (FID) and a model 5973N mass-selective detector (MSD). The analytes were separated on 30 m x 0.25 mm Agilent Technologies capillary columns (HP-1 for FID and HP-5MS for MSD) with a stationary phase of either 1 or 5% crosslinked phenylmethylsiloxane. All compounds except 1-(8-bromooctyl)-4-methoxybenzene were purified using silica gel column chromatography with ethyl acetate/ hexanes mixture as the mobile phase. Once purified, **2**, **3**, and **4** were analyzed by ^1H , ^{13}C , and DEPT NMR spectroscopy using a Varian 400 MHz NMR, **7**, **9**, **10**, and **11** were analyzed by ^1H and ^{13}C NMR spectroscopy using a Bruker 400 MHz NMR, and **1** and **5** were analyzed by ^1H , ^{13}C , and DEPT spectroscopy using both the Bruker 400 MHz NMR and the Varian 400 MHz NMR. ^1H NMR spectra were labeled compared to previous work, and all ^{13}C NMR spectra assignments are detailed in supplemental material.

2.3. Synthesis of 5-(6-Sulphydrylhexyl)salicylaldehyde

2.3.1. Synthesis of 6-bromo-1-(4-methoxyphenyl)-1-hexanone (1).— 4.748 g of 6-bromohexanoyl chloride (MW= 213.50 g/mol) was dissolved in approximately 10 mL dry dichloromethane (DCM) in a round bottom flask. 3.693 g of anhydrous AlCl_3 was added to the round bottom flask and placed under argon with an addition funnel attached. 2.614 g of anisole was mixed with dry DCM containing a small amount of anhydrous AlCl_3 and added into the addition funnel. The apparatus was degassed for 15 to 20 minutes, and the round bottom flask was chilled with ice water. After degassing, the anisole mixture was added dropwise over the course of 10 to 15 minutes to the substrate

in the chilled round bottom flask. After the addition, the mixture was stirred at room temperature for 3 hours under argon. The solution should become more red over that time period. The reaction was stirred at room temperature while open to air for another 8 hours before quenched with deionized water. The water was added dropwise until a reflux occurs. After the reaction was quenched, the aqueous layer was neutralized, and the mixture was extracted three times with equal amounts of DCM, dried over MgSO_4 , and concentrated under vacuum. Impure crystals formed from the concentrate were recrystallized using an ethyl acetate/ hexanes mixture to give white solids. The crude product could also be purified first by column chromatography (5% ethyl acetate–94% hexanes–1% benzene using silica gel, 60–200 mesh) before recrystallization. The pure 6-bromo-1-(4-methoxyphenyl)-1-hexanone (5.684 g, 90% yield, MW= 285.18 g/mol) was analyzed by GC–MS (70 eV) m/z 286, M^+ (0.5%); 284, M^+ (0.5%); 205, $[\text{M}-\text{Br}]^+$ (3.5%); 163, $[\text{M}-(\text{CH}_2)_3\text{Br}]^+$ (2.0%); 150, $[\text{M}-\text{CH}_2=\text{CH}-(\text{CH}_2)_2\text{Br}]^+$ (59.0%); 135, $[\text{M}-(\text{CH}_2)_5\text{Br}]^+$ (100.0%); 107, $[\text{M}-\text{CO}(\text{CH}_2)_5\text{Br}]^+$ (6.0%); 92, $[\text{M}-\text{CO}(\text{CH}_2)_5\text{Br}-\text{CH}_3]^+$ (8.5%); ^1H NMR (CDCl_3): δ 7.95 and 6.94 (2 d, 2H each, ArH), 3.87 (s, 3H, OCH₃), 3.43 (t, 2H, CH₂Br), 2.94 (t, 2H, COCH₂), 1.92 (q, 2H, CH₂CH₂Br), 1.76 (q, 2H, CH₂CH₂CH₂Br), 1.53 (q, 2H, COCH₂CH₂); ^{13}C NMR (CDCl_3): δ 198.75 (**8**), 163.58 (**3**), 130.44 (**1,5**), 130.27 (**6**), 113.88 (**2,4**), 55.62 (**7**), 38.09, 33.77, 32.82, 28.10, 23.72 (**9** through **15**; not directly assigned).

2.3.2. Synthesis of 1-(6-bromohexyl)-4-methoxybenzene (2).— 4.462 g of zinc and 0.260 g of HgCl_2 were combined together, and 6 M HCl was slowly added to create the amalgam catalyst. After fuming, this solution was stirred for 20 minutes, and the catalyst was washed several times with water. The amalgam was added to a round bottom

flask containing 1.040 g of **1** dissolved in 30 mL of benzene, 30 mL of water, and 15 mL of 12 M HCl. A condenser was attached, and the reaction mixture was vigorously stirred for three to five days under darkness at no more than 45 to 50°C. Over that time, 5 mL of 12 M HCl was added each day. At this temperature, zero-valent metal reduction catalyzed by Zn/HCl is inhibited, and the conversion of **2** to 6-hexylanisole is minor.⁹² The crude compound was extracted three times with equal volumes of benzene, dried over MgSO₄, and concentrated under vacuum. The oily product was purified by column chromatography (5% ethyl acetate–95% hexanes using silica gel, 60–200 mesh) to afford 1-(6-bromohexyl)-4-methoxybenzene (0.808 g, 82% yield, MW= 271.19 g/mol). GC–MS (70 eV) *m/z* 272, M⁺ (7.0%); 270, M⁺ (8.0%); 121, [M–(CH₂)₅Br]⁺ (100.0%); ¹H NMR (CDCl₃): δ 7.08 and 6.82 (2 d, 2H each, ArH), 3.78 (s, 3H, OCH₃), 3.39 (t, 2H, CH₂Br), 2.55 (t, 2H, ArCH₂), 1.85 (q, 2H, CH₂CH₂Br), 1.59 (q, 2H, ArCH₂CH₂), 1.45 (q, 2H, CH₂CH₂CH₂Br), 1.34 (q, 2H, ArCH₂CH₂CH₂); ¹³C NMR (CDCl₃): δ 157.77 (**3**), 134.77 (**6**), 129.36 (**1,5**), 113.82 (**2,4**), 55.37 (**7**), 34.98, 34.11, 32.87, 31.61, 28.43, and 28.15 (**8** through **13**; not directly assigned).

2.3.3. Synthesis of 4-(6-bromohexyl)phenol (3).— 3.092 g of **2**, 10 to 15 ml of 48% HBr, and 0.591 g of (n-hexadecyl)tri-n-butylphosphonium bromide were heated and stirred vigorously at 90 to 100°C for least 36 hours. The white phase transfer catalyst dissolved upon heating, and the organic layer turned to red-black. The reaction was tested for completeness by GC prior to the addition of water and extraction with equal amounts of ethyl acetate. The aqueous layer was added dropwise to sodium bicarbonate between each extraction, and the extractions were continued until the organic and aqueous layers became clear. The extracts were dried over MgSO₄ and some sodium bicarbonate to

neutralize any residual acid and concentrated under vacuum. The red-black crude product was purified by column chromatography using a gradient mobile phase (5% ethyl acetate–95% hexanes using silica gel, 60–200 mesh, increased to 10% ethyl acetate–90% hexanes). The purification afforded 4-(6-bromohexyl)phenol as an oil (2.934 g, 97% yield, MW= 257.17 g/mol). GC–MS (70 eV) m/z 258, M^+ (9.0%); 256, M^+ (10.0%); 107, $[M-(CH_2)_5Br]^+$ (100.0%); 1H NMR ($CDCl_3$): δ 7.03 and 6.75 (2 d, 2H each, ArH), 4.79 (s, 1H, OH), 3.39 (t, 2H, CH_2Br), 2.53 (t, 2H, Ar CH_2), 1.84 (q, 2H, CH_2CH_2Br), 1.58 (q, 2H, Ar CH_2CH_2), 1.45 (q, 2H, $CH_2CH_2CH_2Br$), 1.33 (q, 2H, Ar $CH_2CH_2CH_2$). ^{13}C NMR ($CDCl_3$): δ 153.52 (**3**), 134.98 (**6**), 129.58 (**1,5**), 115.22 (**2,4**), 34.98, 34.14, 32.85, 31.57, 28.40, and 28.13 (**7** through **12**; not directly assigned).

2.2.4. Synthesis of 5-(6-bromohexyl)salicylaldehyde (4).— For this reaction, precautions were taken to limit the amount of water present. All glassware were dried in an oven slightly above 100°C overnight, along with paraformaldehyde powder and magnesium turnings. Care was taken with drying paraformaldehyde powder since at higher temperature the polymer will begin to degrade. The powder was covered while in the oven and moved to a desiccator prior to use. Additionally, all solvents were dried, and King seal pipe clamps were used to limit air/water vapor leakage into any apparatus. $CaCl_2$ trap was placed to dry the argon flow into all apparatuses. Finally, all joints were greased, and glassware were kept constantly under argon for the reaction.

0.286 g of dried magnesium turnings was added to 15 to 25 mL of dry diethyl ether in a 100-mL round bottom flask under a dry and inert environment. Using an addition funnel, at least 1.300 g of bromoethane was added dropwise while the mixture

was stirred. The mixture was heated slightly until the reaction started. After all of the magnesium reacted and a clear mixture was obtained, 2.381 g of **3** was dissolved in dry THF and transferred to the addition funnel containing activated 4Å molecular sieves and added dropwise to the Grignard reagent. A white solid should precipitate as the reaction mixture was stirred for 20 to 30 minutes. Subsequently, 30 mL of freshly distilled benzene was added to the flask, and ether and THF were distilled away under argon. Finally, 1.300 g of dried triethylamine and 1.043 g of dried paraformaldehyde powder were added. The mixture was refluxed for 3 to 6 hours under argon and then cooled to room temperature. The mixture should become yellow over this time period. In the end, approximately 40 to 60 mL of 10% aqueous HCl was added directly to the mixture and stirred.

The organic layer was collected, and the aqueous phase was extracted three times with equal volumes of ether and once with benzene. The organic fractions were combined, dried over MgSO₄, and concentrated under vacuum. The resulting crude mixture was purified by column chromatography (5% ethyl acetate–95% hexanes using silica gel, 60-200 mesh) to afford 5-(6-bromohexyl)salicylaldehyde as a yellow solid (1.296 g, 49% yield, MW= 285.18 g/mol). The crystals remained stable at room temperature and were recrystallized in absolute alcohol prior to subsequent use. GC–MS (70 eV) *m/z* 286, M⁺ (12.0%); 284, M⁺ (12.0%); 135, [M–(CH₂)₅Br]⁺ (100.0%); ¹H NMR (CDCl₃): δ 10.86 (s, 1H, ArOH), 9.87 (s, 1H, CHO), 7.36–7.34 and 6.92 (m and d, 2H and 1H, respectively, ArH), 3.41 (t, 2H, CH₂Br), 2.60 (t, 2H, ArCH₂), 1.86 (q, 2H, CH₂CH₂Br), 1.63 (q, 2H, ArCH₂CH₂), 1.48 (q, 2H, CH₂CH₂CH₂Br), 1.37 (q, 2H, ArCH₂CH₂CH₂). ¹³C NMR (CDCl₃): δ 196.72 (**7**), 159.93 (**3**), 137.51 (**5**), 134.08 (**6**),

132.95 (**1**), 120.52 (**4**), 117.62 (**2**), 34.68, 34.01, 32.78, 31.29, 28.31, 28.06 (**8** through **13**; not directly assigned).

2.3.5. Synthesis of 5-(6-sulfhydrylhexyl)salicylaldehyde (5).— Stoichiometric amounts of thiourea (0.175 g) and **4** (0.604 g) were added into a 100-mL round-bottom flask containing 15 mL of absolute ethanol. The apparatus was degassed and the solution was refluxed under argon for overnight. The reaction mixture was cooled to room temperature, the solvent was evaporated, and 25 mL of 30% w/v KOH was added. The apparatus was degassed for ten minutes before the mixture was reheated to reflux for 5 to 6 hours to hydrolyze the isothiuronium salt to a potassium-based salicylaldehyde salt, which was then transferred into a separatory funnel containing 25 mL of 9 M H₂SO₄ to be protonated. After cooling down to room temperature, deionized water was added and the mixture was extracted three times with equal volumes of ether. The organic phases were combined, dried over anhydrous MgSO₄, and the solvent was removed under vacuum. The synthesis afforded 5-(6-sulfhydrylalkyl)salicylaldehyde as a yellow oil (0.287 g, 54% yield, MW= 238.15 g/mol). This product was air sensitive over the time and was used immediately. GC–MS (70 eV) *m/z* 238, M⁺ (16.0%); 187, [M–H₂O–SH]⁺ (5.0%); 173, [M–H₂O–CH₂SH]⁺ (6.0%); 135, [M–(CH₂)₅SH]⁺ (100.0%); ¹H NMR (CDCl₃): δ 10.84 (s, 1H, ArOH), 9.87 (s, 1H, CHO), 7.36–7.33 and 6.91 (m and d, 2H and 1H, respectively, ArH), 2.60 (t, 2H, ArCH₂), 2.52 (q, 2H, CH₂SH), 1.61 (q, 4H, ArCH₂CH₂ and CH₂CH₂SH), 1.46–1.30 (2 m, 2H and 3H, respectively, ArCH₂CH₂CH₂, CH₂CH₂CH₂SH, and SH). ¹³C NMR (CDCl₃): δ 196.71 (**7**), 159.94 (**3**), 137.52 (**5**), 134.19 (**6**), 132.93 (**1**), 120.55 (**4**), 117.62 (**2**), 34.75, 34.00, 31.37, 28.66, 28.27, 24.70 (**8** through **13**; not directly assigned).

2.4. Synthesis of 5-(8-Sulphydryloctyl)salicylaldehyde

2.4.1. Synthesis of 8-bromooctanoyl chloride (6).— 1.411 g of 8-bromooctanoic acid (MW= 223.11 g/mol) was placed in a 100-mL round bottom flask and approximately 10 mL of thionyl chloride was added with stirring. The apparatus was degassed with argon prior to further stirring for 12 hours at 60°C. The thionyl chloride was distilled away, and any residual solvent was quickly removed under vacuum to avoid introduction of excessive moisture. This reaction yielded 1.762 g of crude 8-bromooctanoyl chloride (**6**, MW= 241.56 g/mol), which was used immediately. The acid chloride was not analyzed by NMR or GC-MS due to its extreme water sensitivity.

2.4.2. Synthesis of 8-bromo-1-(4-methoxyphenyl)-1-octanone (7).— 1.762 g of crude **6** was dissolved in approximately 10 mL dry DCM in a round bottom flask. After the addition of 0.8451 g of anhydrous AlCl₃ the apparatus was placed under argon with an additional funnel attached. Subsequently, 0.7040 g of anisole was dissolved in dry DCM containing a small amount of anhydrous AlCl₃. The following procedures were analogous to the synthesis of **1**. Purification afforded 8-bromo-1-(4-methoxyphenyl)-1-octanone as pale yellow crystals (1.602 g, 83% yield, MW= 313.23 g/mol). GC-MS (70 eV) *m/z* 314, M⁺ (0.5%); 312, M⁺ (0.5%); 233, [M-Br]⁺ (2.5%); 163, [M-(CH₂)₅Br]⁺ (6.5%); 150, [M-CH₂=CH(CH₂)₄Br]⁺ (80.0%); 135, [M-(CH₂)₇Br]⁺ (100.0%); 107, [M-CO(CH₂)₇Br]⁺ (5.5%); 92, [M-CO(CH₂)₇Br-CH₃]⁺ (7.5%); ¹H NMR (CDCl₃): δ 7.94 and 6.93 (2 d, 2H each, ArH), 3.87 (s, 3H, OCH₃), 3.40 (t, 2H, CH₂Br), 2.91 (t, 2H, COCH₂), 1.86 (q, 2H, CH₂CH₂Br), 1.73 (q, 2H, CH₂CH₂CH₂Br), 1.49-1.36 (m, 6H, COCH₂CH₂CH₂CH₂); ¹³C NMR (CDCl₃): δ 199.05 (**8**), 163.37 (**3**), 130.32 (**1,5**), 130.21

(6), 113.71 (2,4), 55.47 (7), 38.18, 33.92, 32.77, 29.21, 28.64, 28.03, 24.46 (9 through 15; not directly assigned).

2.4.3. Synthesis of 1-(8-bromooctyl)-4-methoxybenzene (8).— 0.848 g of pure 7 was used and procedures were analogous to the synthesis of 2. The reaction afforded a crude 1-(8-bromooctyl)-4-methoxybenzene yellow oil (0.798 g, MW= 299.34 g/mol), which was used without further purification. GC–MS (70 eV) m/z 300, M^+ (8.0%); 298, M^+ (8.0%); 121, $[M-(CH_2)_7Br]^+$ (100.0%).

2.4.4. Synthesis of 4-(8-bromooctyl)phenol (9).— 0.798 g of crude 8 was used and procedures were analogous to the synthesis of 3. Purification afforded 4-(8-bromooctyl)phenol as an oil (0.614 g, 80% yield, MW= 285.22 g/mol). GC–MS (70 eV) m/z 286, M^+ (9.0%); 284, M^+ (9.0%); 107, $[M-(CH_2)_7Br]^+$ (100.0%); 1H NMR ($CDCl_3$): δ 7.03 and 6.74 (2 d, 2H each, ArH), 4.59 (s, 1H, OH), 3.39 (t, 2H, CH_2Br), 2.52 (t, 2H, Ar CH_2), 1.84 (q, 2H, CH_2CH_2Br), 1.56 (q, 2H, Ar CH_2CH_2), 1.41 (q, 2H, $CH_2CH_2CH_2Br$), 1.33-1.25 (m, 6H, Ar $CH_2CH_2CH_2CH_2CH_2$). ^{13}C NMR ($CDCl_3$): δ 153.41 (3), 135.08 (6), 129.41 (1,5), 115.05 (2,4), 34.99, 33.99, 32.80, 31.63, 29.27, 29.07, 28.68, 28.14 (7 through 14; not directly assigned).

2.4.5. Synthesis of 5-(8-bromooctyl)salicylaldehyde (10).— The preparation of crude compound was analogous to that of 5-(6-bromohexyl)salicylaldehyde. 0.150 g of dried magnesium turnings, 0.700 g of dry bromoethane, 0.869 g of 9, 0.464 g of dried triethylamine, and 0.504 g of dried paraformaldehyde were used. Purification afforded 5-(8-bromooctyl)salicylaldehyde as pale yellow crystals. (0.755 g, 79% yield, MW= 313.23 g/mol). The crystals remained stable at room temperature and were recrystallized in

absolute alcohol prior to subsequent use. GC–MS (70 eV) m/z 314, M^+ (14.0%); 312, M^+ (14.0%); 135, $[M-(CH_2)_7Br]^+$ (100.0%); 1H NMR ($CDCl_3$): δ 10.84 (s, 1H, ArOH), 9.87 (s, 1H, CHO), 7.36–7.33 and 6.91 (m and d, 2H and 1H, respectively, ArH), 3.40 (t, 2H, CH_2Br), 2.59 (t, 2H, Ar CH_2), 1.85 (q, 2H, CH_2CH_2Br), 1.60 (q, 2H, Ar CH_2CH_2), 1.44 (q, 2H, $CH_2CH_2CH_2Br$), 1.37–1.27 (q, 6H, Ar $CH_2CH_2CH_2CH_2CH_2$). ^{13}C NMR ($CDCl_3$): δ 196.74 (**7**), 159.93 (**3**), 137.56 (**5**), 134.36 (**6**), 132.95 (**1**), 120.56 (**4**), 117.60 (**2**), 34.85, 34.10, 32.92, 31.49, 29.40, 29.13, 28.82, 28.27 (**8** through **15**; not directly assigned).

2.4.6. Synthesis of 5-(8-sulphydryloctyl)salicylaldehyde (11).— Stoichiometric amounts of thiourea (0.202 g) and **10** (0.664 g) were dissolved in absolute ethanol. The reaction was mostly analogous to the synthesis of **5**. However, the extraction phase was quickly filtered through copious magnesium sulfate. The synthesis afforded 5-(6-sulphydrylalkyl)salicylaldehyde as a yellow oil (0.480 g, 85% yield, MW= 266.39 g/mol). GC–MS (70 eV) m/z 266, M^+ (5.0%); 248, $[M-H_2O]^+$ (19.0%); 135, $[M-(CH_2)_7SH]^+$ (100.0%); 1H NMR ($CDCl_3$): δ 10.84 (s, 1H, ArOH), 9.87 (s, 1H, CHO), 7.36–7.33 and 6.91 (m and d, 2H and 1H, respectively, ArH), 2.59 (t, 2H, Ar CH_2), 2.52 (q, 2H, CH_2SH), 1.61 (q, 4H, Ar CH_2CH_2 and CH_2CH_2SH), 1.41–1.25 (2 m, 6H and 3H, respectively, Ar $CH_2CH_2CH_2CH_2CH_2$, $CH_2CH_2CH_2SH$, and SH). ^{13}C NMR ($CDCl_3$): δ 196.61 (**7**), 159.84 (**3**), 137.43 (**5**), 134.28 (**6**), 132.83 (**1**), 120.48 (**4**), 117.49 (**2**), 34.75, 34.01, 31.39, 29.36, 29.08, 29.02, 28.36, 24.64 (**8** through **15**; not directly assigned).

2.5. Synthesis of Ni(II) Salen Catalysts with $n=6$ and $n=8$

2.5.1. Synthesis of *N,N'*-bis(salicylidene)ethylenediamine with $n=6$ (**12a**) or $n=8$

(**12b**).— To synthesize the salen ligand with single alkanethiol side chain ($n=6$ or $n=8$), 0.567 g ethylenediamine (0.00943 mol, 5 parts) was dissolved in ethanol and added dropwise into a vigorously stirring chloroform or benzene solution containing 2.073 g salicylaldehyde (0.01698 mol, 9 parts) and 0.449 g 5-(6-sulfhydrylhexyl)salicylaldehyde (0.00189 mol, 1 part) under argon. After 10 to 20 minutes, the reaction mixture was concentrated if necessary until a yellow solid began to precipitate. The precipitate was isolated by vacuum filtration and washed with cold ethanol. The yellow crystals were then transferred to another round bottom flask and dried under vacuum and used immediately. The same procedure was used for synthesis of **12b** using a 5:9:1 molar ratio of ethylenediamine (0.504 g, 0.00839 mol), salicylaldehyde (1.842 g, 0.01508 mol), and 5-(8-sulfhydrylalkyl)salicylaldehyde (0.446 g, 0.00167 mol).

2.5.2. Synthesis of alkanethiol modified Ni(II) salen mixture with $n=6$ (**13a**) or

$n=8$ (**13b**).— The salen ligand mixture was immediately dissolved in chloroform and excess nickel(II) acetate in ethanol (2.432 g for $n=6$) was added dropwise under argon. The solution was stirred to give a dark brown precipitate. The solution was concentrated if too much solvent was used. The product was vacuum filtered, washed with cold ethanol, and stored under vacuum in a sealed vial. The product was used to saturate 40 mL of degassed DMF prior to assembling on gold electrode. The same procedure was employed for the synthesis of **13b** using excess nickel acetate (2.222 g for $n=8$).

2.6. Preparation of SAMs and Cyclic Voltammetry

2.6.1. Preparing the bare Au electrode.— In order to prepare a clean Au electrode surface, the electrode was manually polished with 0.05 micron deagglomerated alumina (Buehler Gamma Micropolish II) followed by suspending the electrode in deionized water and sonicating for 5 to 10 minutes. This was done several times. Subsequently, the electrode was rinsed with deionized water and sonicated in 1.6 M nitric acid for one minute, followed by further polishing with alumina and sonication in deionized water. The Au electrode surface should have a shiny smooth appearance. The electrode was transferred into a DMF solution containing 0.05 M TMABF₄ and degassed with argon for 30 minutes. The electrode was then scanned from 0 V to +1.20 V and 0 V to -1.80 V *vs.* SCE. The procedure was repeated if the CV was not clean. In that case, aqua regia (HCl:HNO₃:water; 15 mL:5 mL:20 mL) was used instead of nitric acid to treat the electrode and sonicated for several seconds.

2.6.2. Cyclic voltammetry of Ni(II) salen and salicylaldehyde in DMF.— The bare Au electrode was placed in a DMF solution containing 0.05 M TMABF₄ and 1.94 mM nickel(II) salen. For CV of salicylaldehyde, a DMF solution containing 0.05 M TMABF₄ and 1.88 mM salicylaldehyde was used instead. The solutions were degassed with argon for 30 minutes prior to collection of any CVs. The CV scan windows were the following: For nickel(II) salen, CVs were obtained in the range of 0 V to +1.09 V and -0.81 V to -1.91 *vs.* SCE. For salicylaldehyde, CVs were obtained in the range of -0.11 V to -1.91 V to +1.09 V to -0.11 V *vs.* SCE for a continuous scan and -0.11 V to -1.91 V and -0.11 V to +1.09 V *vs.* SCE for a discontinuous scan.

2.6.3. Coating the bare Au electrode with 5-(ω -sulfhydrylalkyl)salicylaldehydes.— The bare Au electrode was placed in a degassed 1:1 chloroform:ethanol solution containing 4.24 mM of fresh **5**. The electrode and the solution were sealed in a vial and placed in a vacuum desiccator at room temperature for 40 hours. The electrode was then washed with DMF, placed in DMF overnight, washed with more DMF, and sonicated briefly prior to electrochemical analysis in DMF containing 0.05 M TMABF₄ with and without ferrocene. The desorption of the thiolate was observed in CV by scanning negatively using the scan window of -0.58 V to -2.12 V vs. SCE. The same procedure was repeated for a 4.23 mM solution of **11** dissolved in degassed chloroform in contact with Au electrode for 37 to 64 hours using scan windows of 0 V to -2.12 V to $+0.15$ V to 0 V and -0.58 V to -2.20 V vs. SCE, respectively.

2.6.4. Coating the bare Au electrode with alkanethiol modified Ni(II) salen with $n=6$ or 8.— The bare Au electrode was placed in a 40 mL DMF solution saturated with approximately 10% [nickel(II)salen]C₆SH (**13a**) and 90% nickel(II)salen. The electrode and the solution were sealed in a vial and placed in a vacuum desiccator at room temperature for four days. The surface-modified electrode was then washed with DMF, placed in DMF for overnight, washed with more DMF, and sonicated briefly prior to electrochemical analysis. For **13b**, the coating time was approximately a week.

2.6.5. Cyclic voltammetry analysis.— Both catalyst films were studied by CV in DMF containing 0.05 M TMABF₄ without or with ferrocene. To determine whether the films were robust, a [nickel(II)salen]C₆S-Au film was placed in 0.012 M HCl for overnight after exposed to a scan window of $+0.25$ V to $+1.20$ V vs. SCE for several

sweeps. The electrode was then washed with copious amounts of water and DMF prior to analysis using a scan window of +0.41 V to -1.34 V *vs.* SCE. To determine whether nickel(II) salen binds to the gold electrode surface, the bare gold electrode was submerged in 3.94 mM nickel(II) salen in DMF for 43 hours, followed by washing with DMF prior to CV analysis in DMF containing 0.05 M TMABF₄ using a scan window of -0.20 V to -1.10 V *vs.* SCE.

CHAPTER 3. RESULTS AND DISCUSSION

3.1. CVs of Ferrocene, Nickel(II) Salen, and Salicylaldehyde at a Gold

Electrode.— Prior to the analysis of 5-(ω -sulfhydrylalkyl)salicylaldehydes and [nickel(II)salen] C_n SH films, cyclic voltammograms (CV) were obtained using a gold working electrode in DMF containing 0.05 M TMBF₄ for approximately 2.10 mM ferrocene, 1.94 mM nickel(II) salen, and 1.88 mM salicylaldehyde at a scan rate of 100 mV/s (Figures 18-21). The ferrocene(II)-ferrocene(III) redox couple is at approximately +0.44 V vs. SCE,⁹³ while nickel(II) salen undergoes both oxidation and reduction processes. Nickel(II) salen-nickel(I) salen and nickel(II) salen-nickel(III) salen redox couples can be observed at approximately -1.70 V and +0.77 V vs. SCE, respectively.²⁶ For the CV of salicylaldehyde in DMF, the reductive process taking place at -1.69 V vs. SCE involves an irreversible transfer of an electron to the carbonyl, followed by a reversible protonation of the radical anion to form an alcohol.⁸³ The radical anion can also undergo irreversible anodic dimerization at +0.47 V vs. SCE.⁸³

3.2. Self-Assembled Monolayers on Gold

3.2.1. 5-(6-Sulfhydrylhexyl)salicylaldehyde and 5-(8-sulfhydroctyl)-

salicylaldehyde on gold.— Figure 22 shows the desorption of 5-(6-sulfhydrylhexyl)-salicylaldehyde and 5-(8-sulfhydroctyl)salicylaldehyde from gold electrode surface in

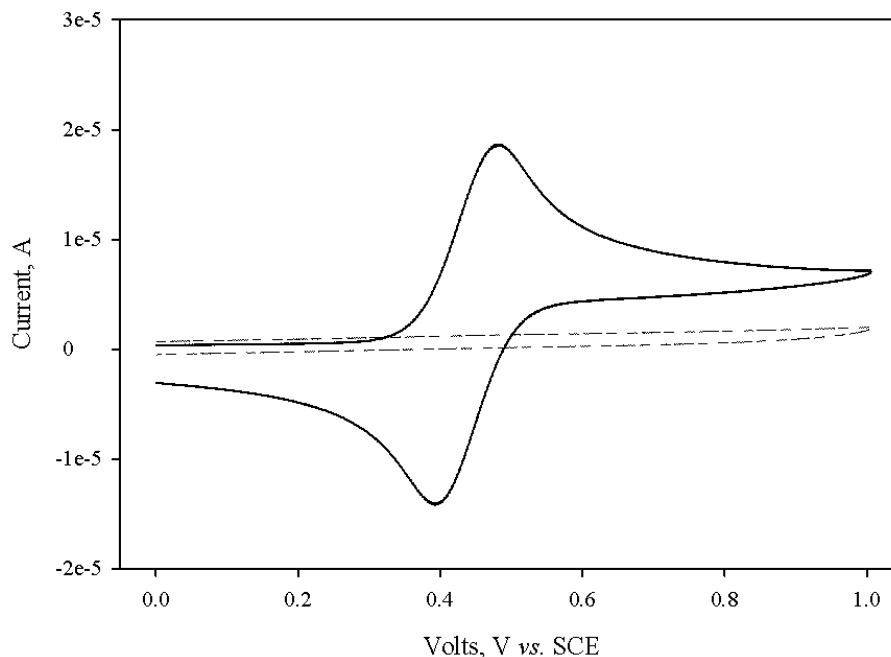


Figure 18. CV of ferrocene in DMF. Cyclic voltammograms of DMF containing 0.05 M TMABF_4 (dashed) and 2.10 mM ferrocene in DMF containing 0.05 M TMABF_4 (solid) at 100 mV/s using a gold working electrode vs. SCE. The ferrocene(II)-ferrocene(III) couple is at +0.44 V vs. SCE.

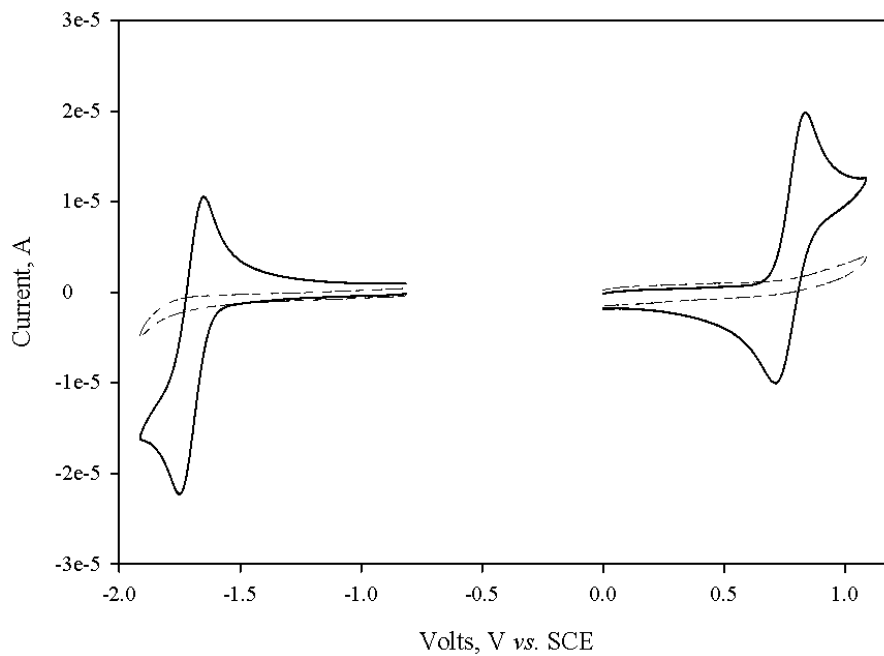


Figure 19. CV of nickel(II) salen in DMF. Cyclic voltammograms of DMF containing 0.05 M TMABF_4 (dashed) and 1.94 mM nickel(II) salen in DMF containing 0.05 M TMABF_4 (solid) at 100 mV/s using a gold working electrode. The nickel(II) salen-nickel(III) salen couple is at +0.77 V vs. SCE. The nickel(II) salen-nickel(I) salen couple is at -1.70 V vs. SCE.

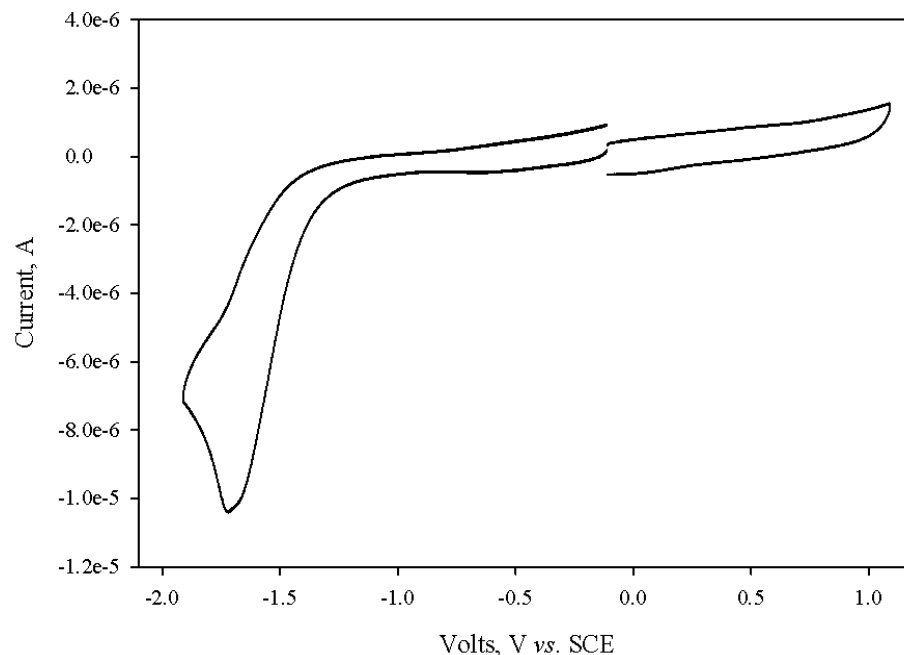


Figure 20. CV of salicylaldehyde in DMF (1). Cyclic voltammogram of 1.88 mM salicylaldehyde in DMF containing 0.05 M TMABF₄ at 100 mV/s using a gold working electrode with separate positive and negative scans.

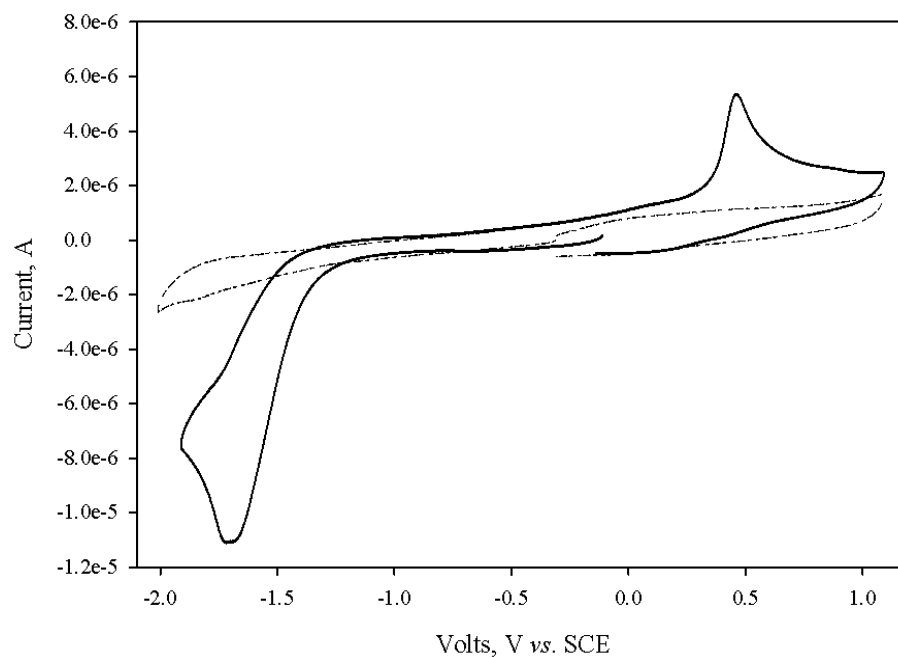


Figure 21. CV of salicylaldehyde in DMF (2). Cyclic voltammograms of DMF containing 0.05 M TMABF₄ (dashed) and 1.88 mM salicylaldehyde in DMF containing 0.05 M TMABF₄ (solid) at 100 mV/s using a gold working electrode. The solid CV was scanned from -0.11 V to -1.91 V to +1.09 V to -0.11 V.

DMF containing 0.05 M TMABF₄ after 40 and 64 hours of submersion in 4.24 and 4.23 mM of the corresponding thiol solutions, respectively. The CVs of the alkylthiolate films on gold are consistent with the electrochemical features previously assigned to many thiolate SAMs on gold.^{54,82,94} The immobilized alkylthiolate undergoes an irreversible one-electron reduction to form alkylthiolate anions (RCH_nS⁻). Subsequent scans (Figures 23 and 24) show that the reduction current decreases and the peak potential shifts slightly positively, indicating the desorption of monolayer.⁵¹ Nevertheless, Figures 22-24 do not show an anodic process which corresponds to the fast oxidative readsorption of alkylthiolate anions onto gold, which could take place for some alkanethiols in aq. KOH.⁸² The reduction potentials of the two thiolate films for the first scans are -1.89 V and -1.85 V vs. SCE, respectively. These potentials may vary slightly over a potential range because the development of the films are dependent on several factors such as cleanliness of the electrode surface, the purity and concentration of the assembly solution, the surface smoothness, and immersion time.⁷⁷ Ideally, longer alkane chain lengths would have a slightly more negative desorption potential with similar surface coverage, but it is not that obvious in our case.⁷⁷ Figures 22 to 24 also indicate that more 5-(8-sulfhydryloctyl)salicylaldehyde molecules are self-assembled to form an ordered alkylthiolate film on the gold surface, likely due to the longer coating time, the better solvent system (chloroform is a much better solvent than ethanol), and a longer chain length. However, using DMF containing 0.05 M TMABF₄ and 2 mM ferrocene (not shown), the corresponding CVs show that the coatings on gold electrode only slightly affect the redox features of ferrocene(II)-ferrocene(III) couple, indicating that the thiolate films have an effect on the diffusion of ferrocene to the electrode surface.

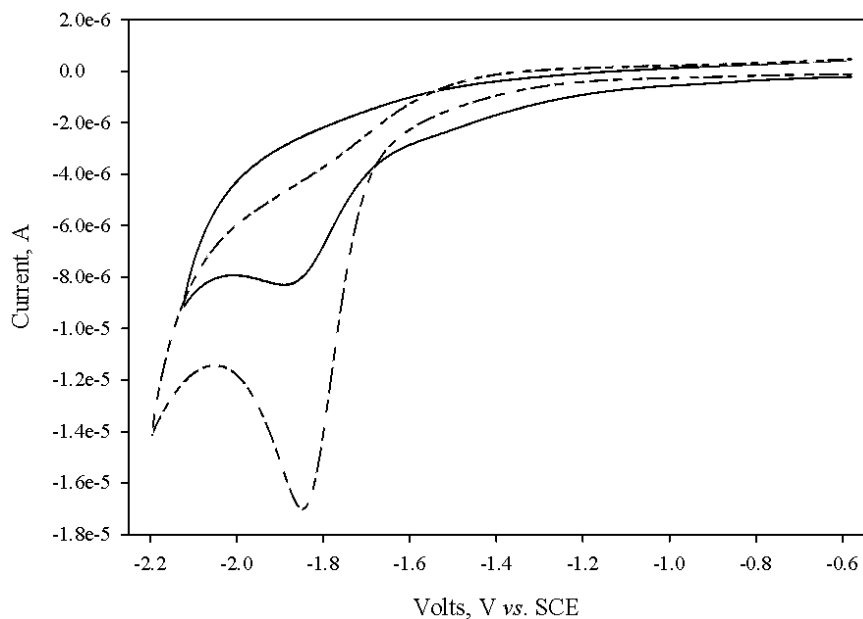


Figure 22. CVs of the desorption of 5-(ω -sulfhydrylalkyl)salicylaldehydes on gold (first scans). Cyclic voltammograms of 5-(6-sulfhydrylhexyl)salicylaldehyde (solid) and 5-(8-sulfhydroctyl)salicylaldehyde (dashed) on gold in DMF containing 0.05 M TMABF₄ at 100 mV/s. 5-(6-Sulfhydrylhexyl)salicylaldehyde was assembled onto a submerged bare gold electrode from a 4.24 mM 50:50 chloroform:ethanol solution for 40 hours. 5-(8-Sulfhydroctyl)salicylaldehyde was assembled onto a submerged bare gold electrode from a 4.23 mM chloroform solution for 64 hours. The reductive desorption potential of the first sweep are -1.89 and -1.85 V vs. SCE, respectively.

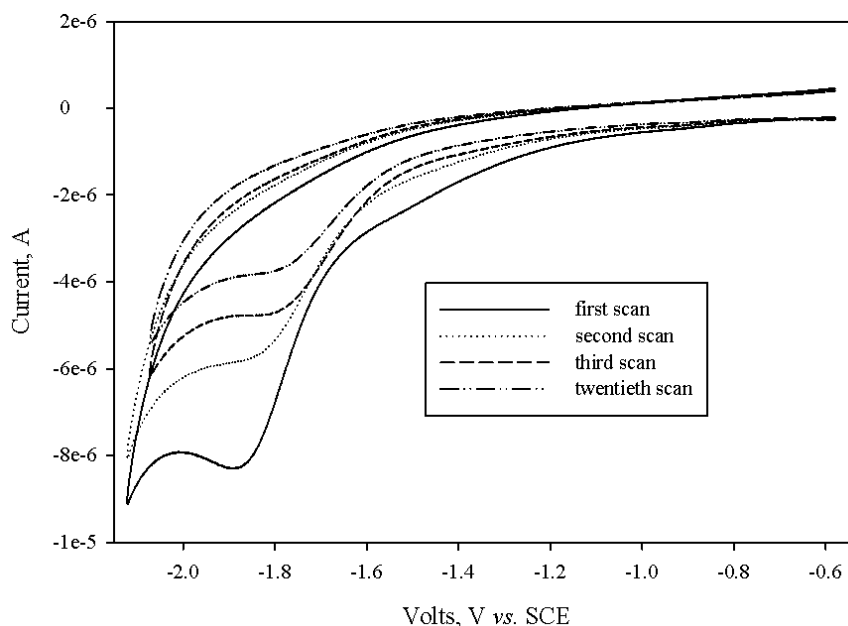


Figure 23. CVs of the desorption of 5-(6-sulfhydrylhexyl)salicylaldehyde on gold. Cyclic voltammograms of 5-(6-sulfhydrylhexyl)salicylaldehyde on gold in DMF containing 0.05 M TMABF₄ at 100 mV/s. The CVs show the desorption of monolayer into the solution with continuous scans. $Q = 1.25 \times 10^{-6}$ C and estimated surface coverage $\Gamma = 1.03 \times 10^{-10}$ mol/cm².

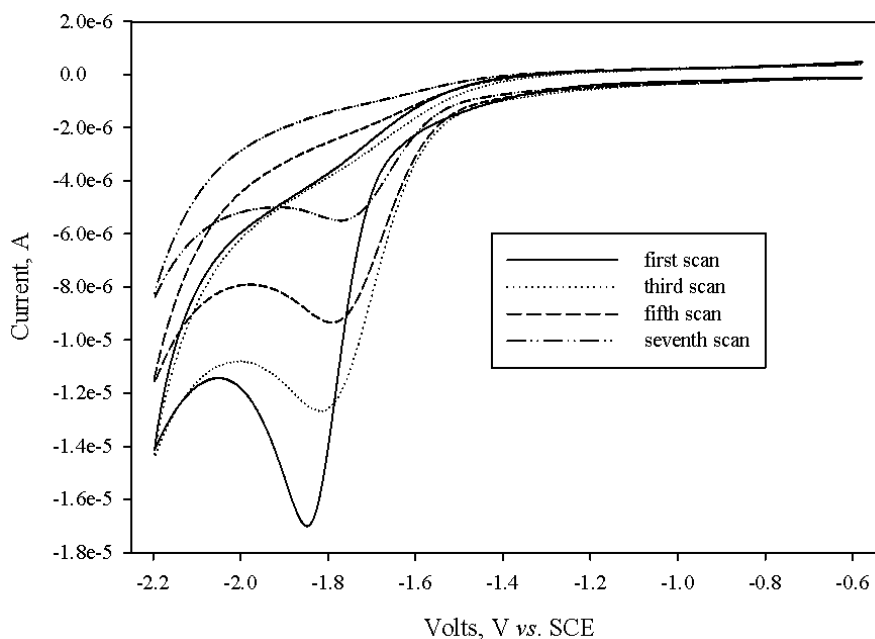


Figure 24. CVs of the desorption of 5-(8-sulphydryloctyl)salicylaldehyde on gold. Cyclic voltammograms of 5-(8-sulphydryloctyl)salicylaldehyde on gold in DMF containing 0.05 M TMABF₄ at 100 mV/s. The CVs show the desorption of monolayer into the solution with continuous scans. $Q = 4.41 \times 10^{-6}$ C and estimated surface coverage $\Gamma = 3.64 \times 10^{-10}$ mol/cm².

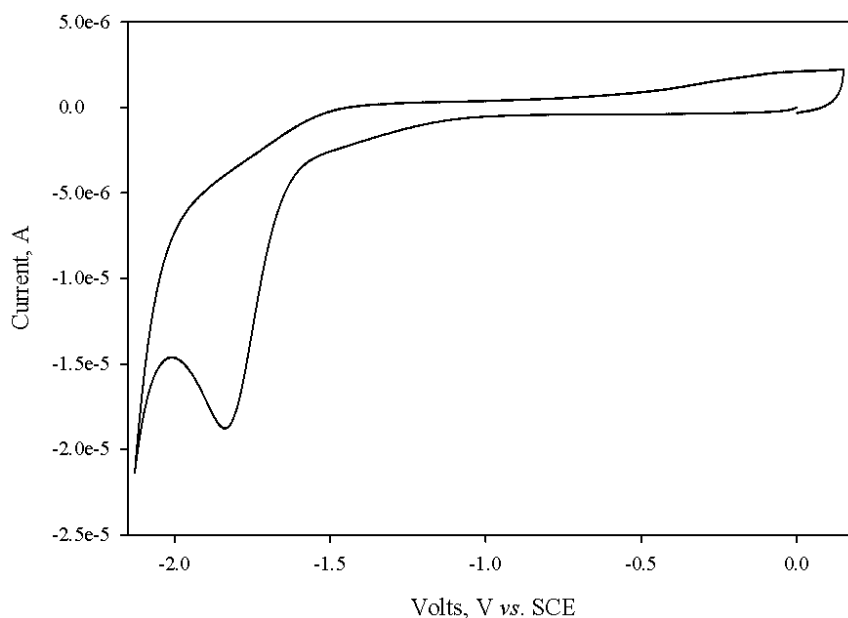


Figure 25. CV of the desorption of 5-(8-sulphydryloctyl)salicylaldehyde on gold (first scan/expanded scan window). Cyclic voltammogram of 5-(8-sulphydryloctyl)salicylaldehyde on gold in DMF containing 0.05 M TMABF₄ at 100 mV/s. 5-(8-Sulphydryloctyl)salicylaldehyde was assembled onto a submerged bare gold electrode from a 4.23 mM chloroform solution for 37 hours. The reductive desorption potential for the first sweep is -1.84 V vs. SCE and the anodic dimerization occurs at -0.07 V vs. SCE.

Figure 25 illustrates the desorption of a 5-(8-sulfhydryloctyl)salicylaldehyde film from gold after 37 hours of submersion in a 4.23 mM thiol solution. The reduction peak current and potential are similar to the data for 64 hours of coating time. However, scanning more positively after desorption gives a small anodic peak at -0.07 V vs. SCE, which maybe the evidence for the irreversible anodic dimerization of radical anions to form the disulfide through a two-electron process. These results are similar to those previously reported for the self-assembly of diphenyl disulfide and thiophenol onto gold.⁵⁴ On the other hand, since this anodic peak is very small, it is also possible that the alkylthiolate anions may slowly readsorb on the gold electrode as the current of the reductive process would noticeably increase between repeating scans if there are several minutes of interval.

3.2.2. [Nickel(II)salen] C_n SH films.— A bare gold electrode was submerged in 3.94 mM nickel(II) salen dissolved in DMF for 43 hours and tested in DMF containing 0.05 M TMABF₄. Figure 26 shows that nickel(II) salen does not bind to the Au surface by itself. A DMF solution saturated with a catalyst mixture of approximately 10% [nickel(II)salen] C_n SH and 90% nickel(II) salen was also used to coat the gold electrode *via* self-assembly. Figure 27 depicts the typical positive CV scans for the immobilized [nickel(II)salen] C_6 S-Au film. The anodic peak at $+0.86$ V decreases significantly after first scan and the oxidation is an irreversible process. Since nickel(II) salen can electrochemically polymerize on the electrode surface in aprotic organic solvents *via* oxidation, this CV response is likely due to the electrochemical chain polymerization of nickel(II) salen immobilized on gold.^{36,38} Because DMF has a high solvent coordination ability, it also stabilizes the nickel salen catalyst in an octahedral complex by axial

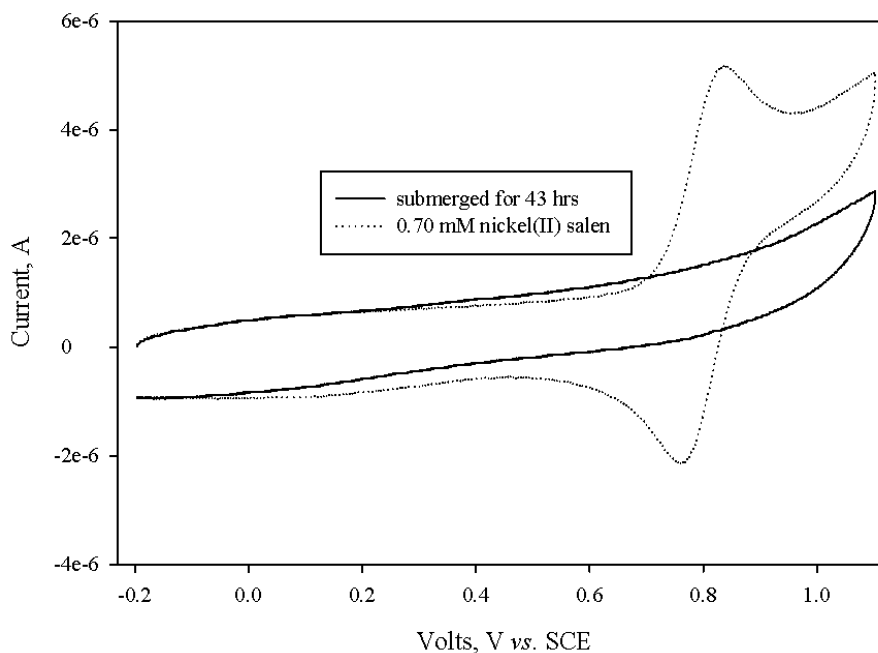


Figure 26. CV for a gold electrode after submerged in DMF containing nickel(II) salen. Cyclic voltammogram for gold electrode in DMF containing 0.05 M TMABF₄ at 100 mV/s after submerged in 3.94 mM nickel(II) salen dissolved in DMF for 43 hours (solid). The dotted line is the cyclic voltammogram of 0.70 mM nickel(II) salen.

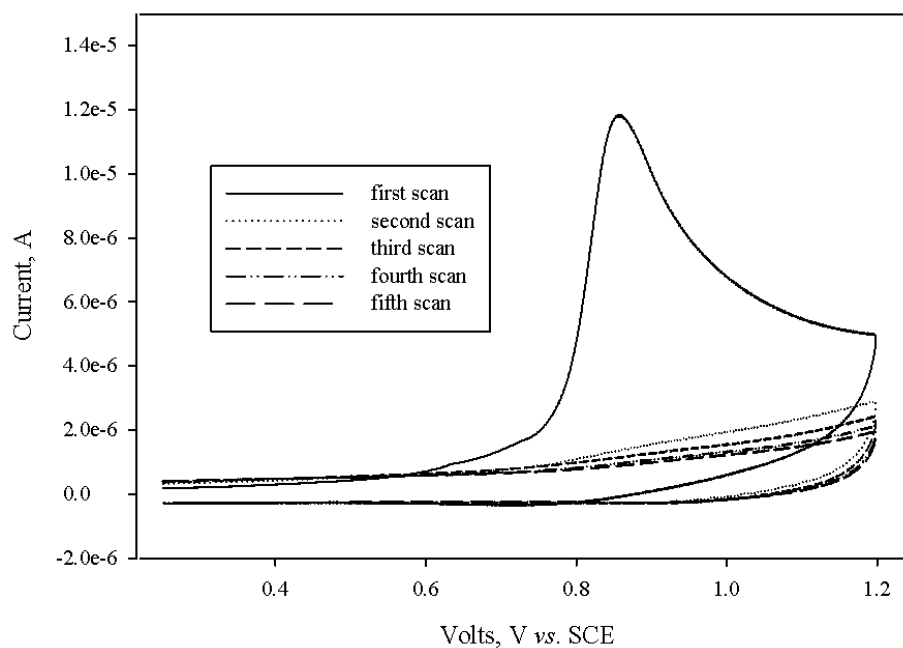


Figure 27. CVs of the electrochemical chain polymerization of a [nickel(II)salen]C₆S-Au film. Cyclic voltammograms from +0.25 to +1.20 V vs. SCE showing oxidative electrochemical chain polymerization of a [nickel(II)salen]C₆S-Au film in DMF containing 0.05 M TMABF₄ at 100 mV/s where the anodic potential of the first sweep is +0.86 V vs. SCE. A bare gold electrode was submerged for four days in a DMF solution saturated with 10% [nickel(II)salen]C₆SH and 90% nickel(II) salen prior to the CVs.

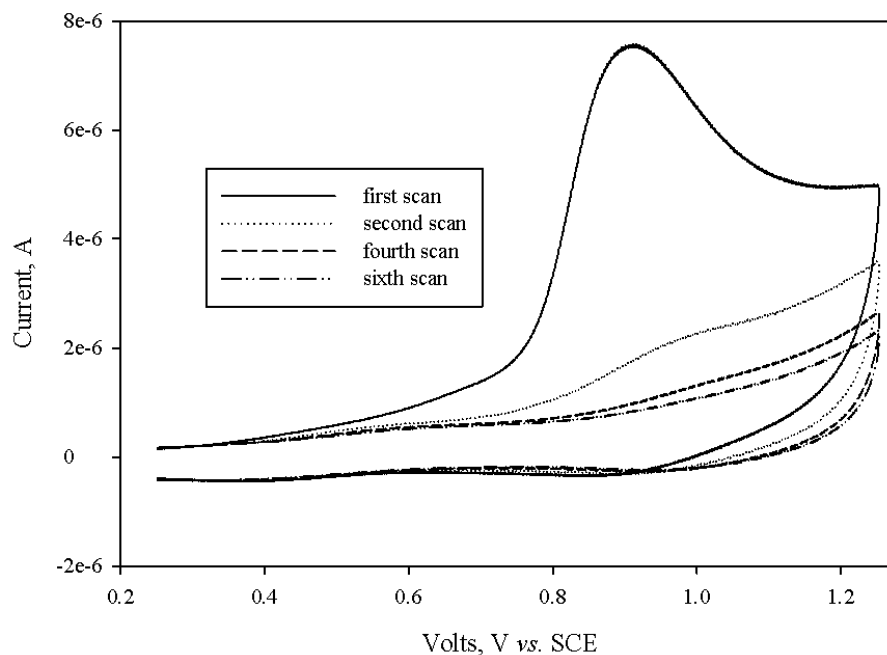


Figure 28. CVs of the electrochemical chain polymerization of a [nickel(II)salen] C_8S -Au film. Cyclic voltammograms from +0.25 to +1.25 V vs. SCE showing oxidative electrochemical chain polymerization of [nickel(II)salen] C_8S -Au film in DMF containing 0.05 M $TMABF_4$ at 100 mV/s where the anodic potential of the first sweep is +0.91 V vs. SCE. A bare gold electrode was submerged for one week in a DMF solution saturated with a mixture of 10% [nickel(II)salen] C_8SH and 90% nickel(II)salen prior to the CVs.

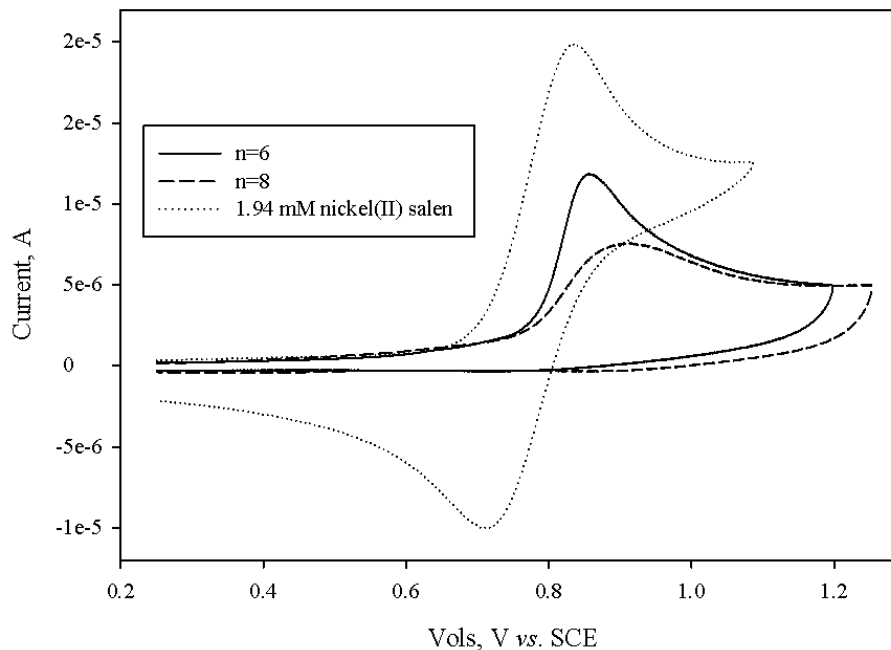


Figure 29. CVs of the electrochemical chain polymerization of [nickel(II)salen] C_nS -Au films vs. nickel(II) salen in DMF. Cyclic voltammograms from +0.25 to +1.25 V vs. SCE showing oxidative electrochemical chain polymerization of [nickel(II)salen] C_6S -Au film (solid) and [nickel(II)salen] C_8S -Au film (dashed) in DMF containing 0.05 M $TMABF_4$ at 100 mV/s. The dotted line is the CV 1.94 mM nickel(II) salen in DMF containing 0.05 M $TMABF_4$ at 100 mV/s.

ligation.^{36,38} This effect usually makes close-packed stack polymerization impossible, but does not impede chain polymerization since the phenolic portion of the ligand is free of substituents at the ortho and para positions.^{36,38} Stack polymerization is also less possible due to the orientation of the catalyst molecules in the SAMs on gold. Thus, chain polymerization is more likely to take place and following this process a more negative redox CV peak is observed for the reduction of polymerized film (Figures 31 and 32). The same behavior can also be observed for [nickel(II)salen] C_nS -Au films with an anodic CV potential at +0.91 V vs. SCE (Figure 28). Both of these anodic potentials are slightly

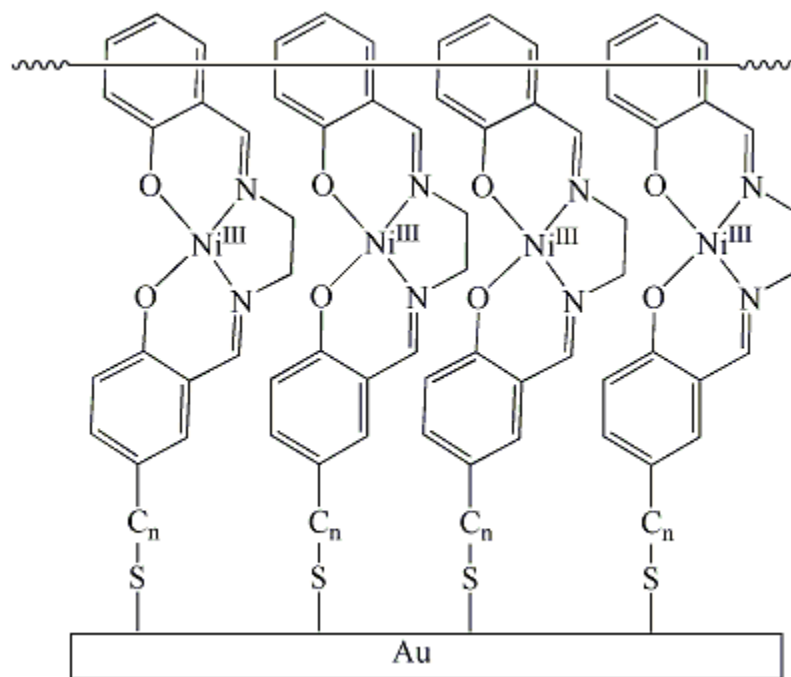


Figure 30. Electrochemical chain polymerization of a [nickel(II)salen] C_nS -Au film in DMF. An illustration of a poly[(nickel(II)salen)] C_nS -Au film on a gold working electrode after the electrochemical chain polymerization through the ortho and para positions of the exposed ligand.

more positive than the free nickel(II) salen-nickel(III) salen couple at +0.77 V vs. SCE, a characteristic behavior for a metal complex that is bound to electrode surface (Figure 29).⁸⁶ The proposed structure of the polymer, poly[(nickel(II)salen)] C_nS -Au, is illustrated in Figure 30.

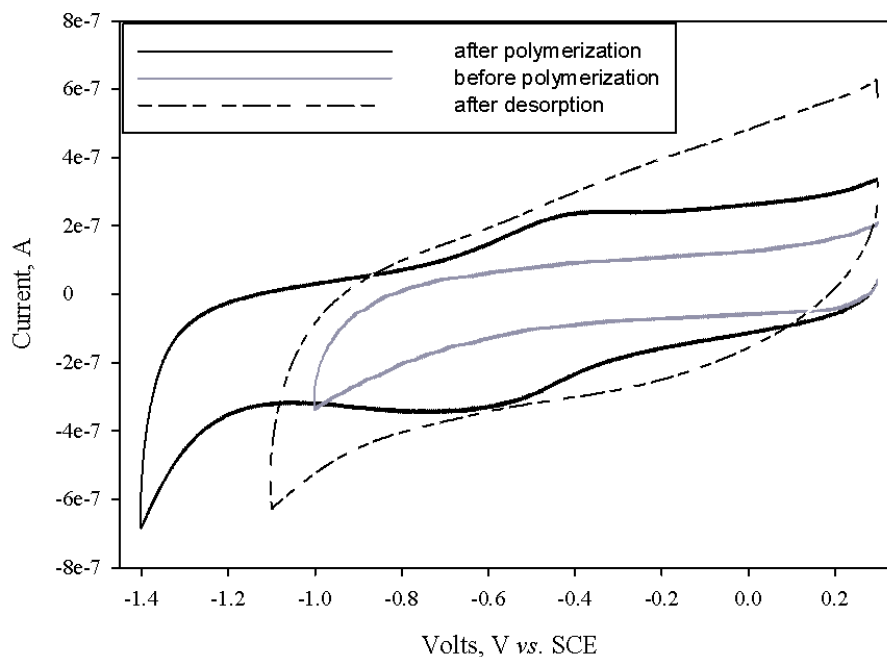


Figure 31. CV of the reduction of poly[nickel(II)salen]C₆S-Au film. Cyclic voltammogram from +0.25 to -1.40 V vs. SCE showing the reduction of poly[nickel(II)salen]C₆S-Au film (solid) in DMF containing 0.05 M TMABF₄ at 100 mV/s (solid) where the redox potential is at -0.56 V vs. SCE. Also shown is the CVs before polymerization (gray) and after desorption (dashed) of the catalyst.

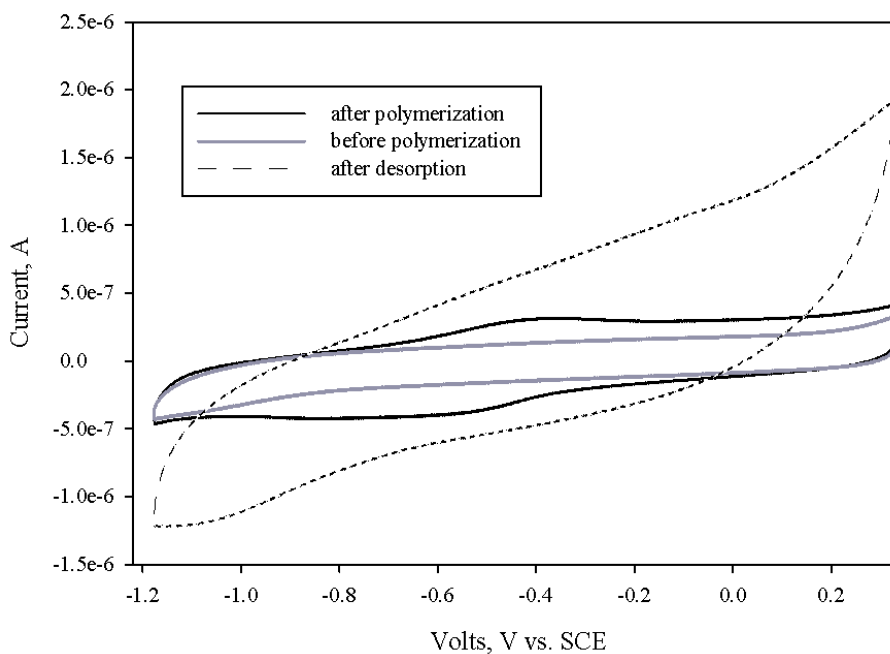


Figure 32. CV of the reduction of poly[nickel(II)salen]C₈S-Au film. Cyclic voltammogram from +0.25 to -1.20 V vs. SCE showing the reduction of poly[nickel(II)salen]C₈S-Au film (solid) in DMF containing 0.05 M TMABF₄ at 100 mV/s where the redox potential is -0.56 V vs. SCE. Also shown is the CVs before polymerization (gray) and after desorption (dashed) of the catalyst.

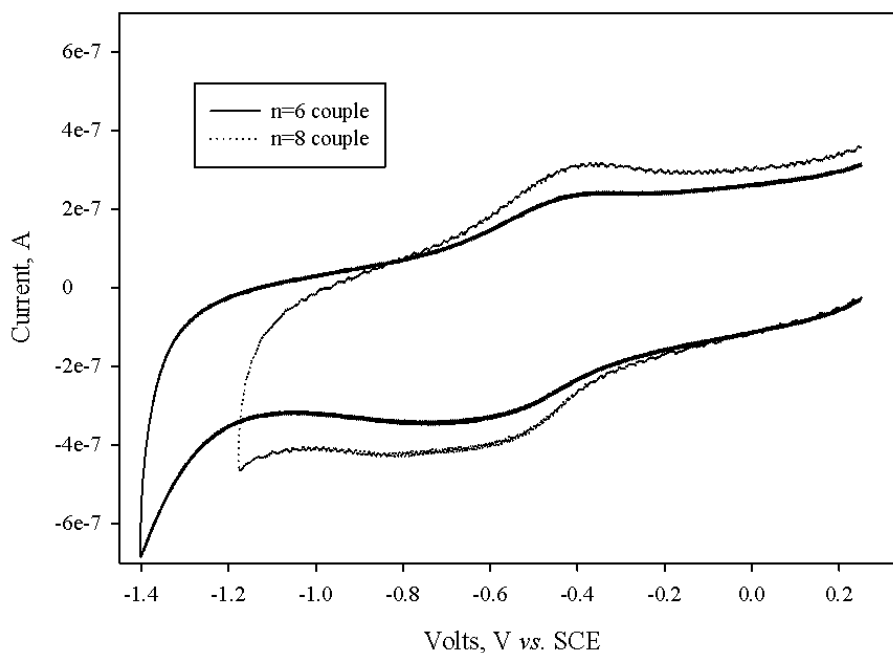


Figure 33. CVs of the reduction of poly[nickel(II)salen] C_n S-Au films. Cyclic voltammograms showing the reduction of poly[nickel(II)salen] C_6 S-Au film (solid) and poly[nickel(II)salen] C_8 S-Au film (dotted) in DMF containing 0.05 M TMABF₄ at 100 mV/s.

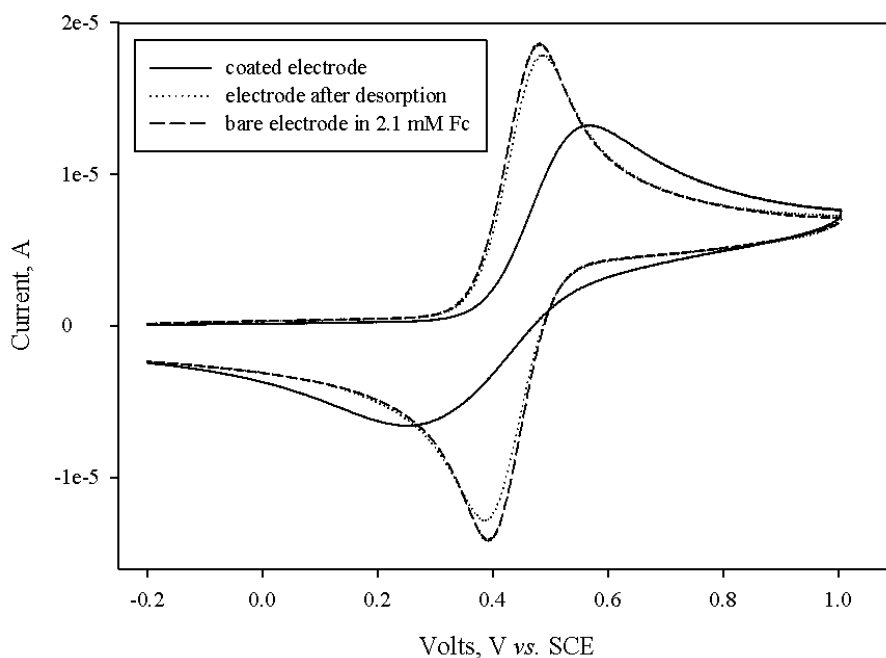


Figure 34. CVs of ferrocene in DMF before and after desorption of poly[nickel(II)salen] C_6 S-Au film. Cyclic voltammograms of 2.1 mM ferrocene in DMF containing 0.05 M TMABF₄ at (a) bare gold electrode and the surface-modified gold electrode (b) before or (c) after the desorption of poly[nickel(II)salen] C_6 S-Au film with a scan rate of 100 mV/s. The larger peak separation with decreased peak current for the ferrocene(II)-ferrocene(III) couple in curve (b) indicates that a film is present on the gold surface.

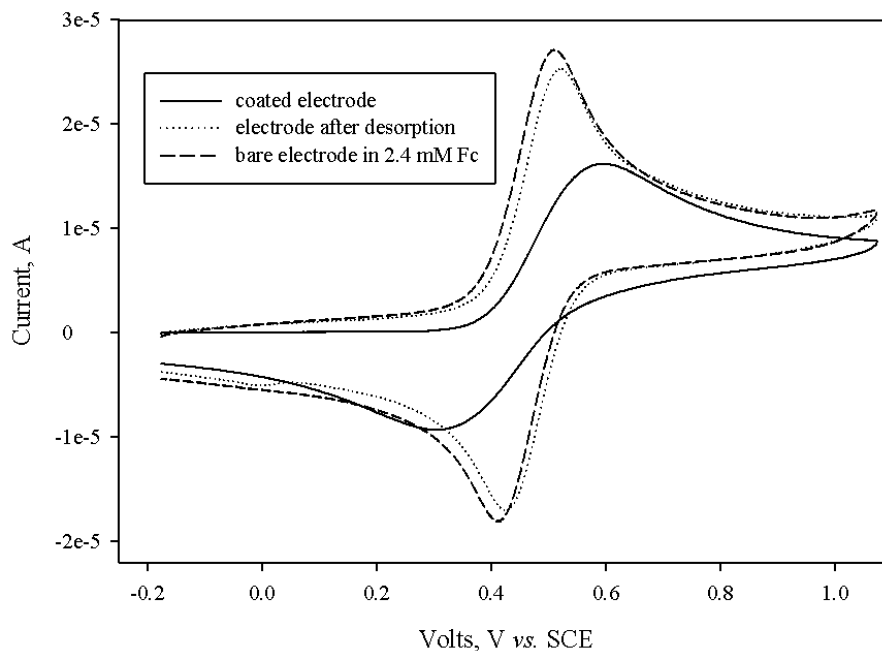


Figure 35. CVs of ferrocene in DMF before and after desorption of poly[nickel(II)salen] C_8S -Au film. Cyclic voltammograms of 2.4 mM ferrocene in DMF containing 0.05 M $TMABF_4$ at (a) bare gold electrode and the surface-modified gold electrode (b) before or (c) after the desorption of poly[nickel(II)salen] C_8S -Au film with a scan rate of 100 mV/s.

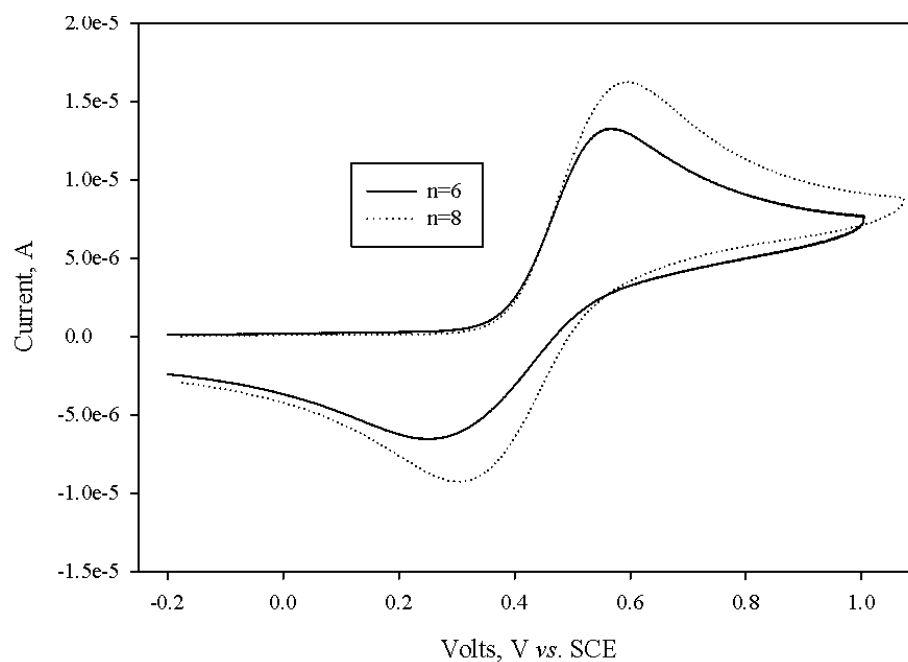


Figure 36. CVs of ferrocene in DMF before desorption of poly[nickel(II)salen] C_nS -Au films. Cyclic voltammograms of 2.1 mM and 2.4 mM ferrocene in DMF containing 0.05 M $TMABF_4$ at the surface-modified gold electrode before the desorption of poly[nickel(II)salen] C_6S -Au film (solid) and poly[nickel(II)salen] C_8S -Au film (dotted) with a scan rate of 100 mV/s.

Prior to polymerization of the nickel salen catalyst on the gold surface, the negative CV scan before the desorption of the film was taken but no electrochemical activity was detected in this region (Figures 31-32). However, after polymerization both films gave rise to a redox couple at -0.56 V vs. SCE with similar currents (Figure 33). This reversible peak could be assigned to the reduction of polymerized nickel salen. For a metal complex that is bound to an electrode surface, ideally the ΔE_p between the redox peak potentials is zero, though deviation is commonly observed in experiments. This phenomenon can be attributed to (1) a change in solvation of the redox molecule, (2) a change in intermolecular interactions between the redox centers, or (3) structural alteration of the monolayer according to Nielson et al.⁴¹ Since chain polymerization can occur, it may bring out nonideal conditions on the surface to cause this distortion in CV. Furthermore, this result suggests that the immobilized catalyst not be capable of reducing many organohalides, which usually takes place at much more negative potentials.²⁶ Our data also shows that after desorption of the alkylthiolate monolayer, the redox couple at -0.56 V disappears, indicating that this CV signal is directly related to the monolayer and specifically the polymerized nickel salen on gold electrode.

Figures 34-36 illustrate the effect of the coated gold electrodes on the CVs of ferrocene dissolved in DMF containing 0.05 M TMBF₄. For both poly[nickel(II)salen] modified gold electrodes, the peak separation of the Fc(II)-Fc(III) redox couple increases with decreased currents, strongly suggesting that the film act as a blocking layer on the surface. Figure 34 and 35 also show that the reversibility of ferrocene can be restored after the desorption process. These results demonstrate that both modified gold electrodes have ordered films (though not very dense) covering the surface.⁹⁵ Figures 37-

40 show the desorption of poly[nickel(II)salen]C_nS-Au films in DMF containing 0.05 M TMABF₄ with the reductive desorption peaks at -2.04 and -2.02 V vs. SCE, respectively. The continuous CV scans show a decrease in the current and a positive potential shift, indicating desorption of the monolayer.⁵¹ Figure 39 also gives each of the three characteristics involved in the desorption of poly[nickel(II)salen]C₆S-Au films: the reductive desorption, the readsorption of alkylthiolate anions at -1.64 V vs. SCE, and the dimerization of the anions at -0.02 V vs. SCE.^{54,82,94} However, the readsorption process is less obvious for poly[nickel(II)salen]C₈S-Au film and the reason is not clear at this point (Figure 40).

In order to determine which film is more ordered, the peak currents for polymerization (Figure 29) and desorption (Figure 40) of each film are compared, and the estimated surface coverage of the polymer films is calculated. It is ideal that longer alkane chain length should afford more densely packed films. At first glance, the larger current indicates that more [nickel(II)salen]C₆SH may assemble on gold over the allotted time in our case.⁷⁷ To confirm this, both desorption processes were integrated to obtain the charge Q to calculate an estimated surface coverage Γ for the polymerized films (see Figures 37 and 38). The estimated surface coverage Γ for poly[nickel(II)salen]C₆S-Au and poly[nickel(II)salen]C₈S-Au films are 5.64×10^{-11} and 3.11×10^{-11} mol/cm², respectively indicating that poly[nickel(II)salen]C₆S-Au developed a slightly more ordered polymerized film. Since the alkylthiolate film development is affected by several factors and significantly by concentration of the catalyst in the coating solution, it is likely that the lower solubility of [nickel(II)salen]C₈SH in DMF causes this discrepancy.^{51,77} Finally, the robustness of poly[nickel(II)salen]C₆S-Au film

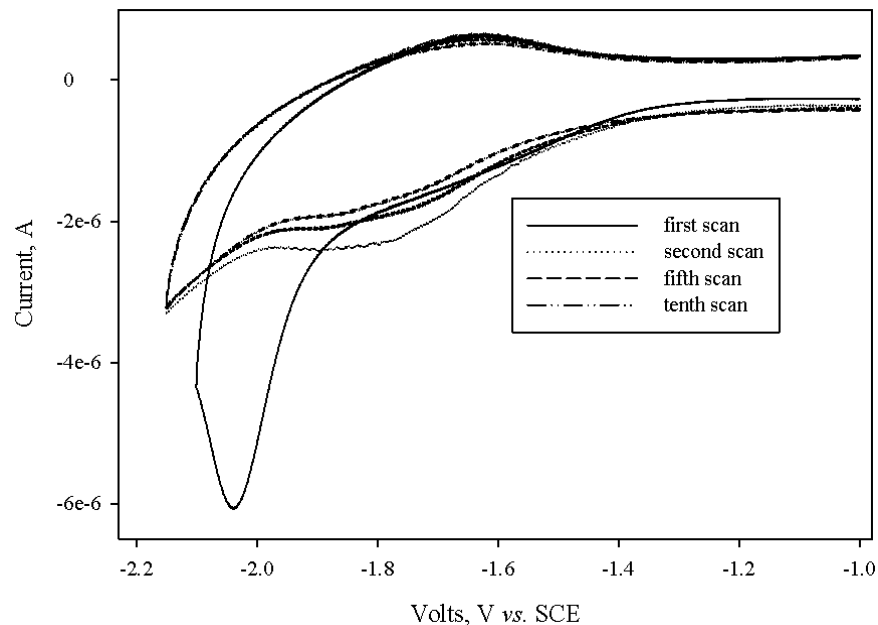


Figure 37. CVs of the desorption of poly[nickel(II)salen] C_6S -Au film in DMF. Cyclic voltammograms from -1.00 to -2.15 V vs. SCE showing the desorption of poly[nickel(II)salen] C_6S -Au film in DMF containing 0.05 M $TMABF_4$ at 100 mV/s. The reductive desorption potential of the first sweep is -2.04 V vs. SCE. $Q = 6.84 \times 10^{-7}$ C. The estimated surface coverage Γ for poly[nickel(II)salen] C_6S -Au is 5.64×10^{-11} mol/cm 2 .

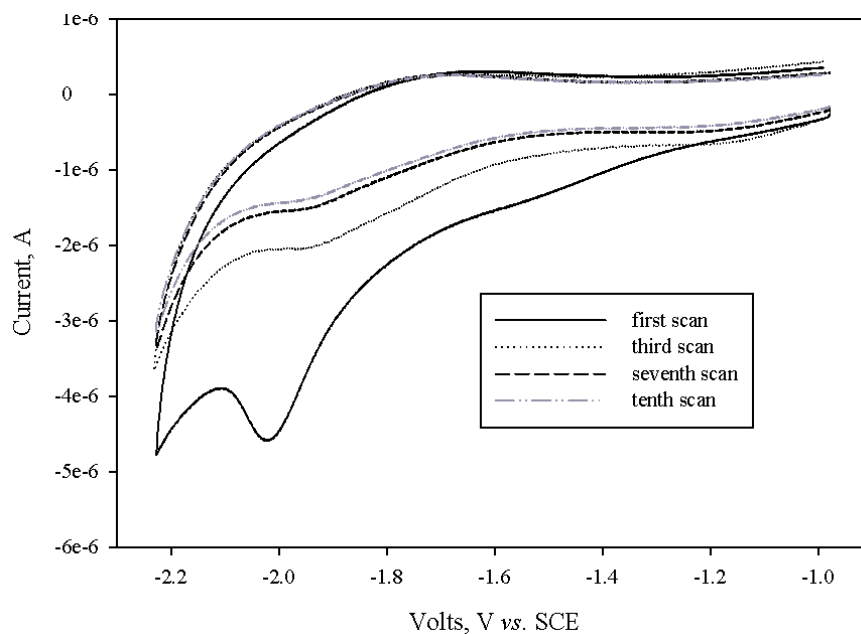


Figure 38. CVs of the desorption of poly[nickel(II)salen] C_8S -Au film in DMF. Cyclic voltammograms from -1.00 to -2.23 V vs. SCE showing the desorption of poly[nickel(II)salen] C_8S -Au film on gold in DMF containing 0.05 M $TMABF_4$ at 100 mV/s. The reductive desorption potential of the first sweep is -2.02 V vs. SCE. $Q = 3.77 \times 10^{-7}$ C. The estimated surface coverage Γ for poly[nickel(II)salen] C_6S -Au is 3.11×10^{-11} mol/cm 2 .

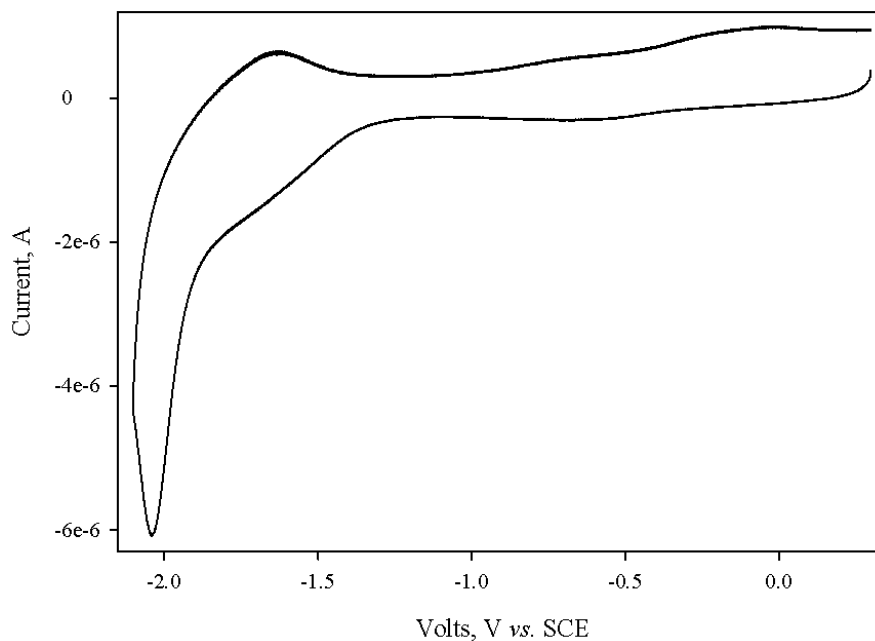


Figure 39. CV of the desorption of poly[nickel(II)salen]C₆S-Au film in DMF (first scan/expanded scan window). Cyclic voltammogram from +0.30 to -2.15 V vs. SCE showing the desorption of poly[nickel(II)salen]C₆S-Au film on gold in DMF containing 0.05 M TMABF₄ at 100 mV/s in four segments. Readsorption of alkylthiolate anions is observed as an anodic peak at -1.64 V vs. SCE. Dimerization of the anions occurs at -0.02 V vs. SCE.

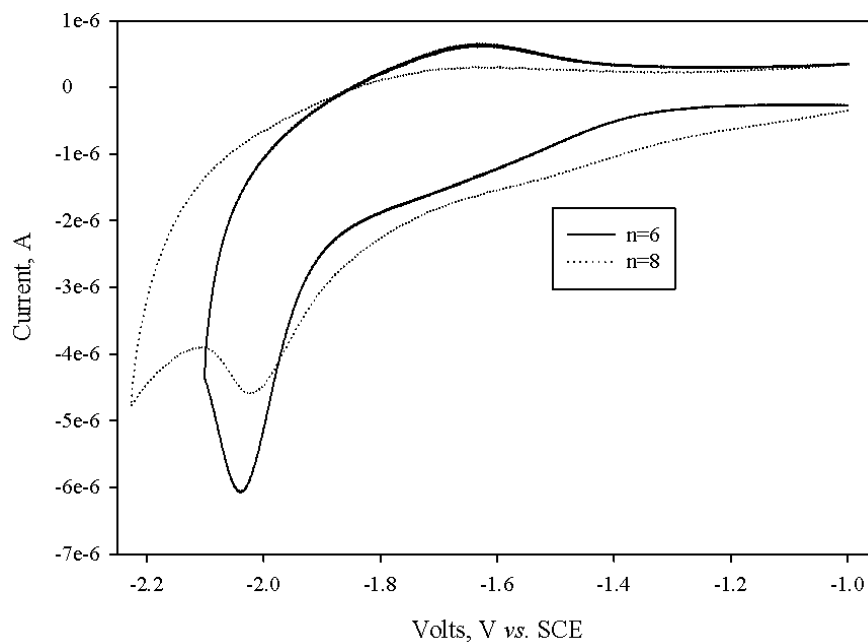


Figure 40. CVs of the desorption of poly[nickel(II)salen]C_nS-Au films in DMF. Cyclic voltammograms from -1.0 to -2.23 V vs. SCE showing the desorption of poly[nickel(II)salen]C₆S-Au film (solid) and poly[nickel(II)salen]C₈S-Au film (dotted) in DMF containing 0.05 M TMABF₄ at 100 mV/s.

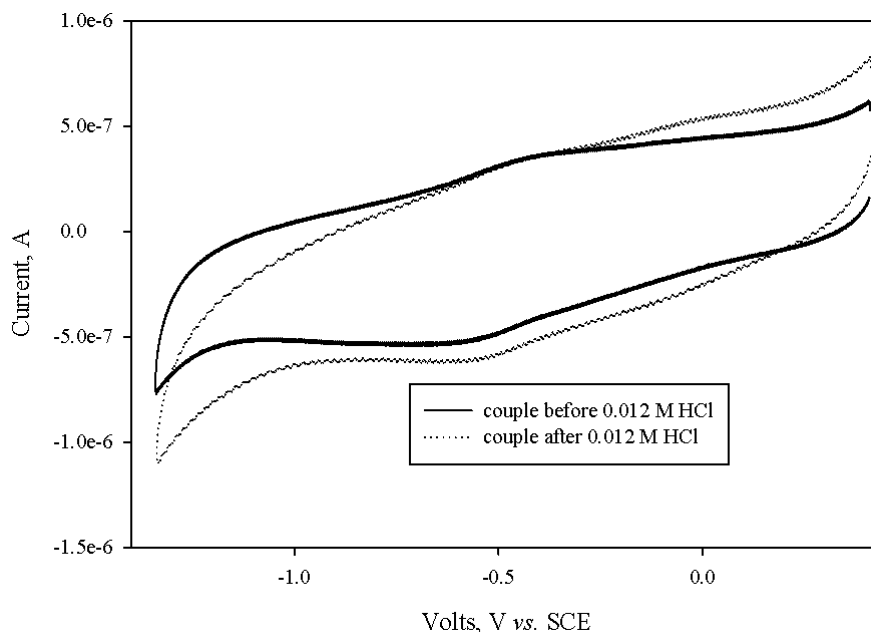


Figure 41. CVs of the reduction of poly[nickel(II)salen] C_6S -Au film before and after treatment with **0.012 M HCl**. Cyclic voltammograms from +0.41 to -1.34 V vs. SCE showing poly[nickel(II)salen] C_6S -Au film in DMF containing 0.05 M $TMABF_4$ at 100 mV/s before (solid) and after (dotted) treatment with 0.012 M HCl for 24 hours.

was tested by submerging the coated electrode in 0.012 M aq. HCl for overnight and collecting the CV afterwards (Figure 41). After 24 hours, the polymer film remained on the gold electrode surface as the redox couple at -0.56 V was still detectable, indicating the film can stand low acidic concentrations.

3.2.3. Final remarks.— In conclusion, 5-(6-sulphydrylhexyl)salicylaldehyde and 5-(8-sulphydryloctyl)salicylaldehyde were synthesized and self-assembled on gold working electrode for CV analysis. It was found that their SAM films only slightly affect the diffusion of ferrocene to the electrode surface and the corresponding desorption process in DMF gives characteristic CV features. These two compounds were also used to synthesize [nickel(II)salen] C_6SH and [nickel(II)salen] C_8SH to be self-assembled on gold working electrode for CV analysis. It was shown that both [nickel(II)salen] C_nS -Au films could undergo electrochemical chain polymerization to form poly[nickel(II)

salen]C_nS-Au films. These polymerized films can more efficiently block the diffusion of ferrocene to the electrode surface and are stable in slightly acidic solutions. Moreover, the polymerized films give a redox peak at -0.56 V vs. SCE, indicating that the surface-modified Au electrode could be used for detection of some substrates *via* electrocatalytic oxidation or reduction. Finally, the desorption process for the polymer films can also be detected in the CV in DMF.

3.3. Future Research.— For future research, there are many other aspects that could be further examined. Some are the following: (1) isolation and analytical characterization of pure [nickel(II)salen]C₆SH and [nickel(II)salen]C₈SH, (2) synthesis of [cobalt(II) salen]C₆SH and [cobalt(II)salen]C₈SH, (3) synthesis of symmetrical disulfides from 5-(ω -sulfhydrylalkyl)salicylaldehydes in high yield to make the catalyst [metal(II)salen]C_nS-SC_n[metal(II)salen], and (4) development of “bulky” metal salens or salophens by using specially designed ethylenediamine and salicylaldehyde derivatives. Aspects 3 and 4 will be discussed in detail.

3.3.1. Proposed changes to methodology for [nickel(II)salen]C_nS-Au film development.— To obtain well coated [nickel(II)salen]C_nS-Au films consistently could be rather difficult through direct synthesis and self-assembly by the method discussed in this thesis. The low amount of the [nickel(II)salen]C_nSH present in the synthesized mixture and its low solubility in DMF make the coating process take a long period of time. Moreover, the immobilized films are less predictable and comparable due to the uncertain amounts of the catalysts dissolved in DMF. An alternative method should be developed so that [nickel(II)salen]C_nSH films on gold electrode can be formed more

easily for electrochemical studies. The following sections will discuss two possible routes where the concentration of the catalyst in solution might be controlled for future research.

3.3.2. [Metal salen] disulfides.— Oxidation of sulfhydryl groups is synthetically important for the formation of disulfides.⁹⁶ It is particularly interesting to oxidize 5-(ω -sulfhydrylalkyl)salicylaldehydes because various asymmetrical and symmetrical dialkyl disulfides can assemble efficiently on a gold surface at room temperature.⁹⁷ Symmetrical disulfides from 5-(ω -sulfhydrylalkyl)salicylaldehydes, which have not been previously synthesized, should also be able to assemble on gold to form an analogous gold-alkylthiolate monolayer because unlike thiols, the disulfides are much less prone to air oxidation and therefore easier to isolate or purify.⁸¹ It could be an attractive starting material for the development of [metal salen] C_nS -Au films (see Figure 42).

To selectively oxidize 5-(ω -sulfhydrylalkyl)salicylaldehydes to a symmetrical disulfide, a method reported by Yiannios et al. could be employed. The disulfides could be synthesized using dimethylsulfoxide (DMSO) at 80 to 90°C in high yield (see Eq. 6).⁹⁸ The by-product dimethylsulfide could be converted back to DMSO upon exposure



to oxygen. The authors suggested that their method should not affect other oxidizable sites such as aldehyde or amino groups. Consequently, the synthesis of symmetrical disulfides from 5-(ω -sulfhydrylalkyl)salicylaldehydes might be possible using this methodology since salicylaldehyde has been shown to be stable in DMSO at 110°C for several hours.⁹⁹ On the basis of that, the disulfides could be employed as the precursors for making the new salen ligands (Figure 42). Since it has been shown that metal acetates

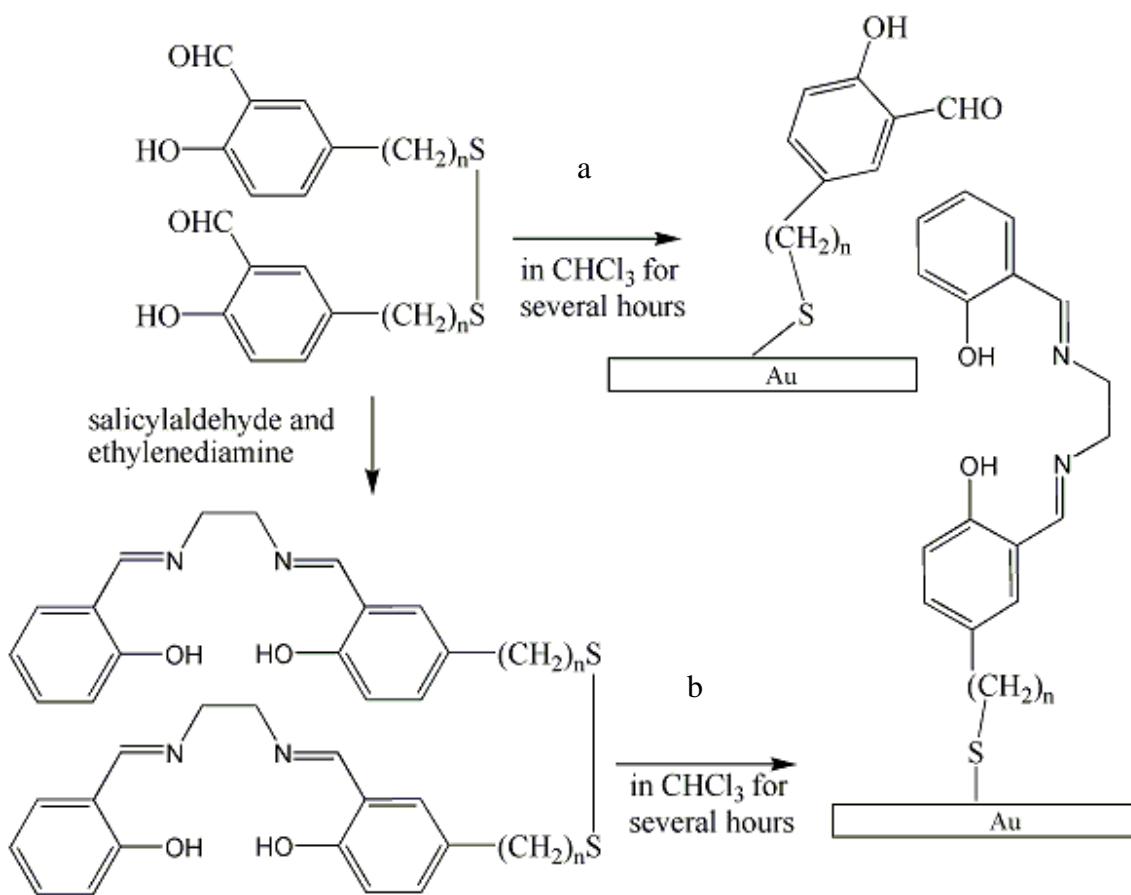


Figure 42. Proposed synthesis of salen ligand on gold using disulfides. An illustration of the proposed (a) symmetrical disulfides from 5-(ω -sulhydrylalkyl)salicylaldehydes and (b) corresponding salen ligand complexes and their self-assembly onto gold from chloroform.

and chlorides can be used to coordinate metal ions into self-assembled salen ligands on gold, this strategy might be helpful to develop consistent, well controlled, and very dense [metal salen] C_nS -Au films using a concentrated salen ligand solution.⁴¹

3.3.3. Proposed synthesis of new “bulky” salen and salophen ligands.— Nielson et al. reported the first example of thiol-derivatized salen complexes self-assembled onto gold via *p*-acylthio(phenylacetylene) $_n$ -substituted chiral salen ligands ($n=1$ and 2).⁴¹ Interestingly, they synthesized a free amine from the condensation reaction of commercially available (1*S*,2*S*)-1,2-diphenylethylenediamine and 3,5-di-*tert*-butylsalicylaldehyde (see Figures 43 and 44). A further 1:1 condensation reaction with *p*-

acylthio(phenylacetylene)_n derivatized salicylaldehyde would give the desired salen ligands.¹³ This was followed by deprotection of the sulfur, immobilization of the ligand, and metal coordination of the immobilized films to develop the surface-modified gold electrode.

As Figure 44 shows, several similar amines and their synthetic routes have also been published.¹⁰⁰⁻¹⁰¹ By synthesizing these amines and reacting them with 5-(ω-sulfhydrylalkyl)salicylaldehydes, pure salen or salophen ligands with an alkanethiol side chain could be obtained for self-assembly onto gold. The metal ions can be subsequently coordinated into the ligand film from a metal acetate solution. For example, reacting c in

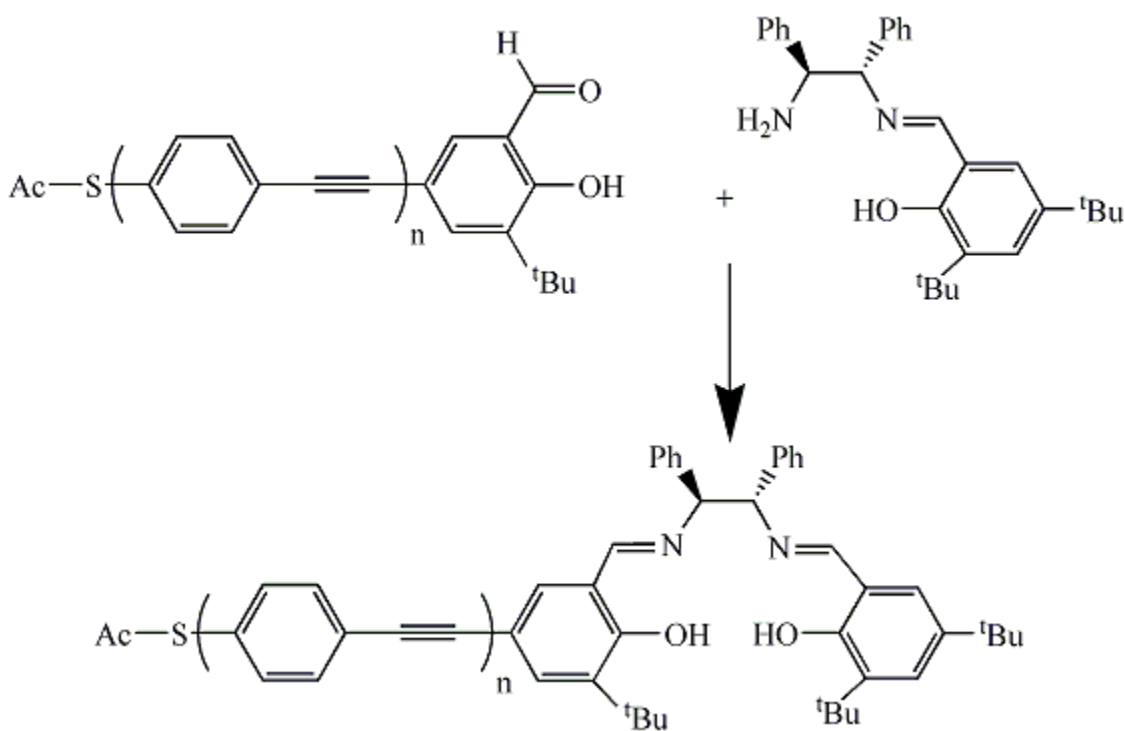


Figure 43. *p*-Acylthio(phenylacetylene)_n-substituted chiral salen ligands (*n*=1 and 2). A 1:1 condensation reaction with *p*-acylthio(phenylacetylene)_n derivatized salicylaldehyde and a free amine made desired salen ligands. From ref 41.

Figure 44 with 5-(ω-sulfhydrylalkyl)salicylaldehydes would likely lead to a high yield of a salophen ligand containing a single side alkanethiol side chain (Figure 45). Once

metallated, these films might still undergo polymerization like [nickel(II)salen] C_nS -Au films at the phenolic sites of the ligand since oxidative coupling is not inhibited as the ortho and para positions are free of substituents.^{36,38} However, by reacting a or b (Figure 44) with 5-(ω -sulfhydrylalkyl)salicylaldehydes, the corresponding chain polymerization

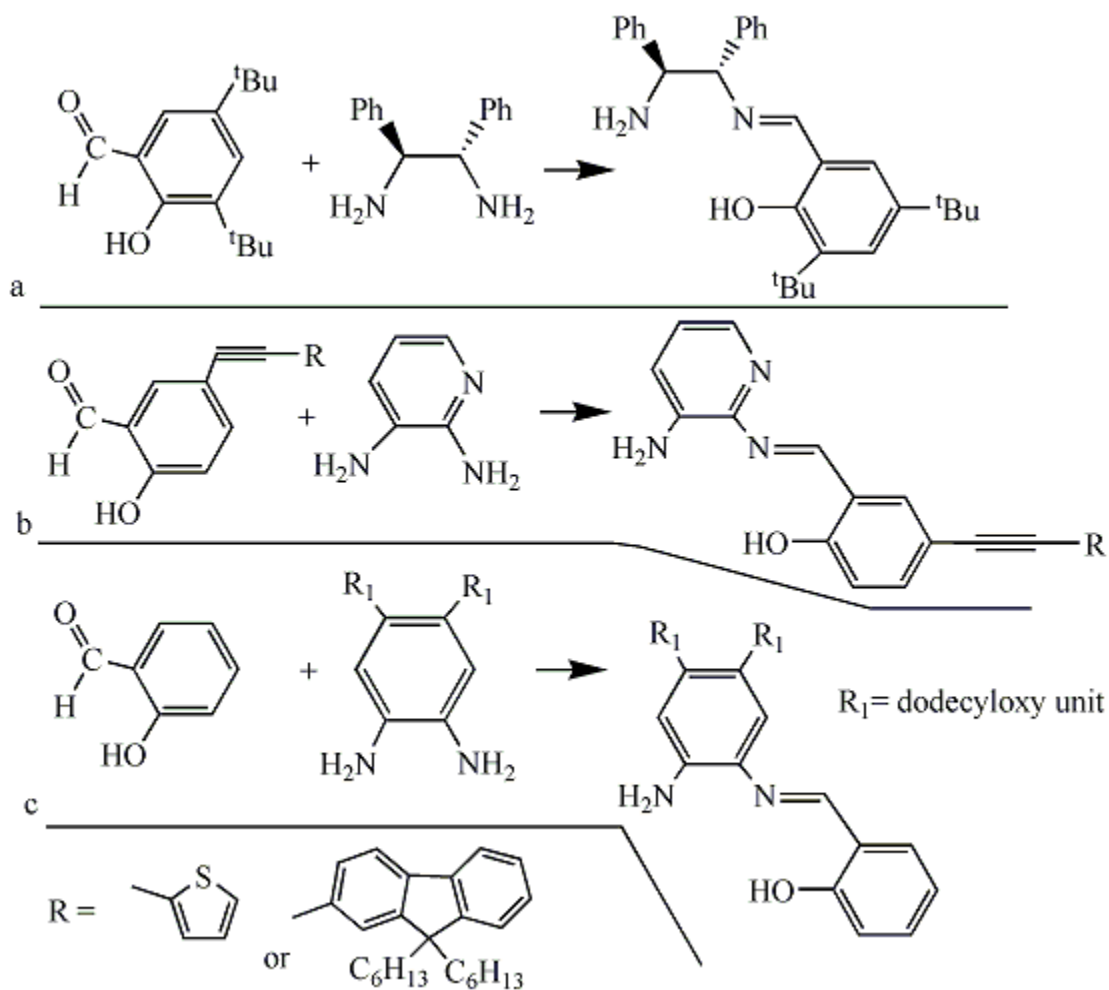


Figure 44. Several examples of syntheses of free amines from the condensation reaction of various diamines and salicylaldehydes. These can be used to synthesize salen and salophen ligands with an alkanethiol side chain *via* a 1:1 molar reaction. From ref. 41, 100, and 101.

of the film might be inhibited. Additionally, it would be interesting to see if 5-(ω -sulfhydrylalkyl)salicylaldehyde or their symmetrical disulfides could be assembled onto gold and used as a linker molecule to develop the catalyst SAMs in a stepwise fashion.

New “bulky” thiol-derivatized salen or salophen complexes synthesized by this methodology could be potentially used in various electrochemical applications.

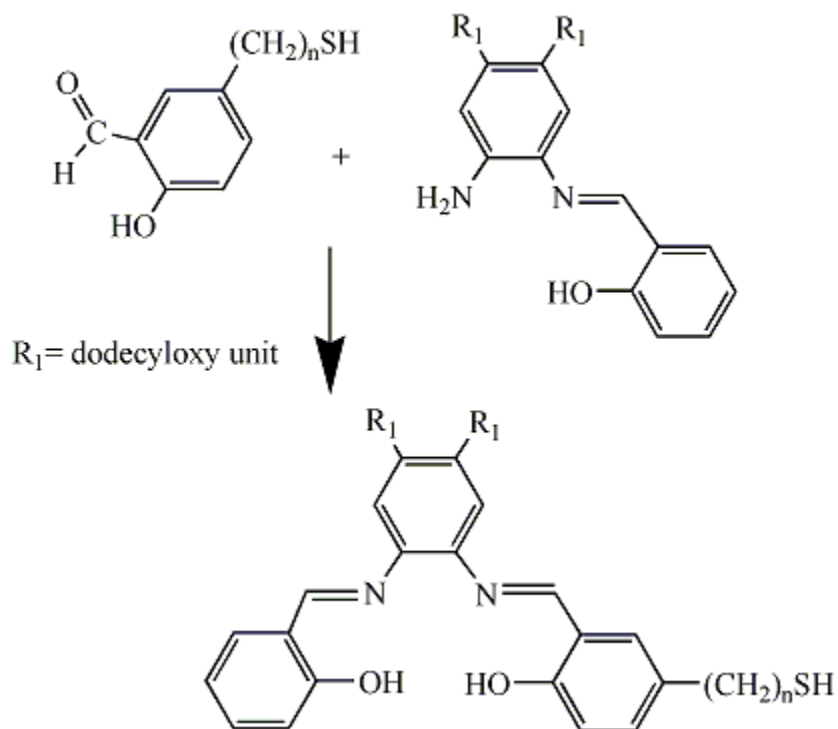
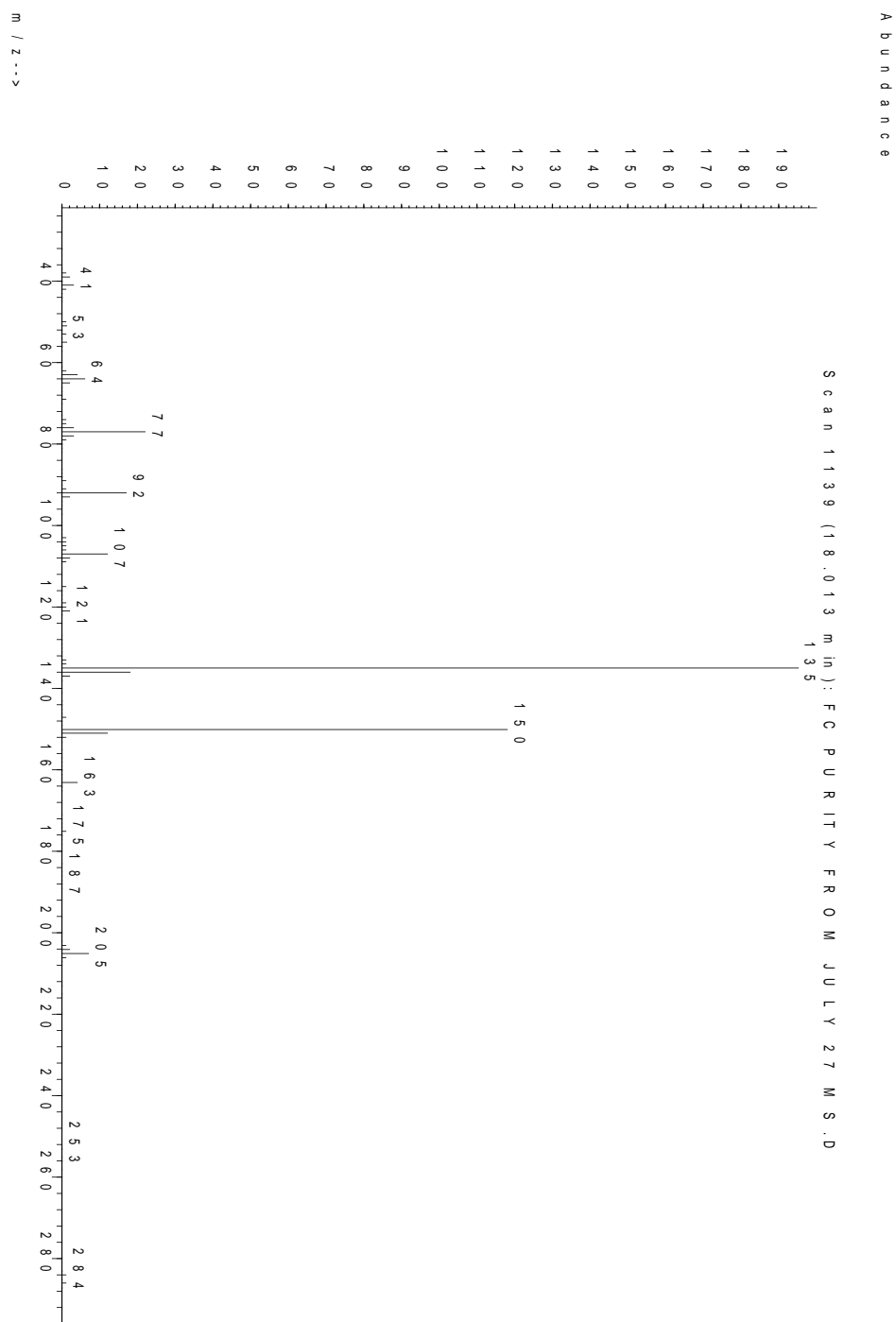


Figure 45. Proposed synthesis of salophen ligand with a single alkanethiol side chain. reacting c in Figure 44 with 5-(ω -sulfhydrylalkyl)salicylaldehydes would likely lead to a high yield of a salophen ligand containing a single side alkanethiol side chain.

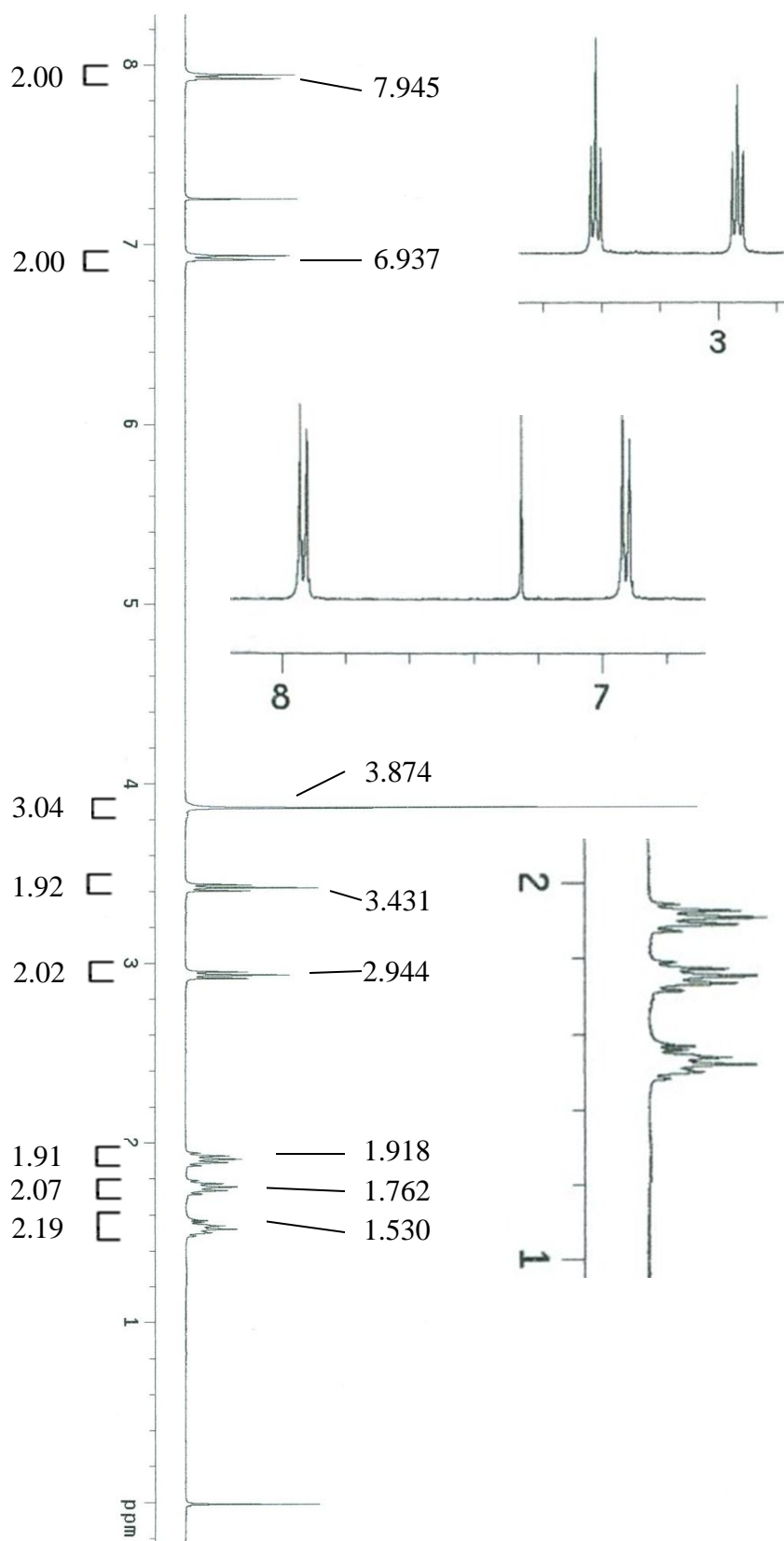
SUPPLEMENTAL MATERIAL

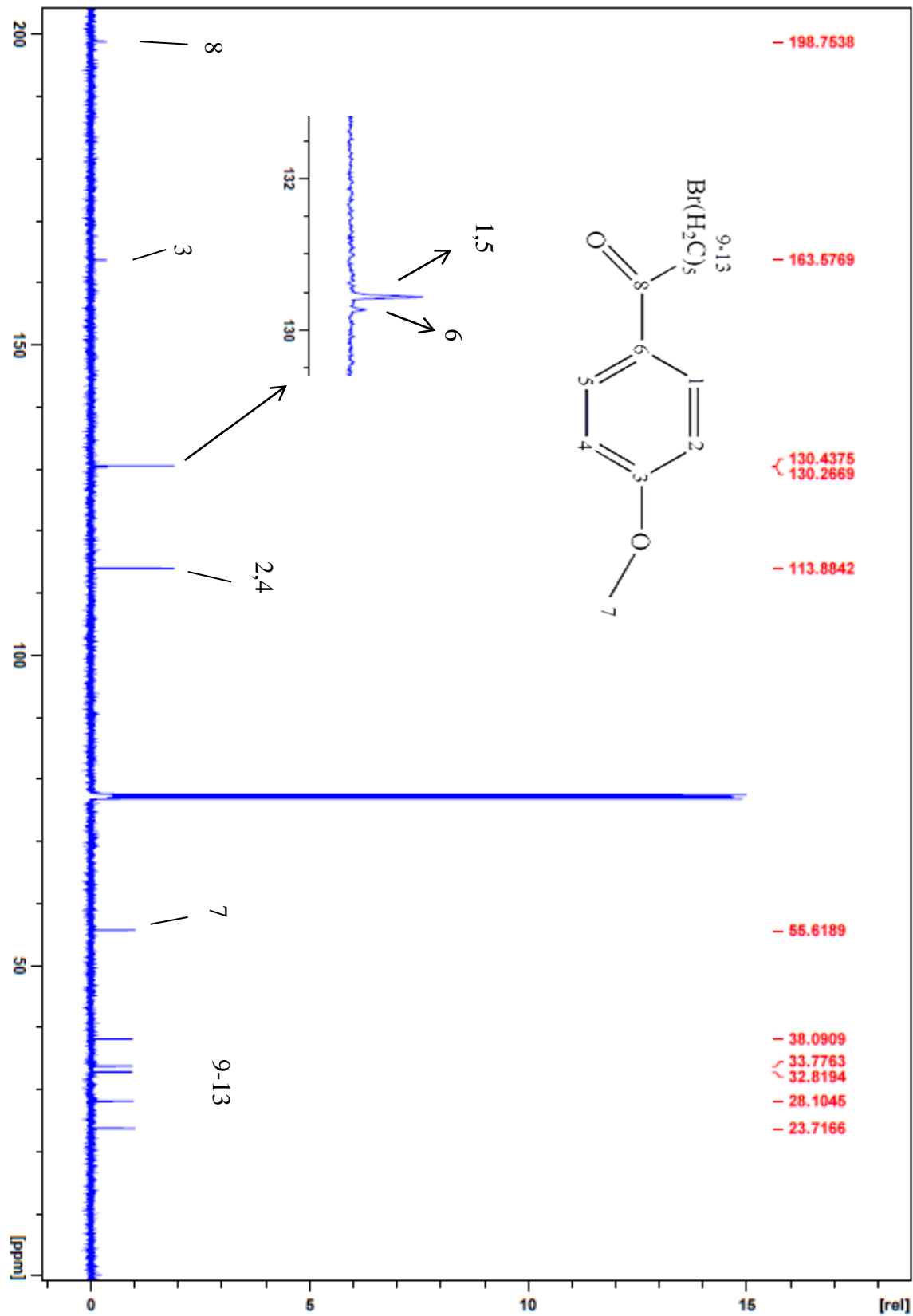
Before any NMR spectrum was collected, all ^1H and ^{13}C spectra were predicted using two software packages: (1) NMRShiftDB software that is available for free online through web-based java and software download and (2) Advanced Chemistry Development (ACD/Labs) Software V11.02 (© 1994-2011 ACD/Labs) available through SciFinder.^{102,103} All NMR spectra were obtained using deuterated chloroform containing 0.03% v/v TMS as the solvent. 1-(8-Bromooctyl)-4-methoxybenzene, the precursor of 5-(8-sulfhydryloctyl)salicylaldehyde, was the only compound that was analyzed solely using GC-MS because it was not purified. However, its NMR spectra should be very similar to that of 1-(6-bromohexyl)-4-methoxybenzene. DEPT NMR spectra were not obtained for any precursor of 5-(8-sulfhydryloctyl)salicylaldehyde. All major impurities in NMR spectra were identified and usually were water (^1H NMR (CDCl_3): 1.56 (s); ^{13}C NMR: none), acetone (^1H NMR (CDCl_3): 2.17 (s); ^{13}C NMR (CDCl_3): 207.07 (CO), 30.92 (CH_3)), residue solvents, preservatives, etc.^{104,105}

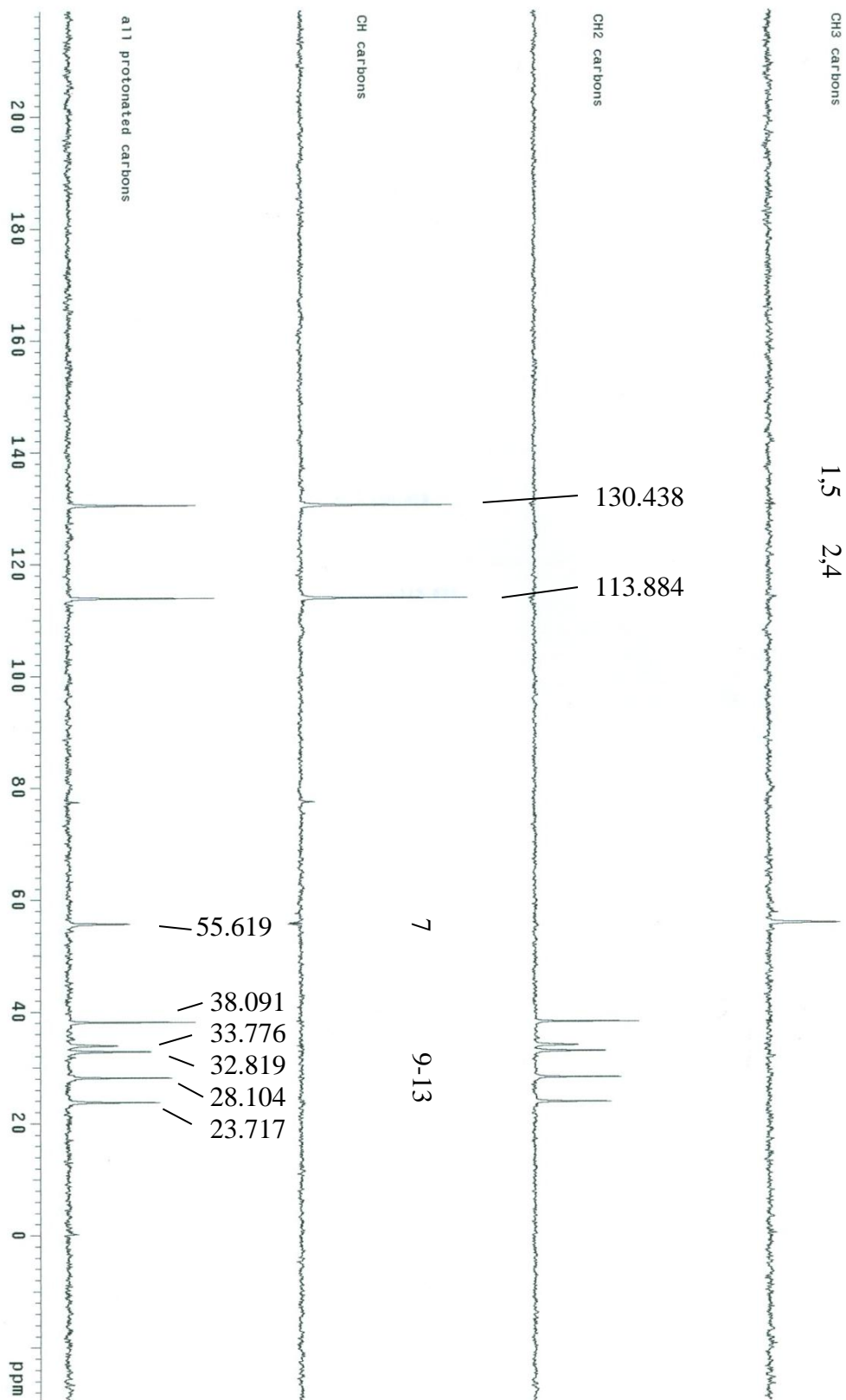
MS of 6-bromo-1-(4-methoxyphenyl)-1-hexanone



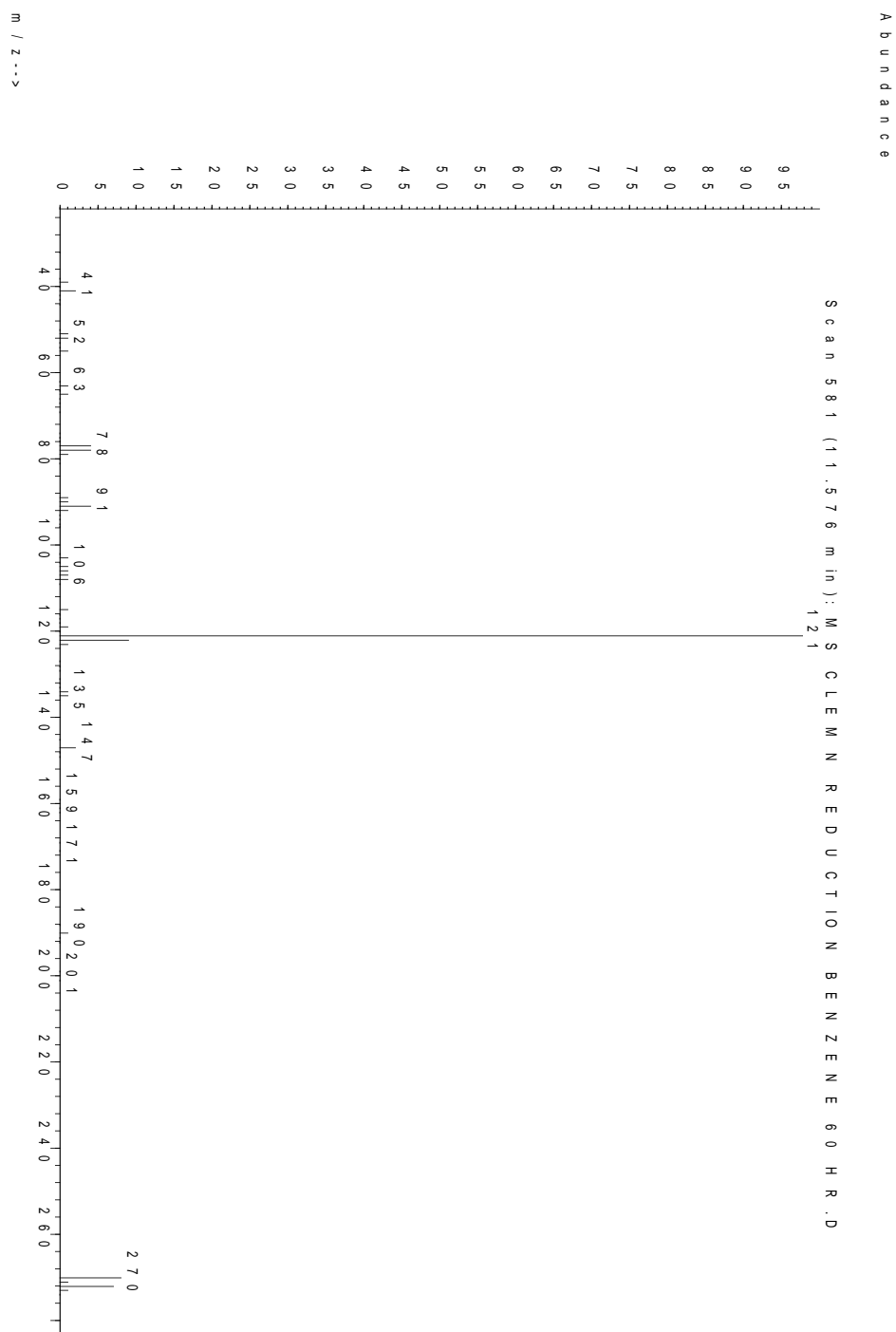
^1H NMR ($\text{CDCl}_3/0.03\%$ v/v TMS) of 6-bromo-1-(4-methoxyphenyl)-1-hexanone



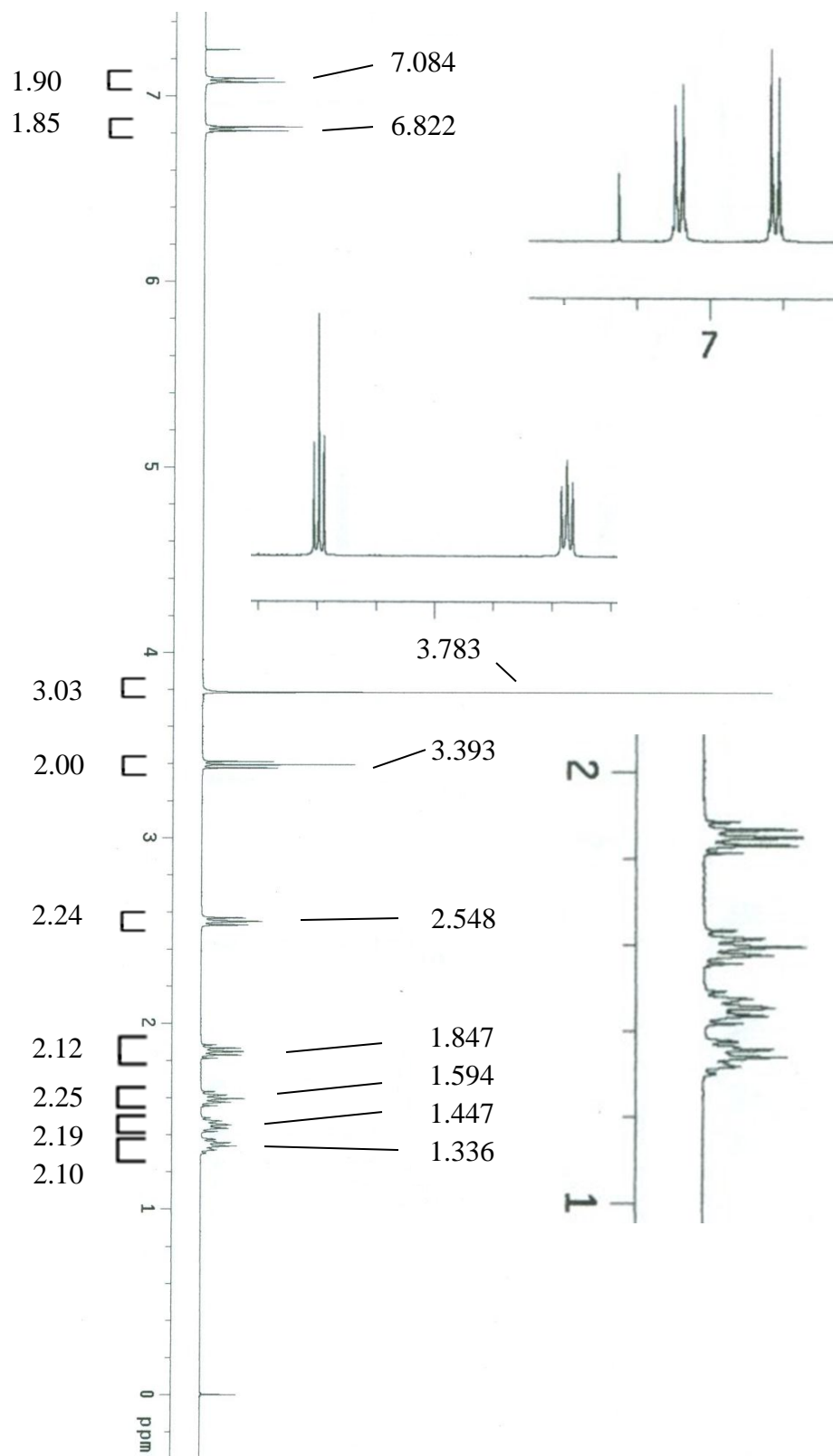
^{13}C NMR ($\text{CDCl}_3/0.03\%$ v/v TMS) of 6-bromo-1-(4-methoxyphenyl)-1-hexanone

DEPT NMR (CDCl₃/0.03% v/v TMS) of 6-bromo-1-(4-methoxyphenyl)-1-hexanone

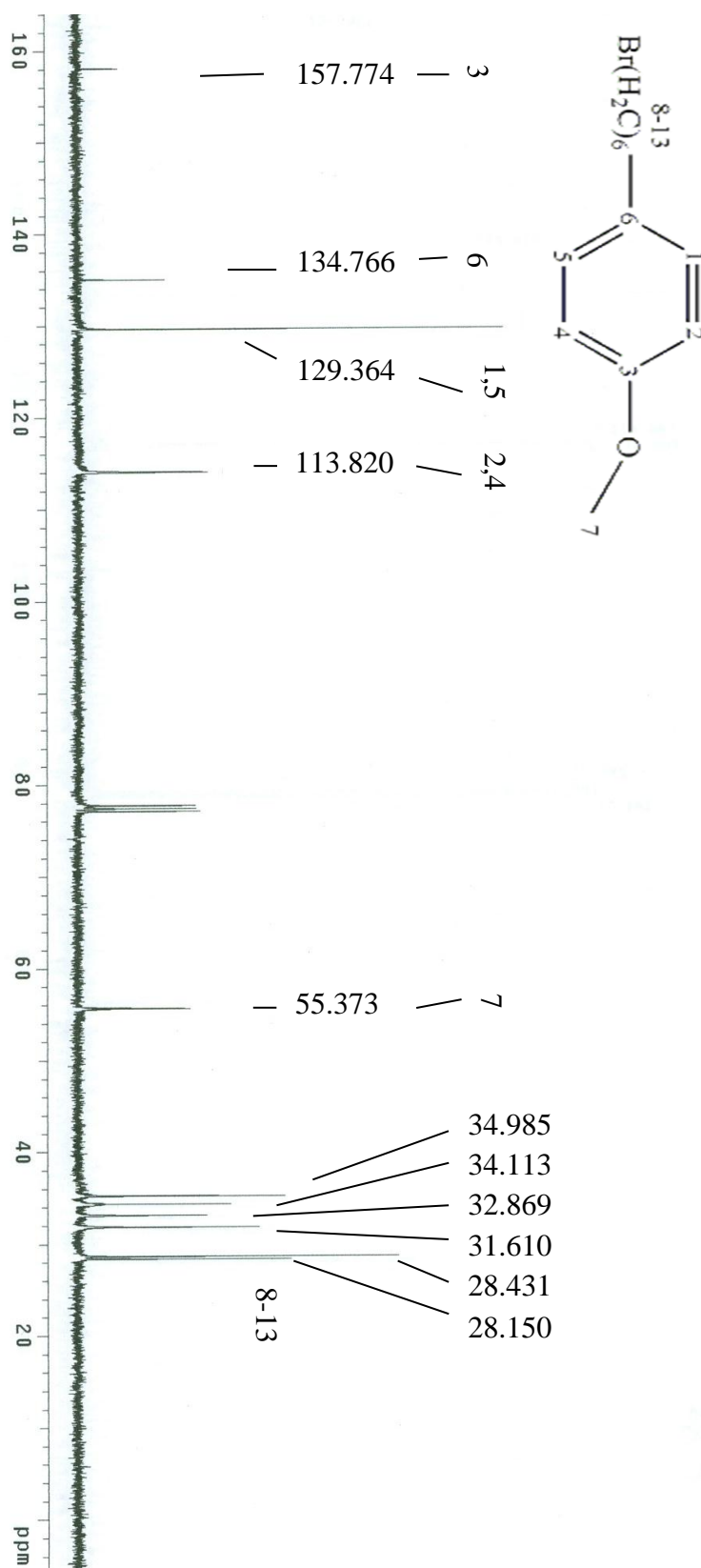
MS of 1-(6-bromohexyl)-4-methoxybenzene

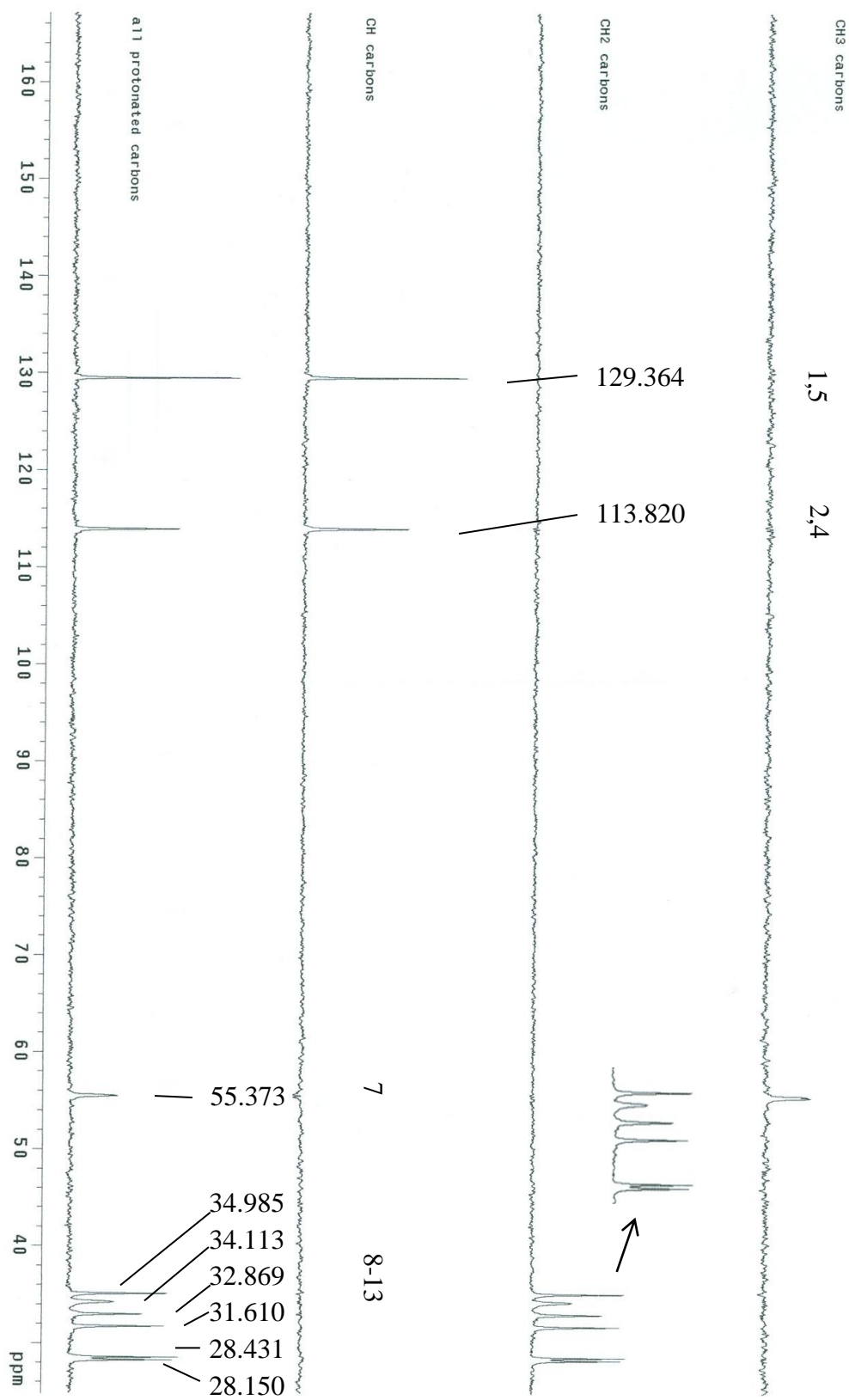


^1H NMR ($\text{CDCl}_3/0.03\%$ v/v TMS) of 1-(6-bromohexyl)-4-methoxybenzene

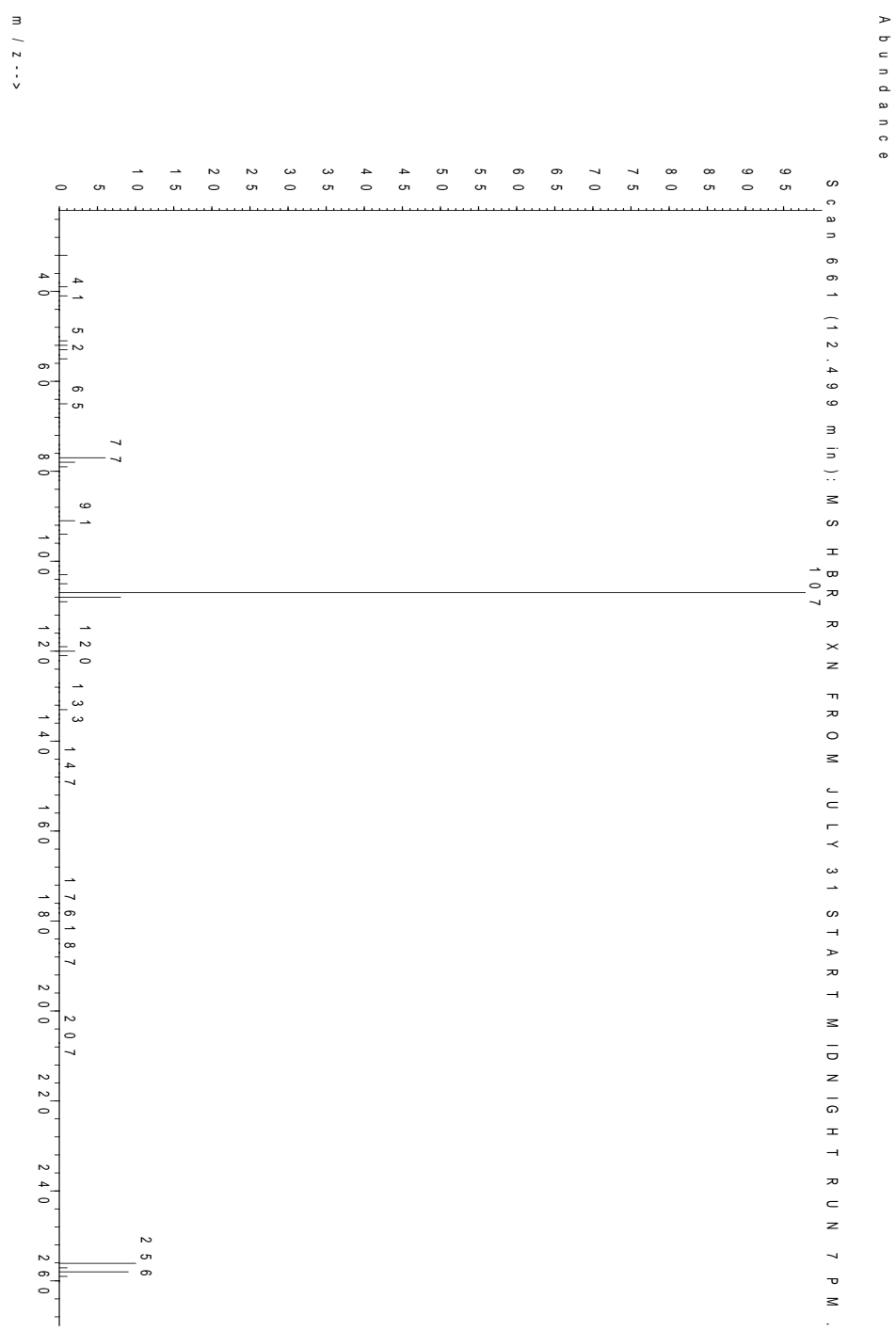


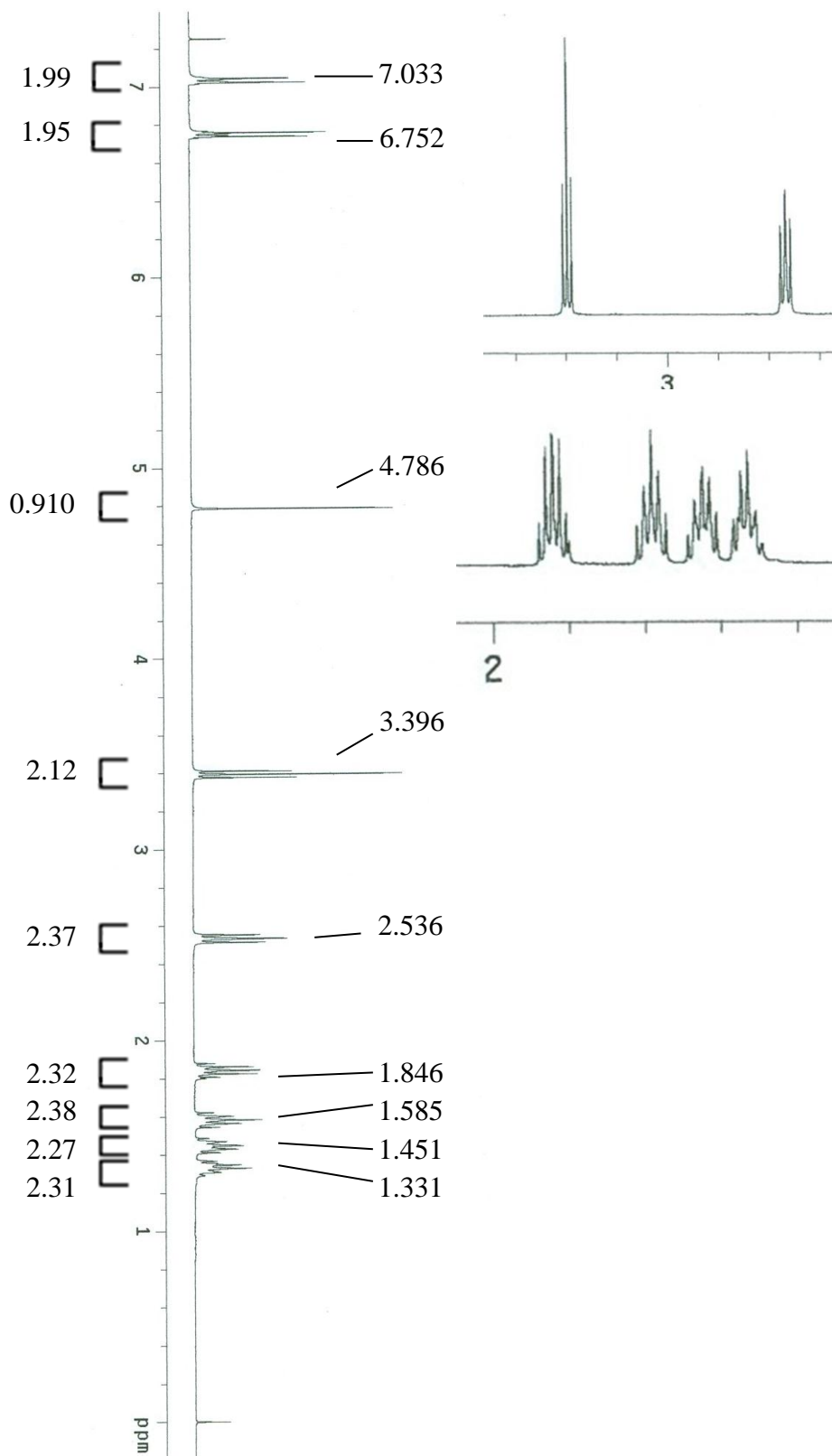
^{13}C NMR ($\text{CDCl}_3/0.03\%$ v/v TMS) of 1-(6-bromohexyl)-4-methoxybenzene

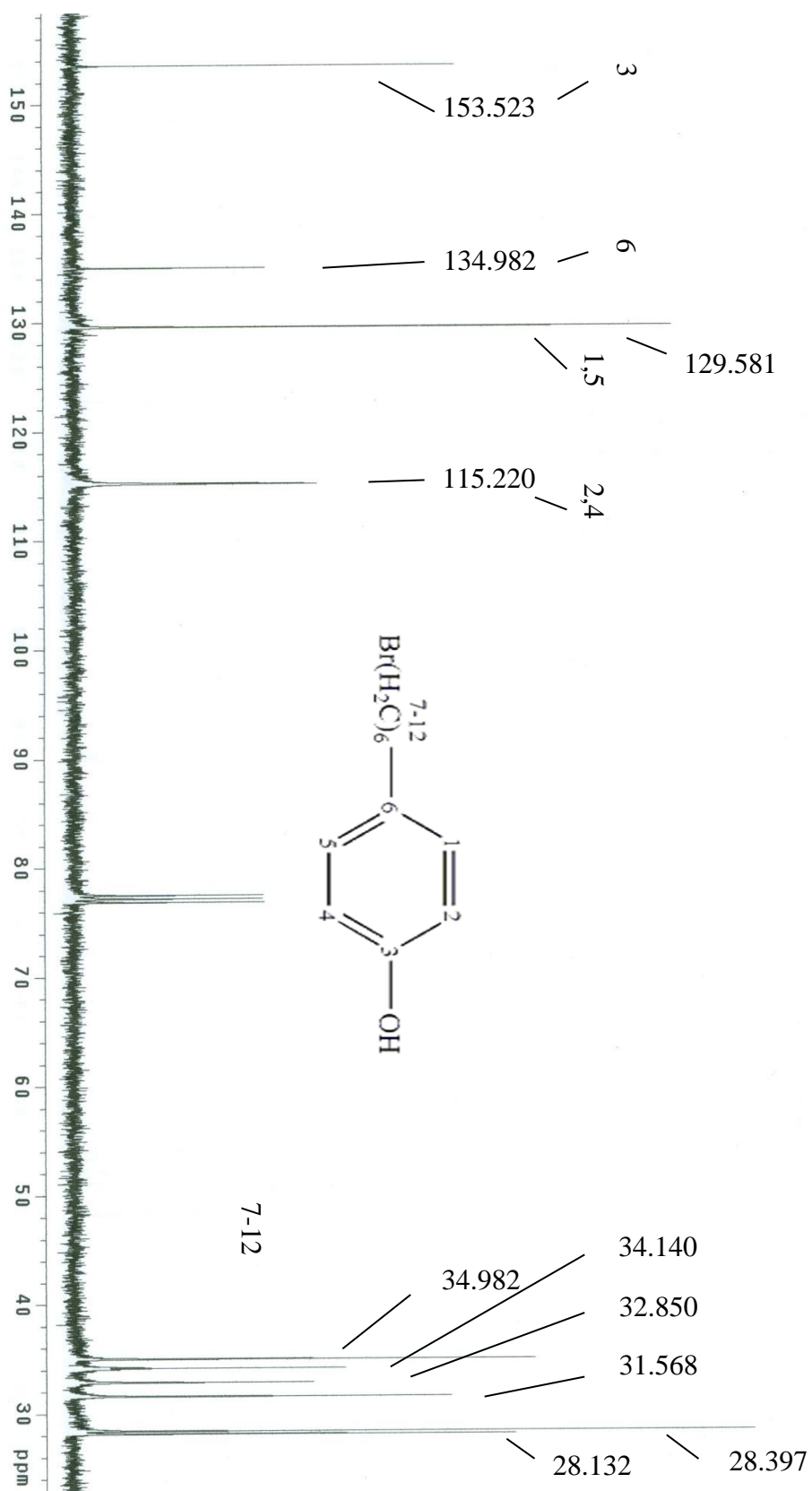


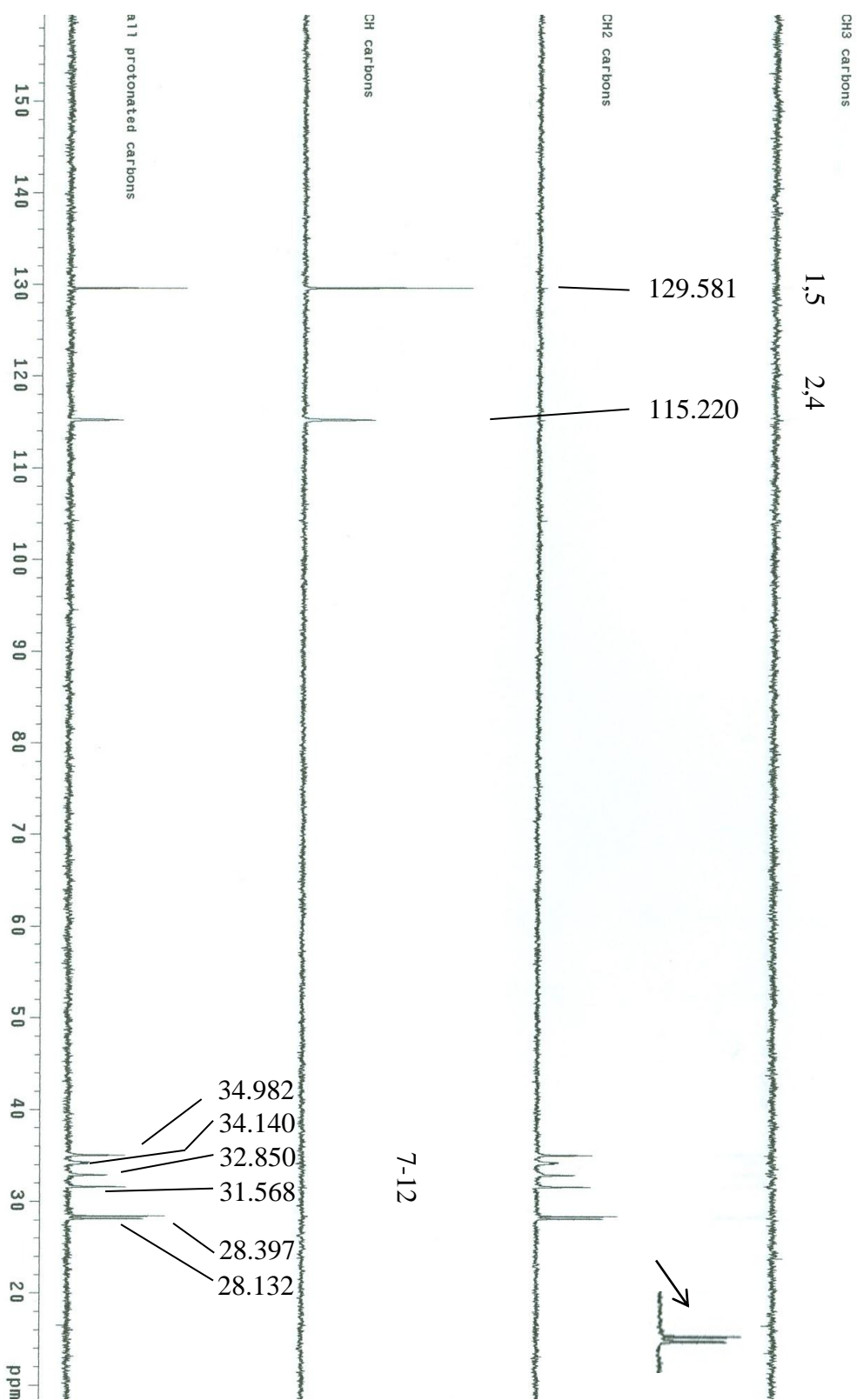
DEPT NMR ($\text{CDCl}_3/0.03\%$ v/v TMS) of 1-(6-bromohexyl)-4-methoxybenzene

MS of 4-(6-bromohexyl)phenol

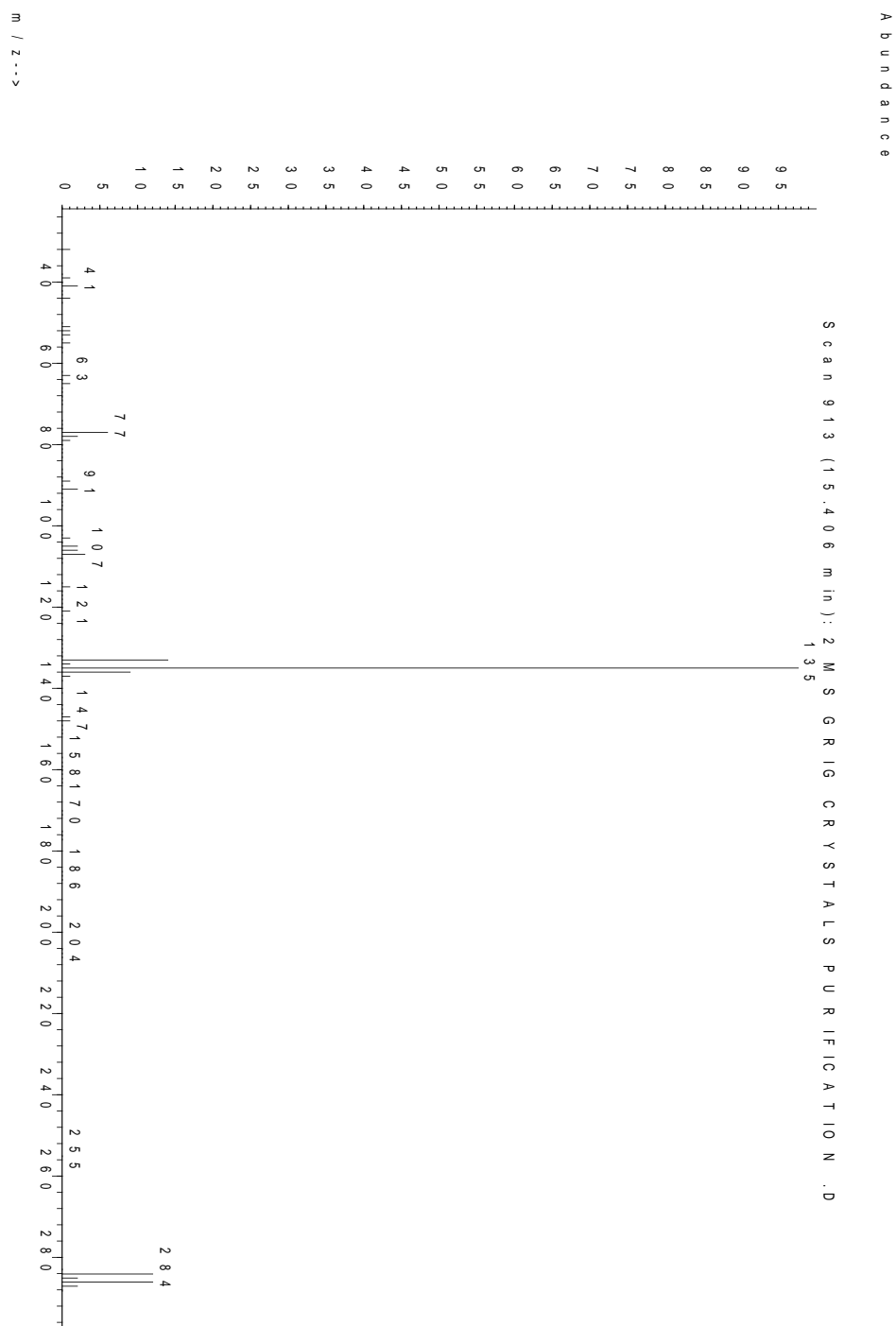


^1H NMR ($\text{CDCl}_3/0.03\%$ v/v TMS) of 4-(6-bromohexyl)phenol

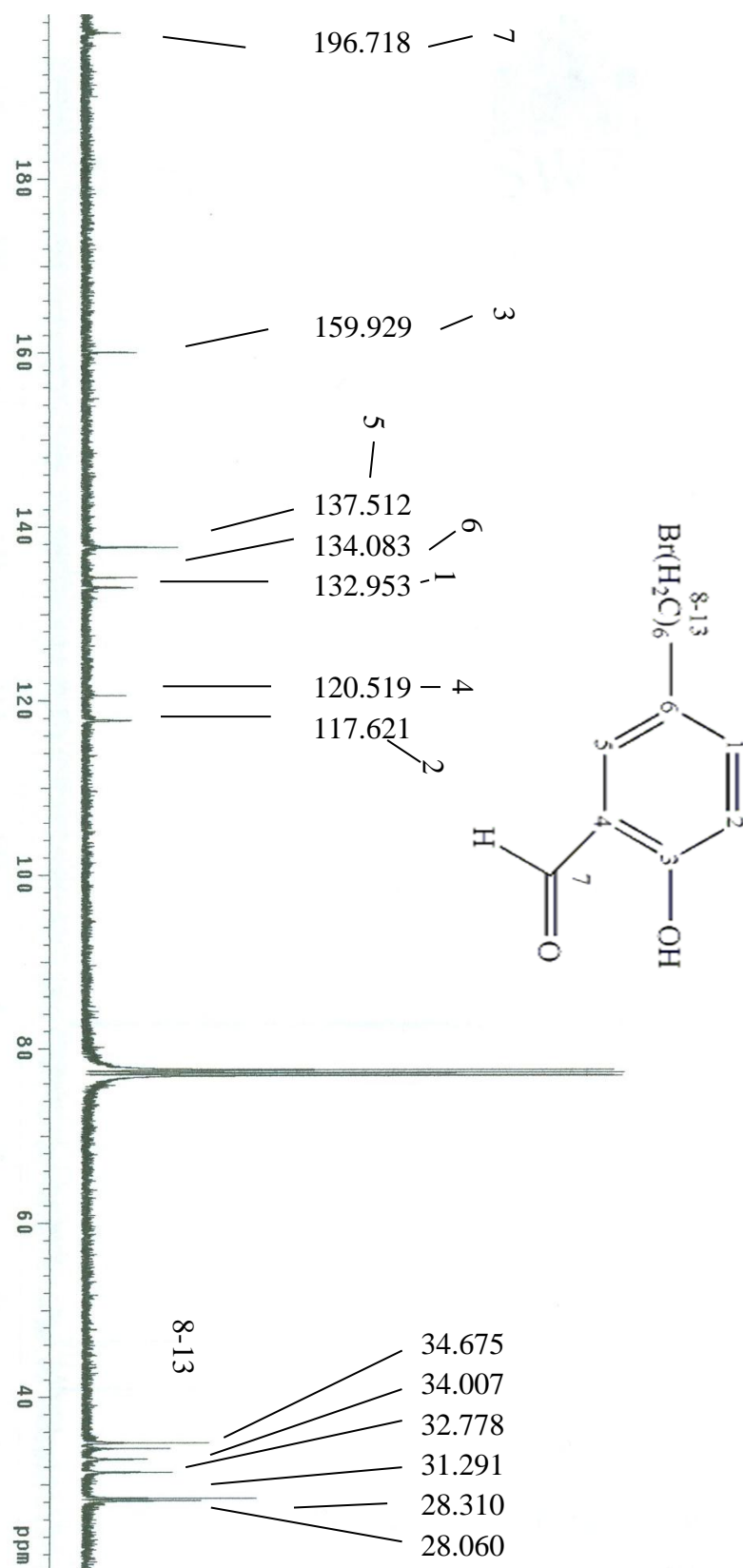
^{13}C NMR ($\text{CDCl}_3/0.03\%$ v/v TMS) of 4-(6-bromohexyl)phenol

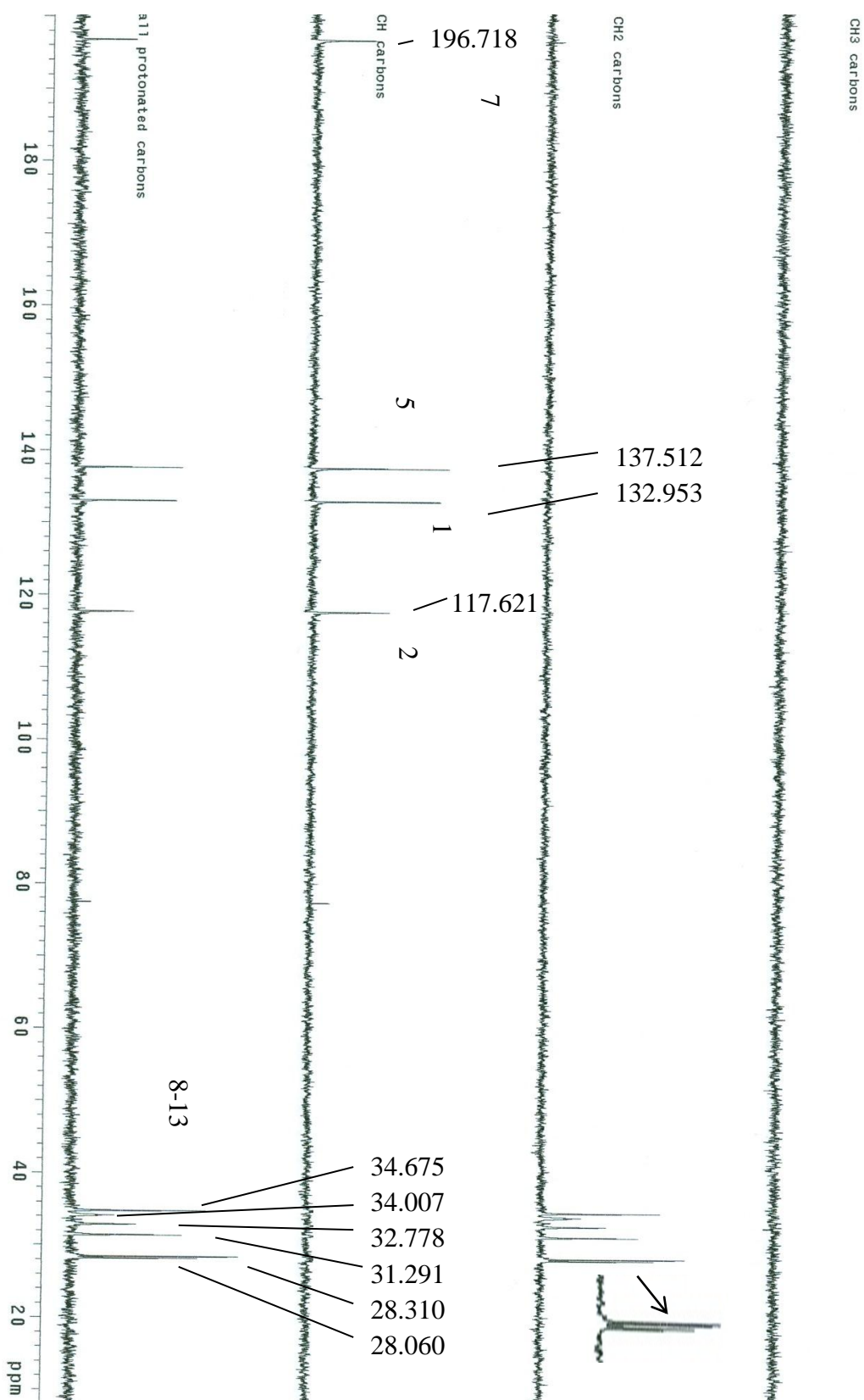
DEPT NMR (CDCl₃/0.03% v/v TMS) of 4-(6-bromohexyl)phenol

MS of 5-(6-bromohexyl)salicylaldehyde

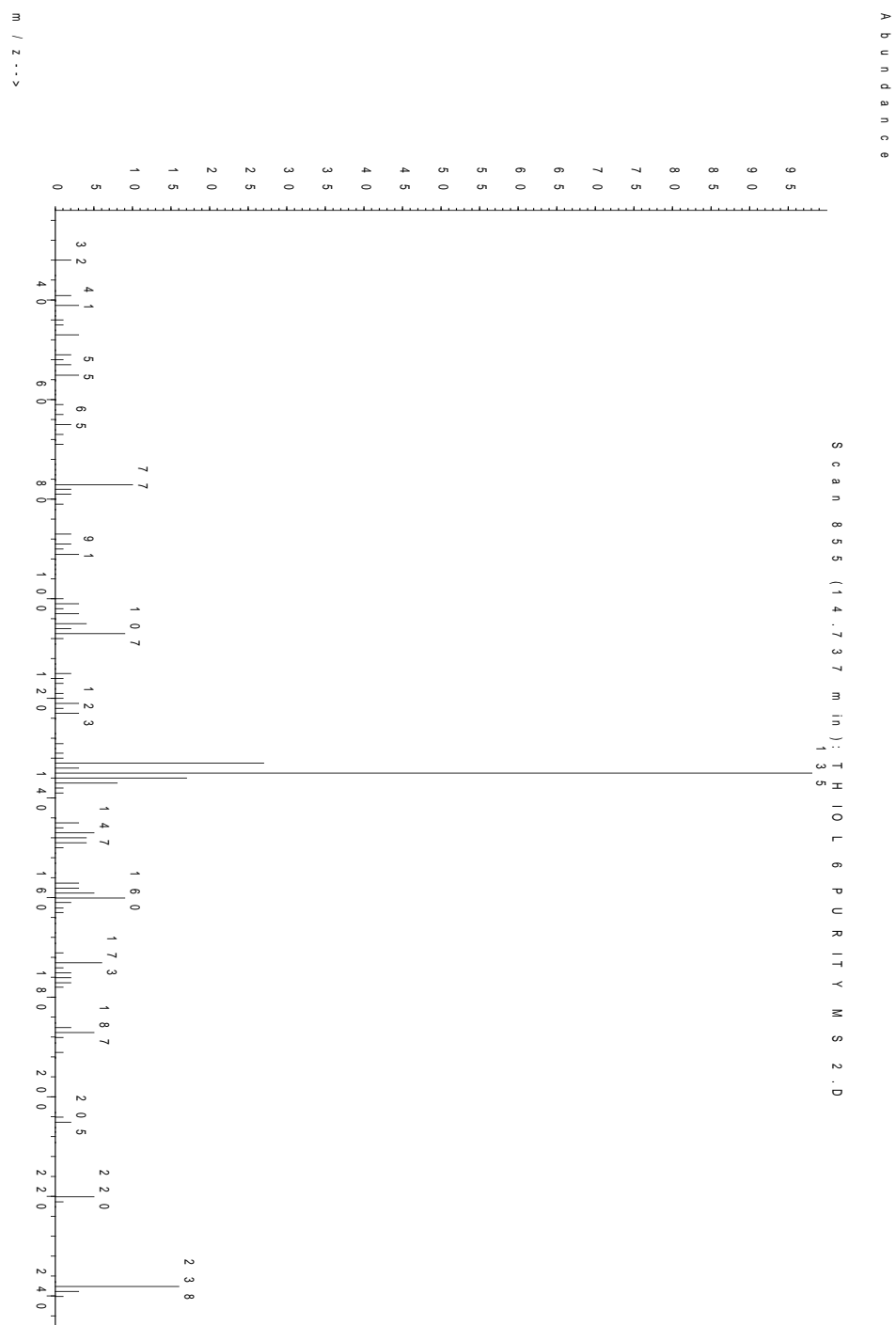


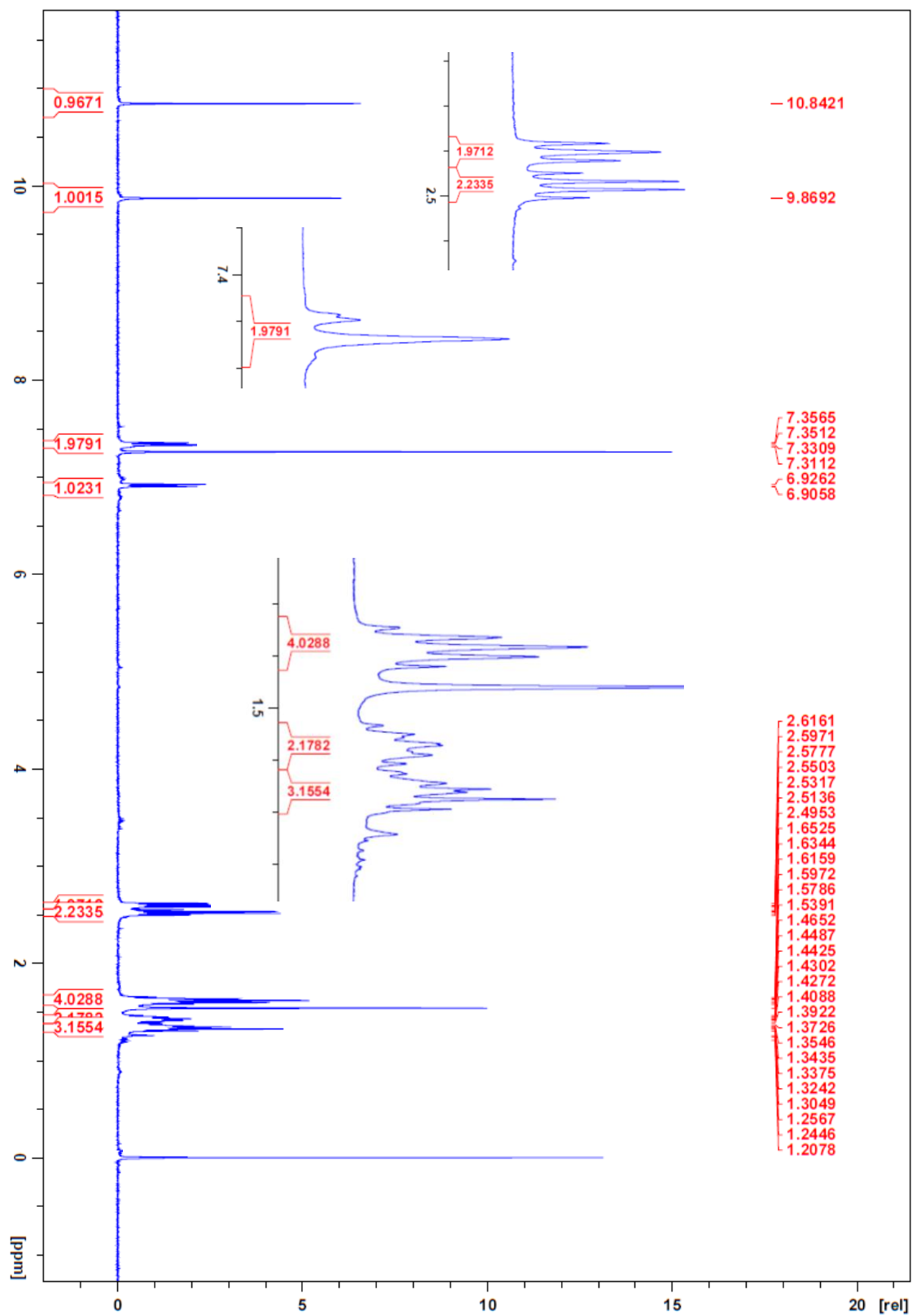
^{13}C NMR ($\text{CDCl}_3/0.03\%$ v/v TMS) of 5-(6-bromohexyl)salicylaldehyde

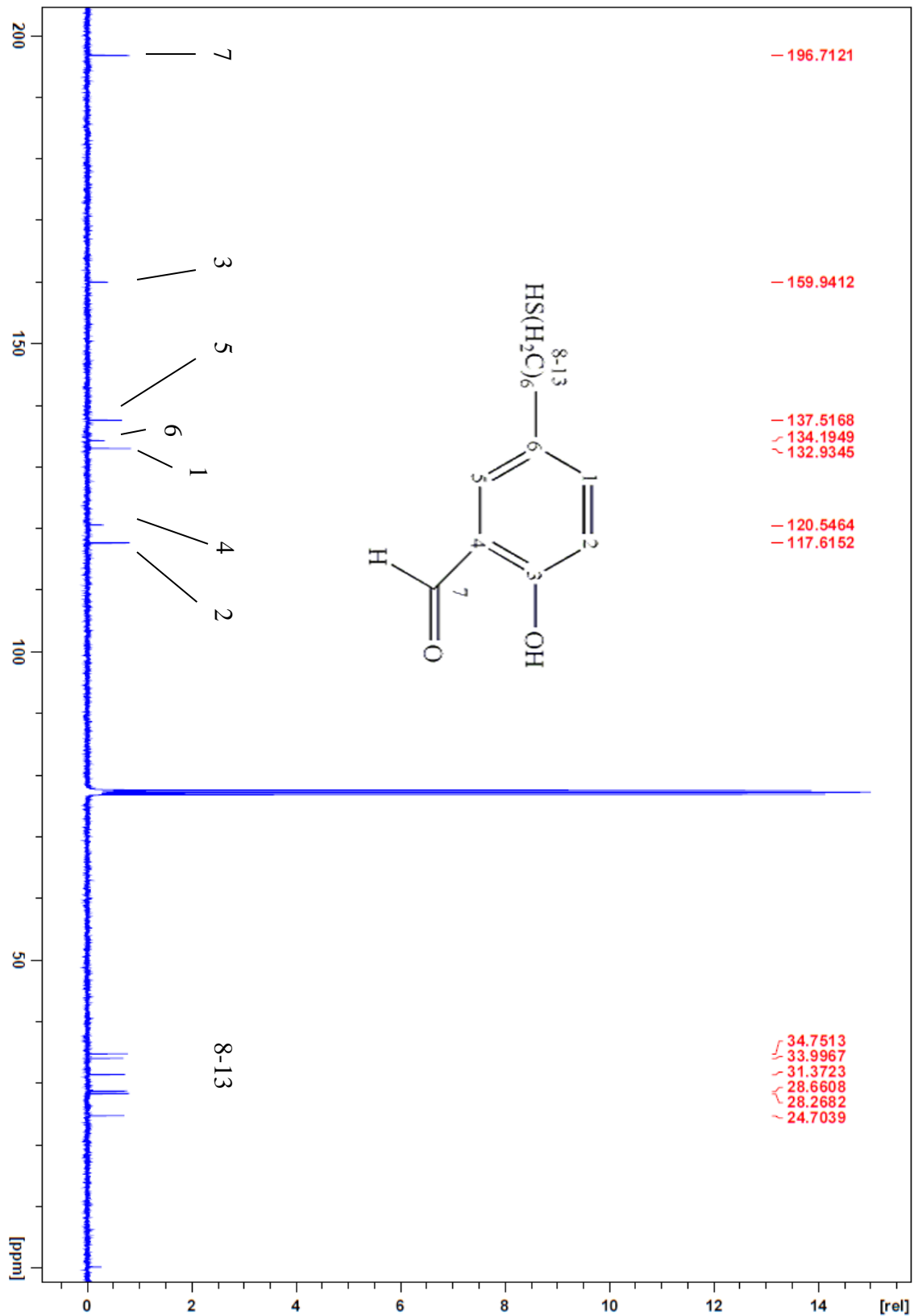


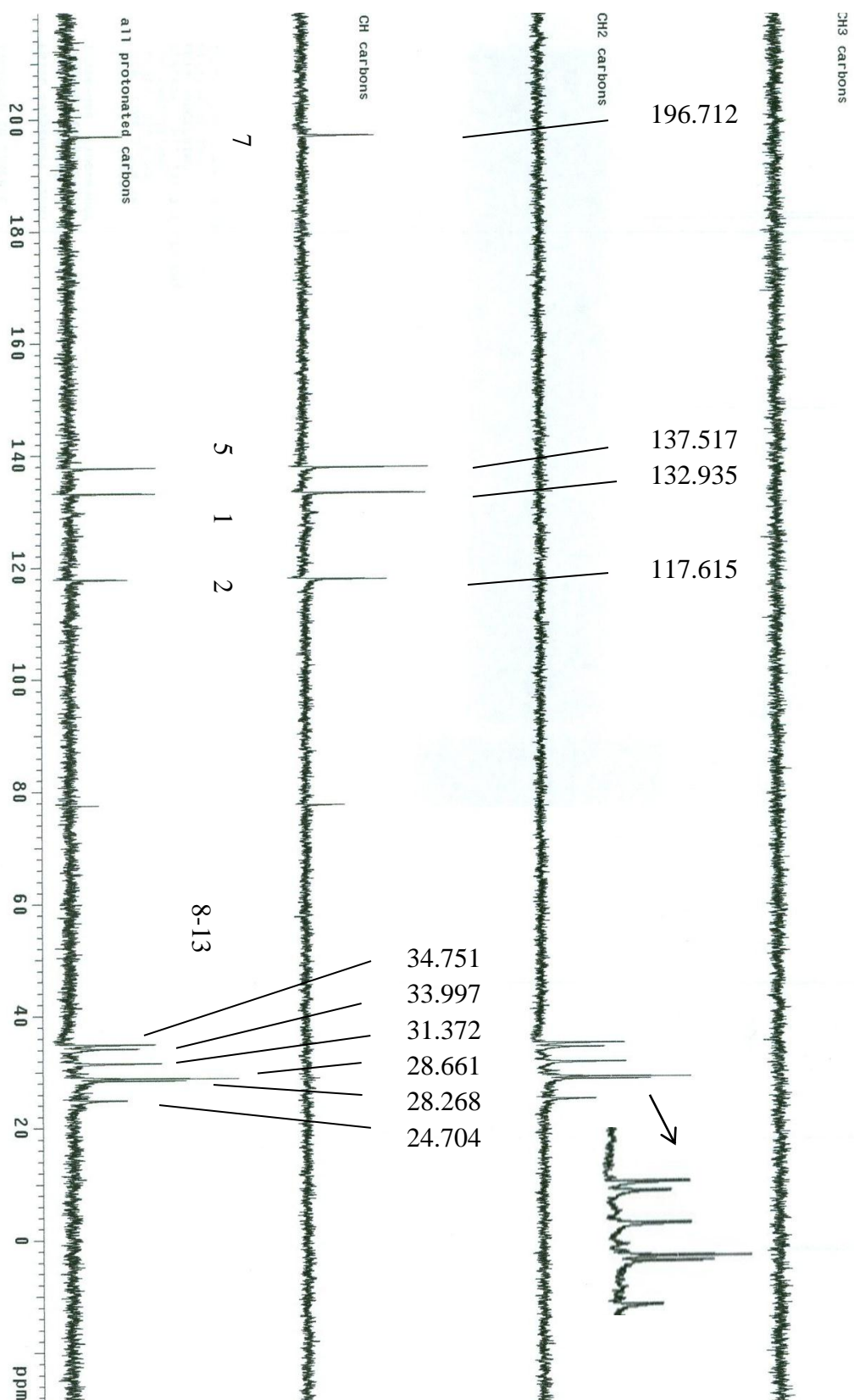
DEPT NMR (CDCl₃/0.03% v/v TMS) of 5-(6-bromohexyl)salicylaldehyde

MS of 5-(6-sulfhydrylhexyl)salicylaldehyde

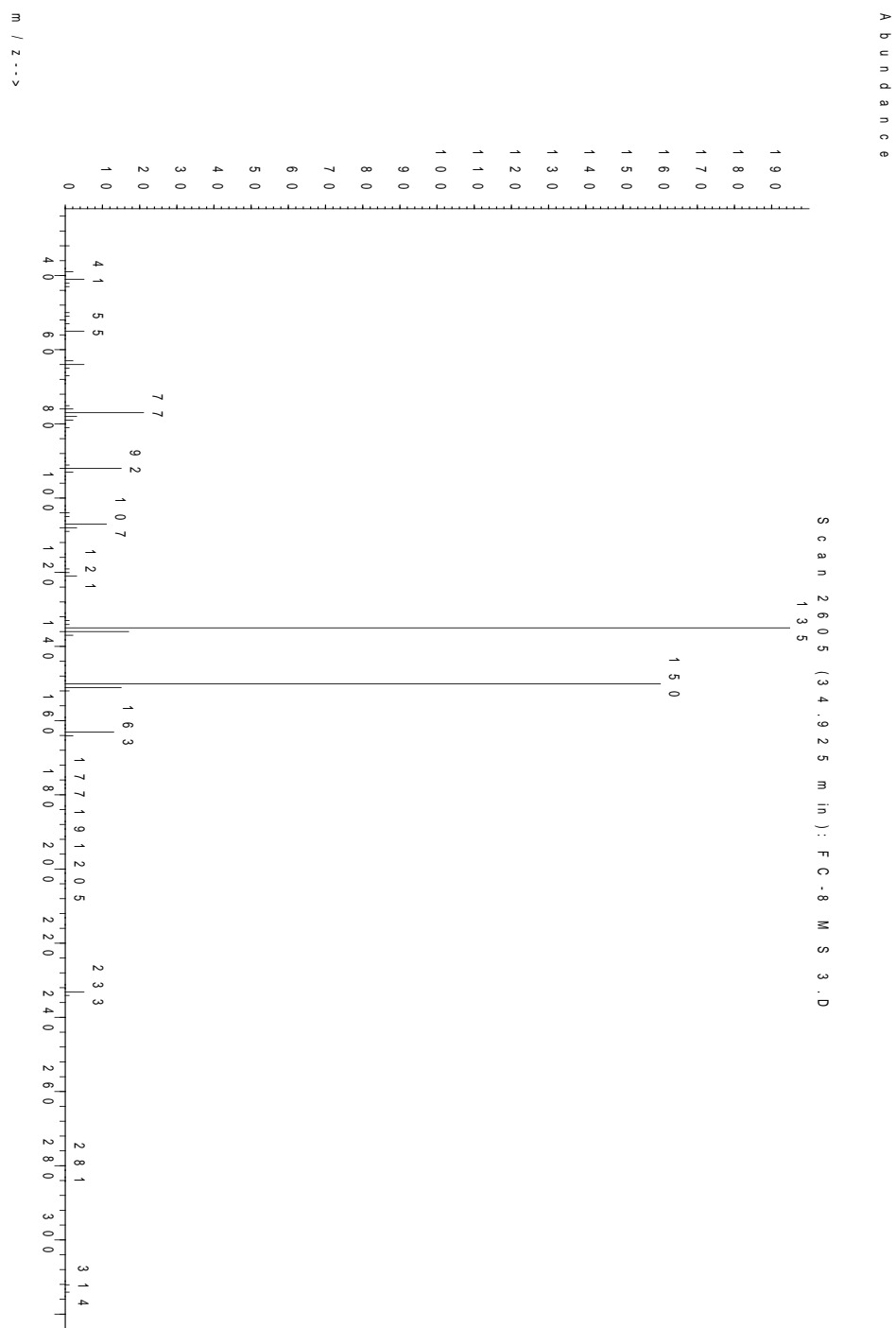


^1H NMR ($\text{CDCl}_3/0.03\%$ v/v TMS) of 5-(6-sulfhydrylhexyl)salicylaldehyde

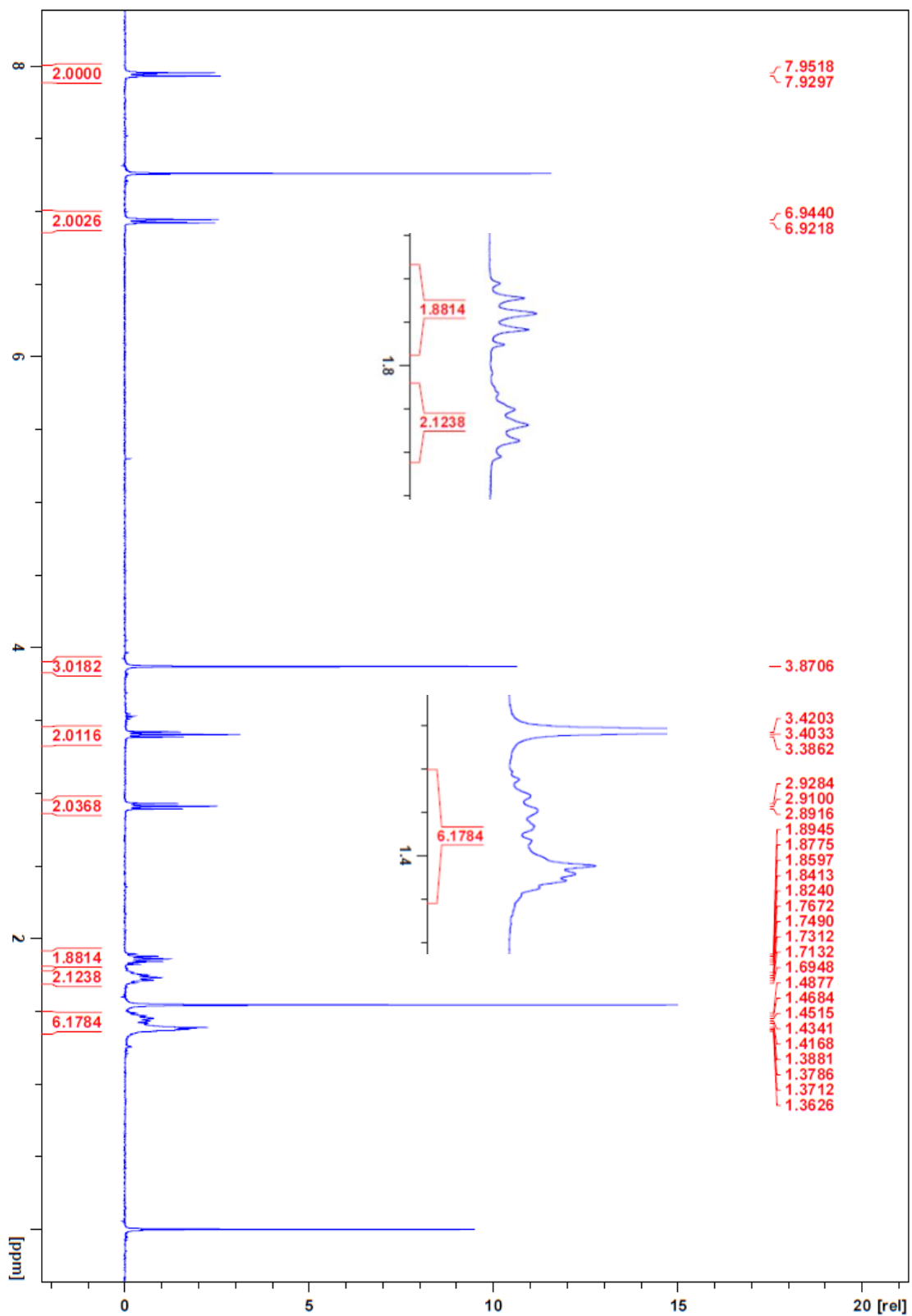
^{13}C NMR ($\text{CDCl}_3/0.03\%$ v/v TMS) of 5-(6-sulphydrihexyl)salicylaldehyde

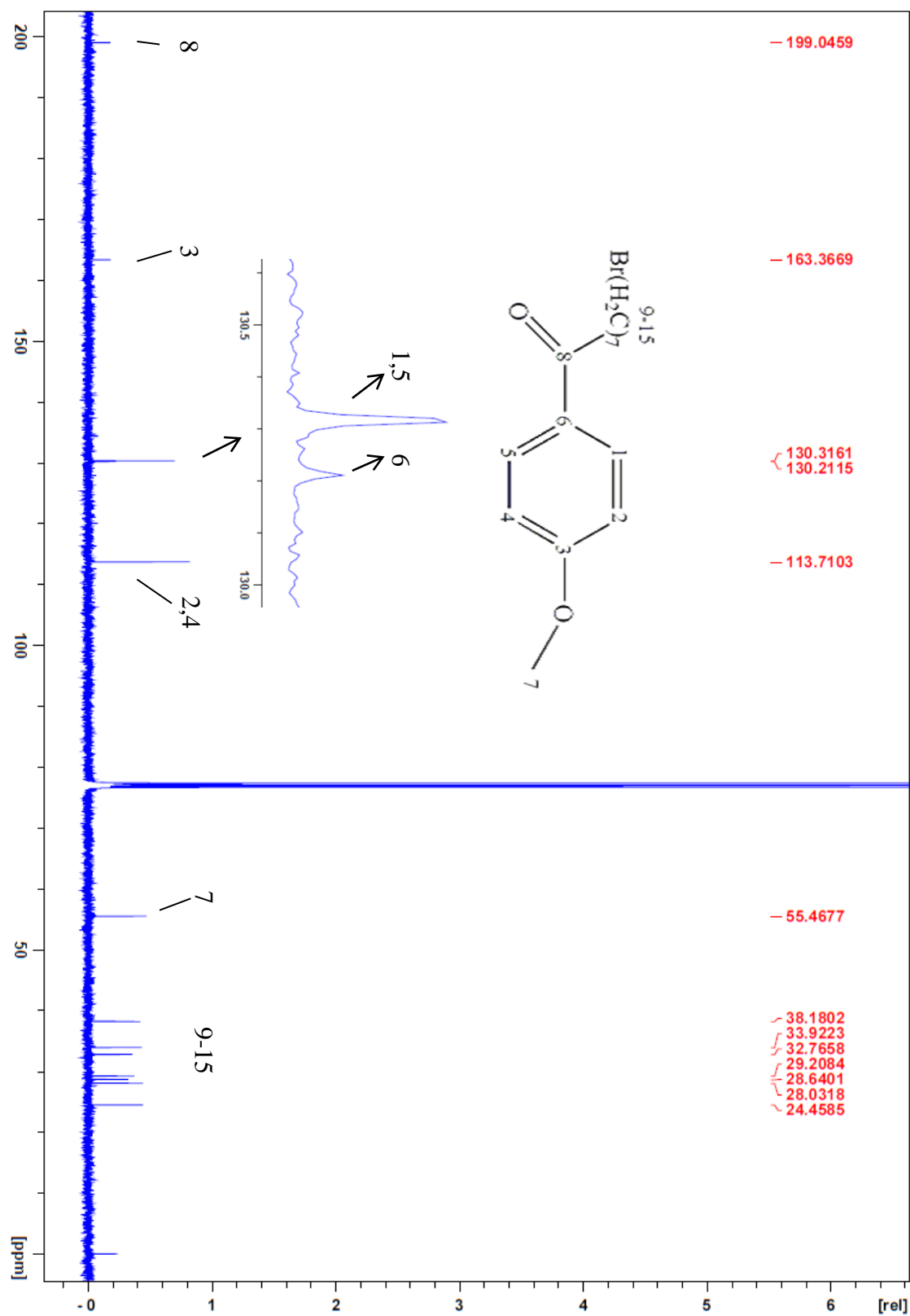
DEPT NMR (CDCl₃/0.03% v/v TMS) of 5-(6-sulphydrihexyl)salicylaldehyde

MS of 8-bromo-1-(4-methoxyphenyl)-1-octanone

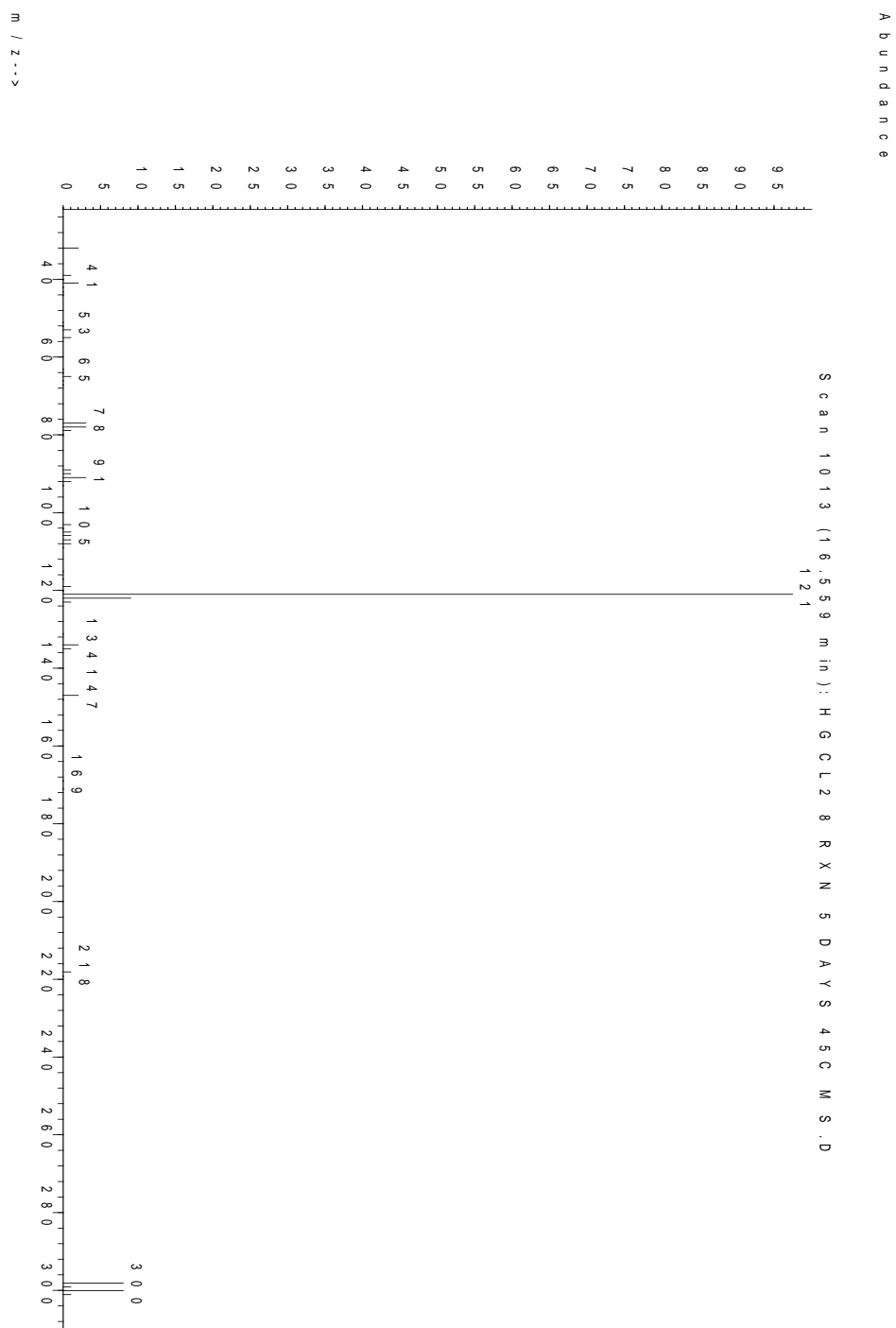


^1H NMR ($\text{CDCl}_3/0.03\%$ v/v TMS) of 8-bromo-1-(4-methoxyphenyl)-1-octanone

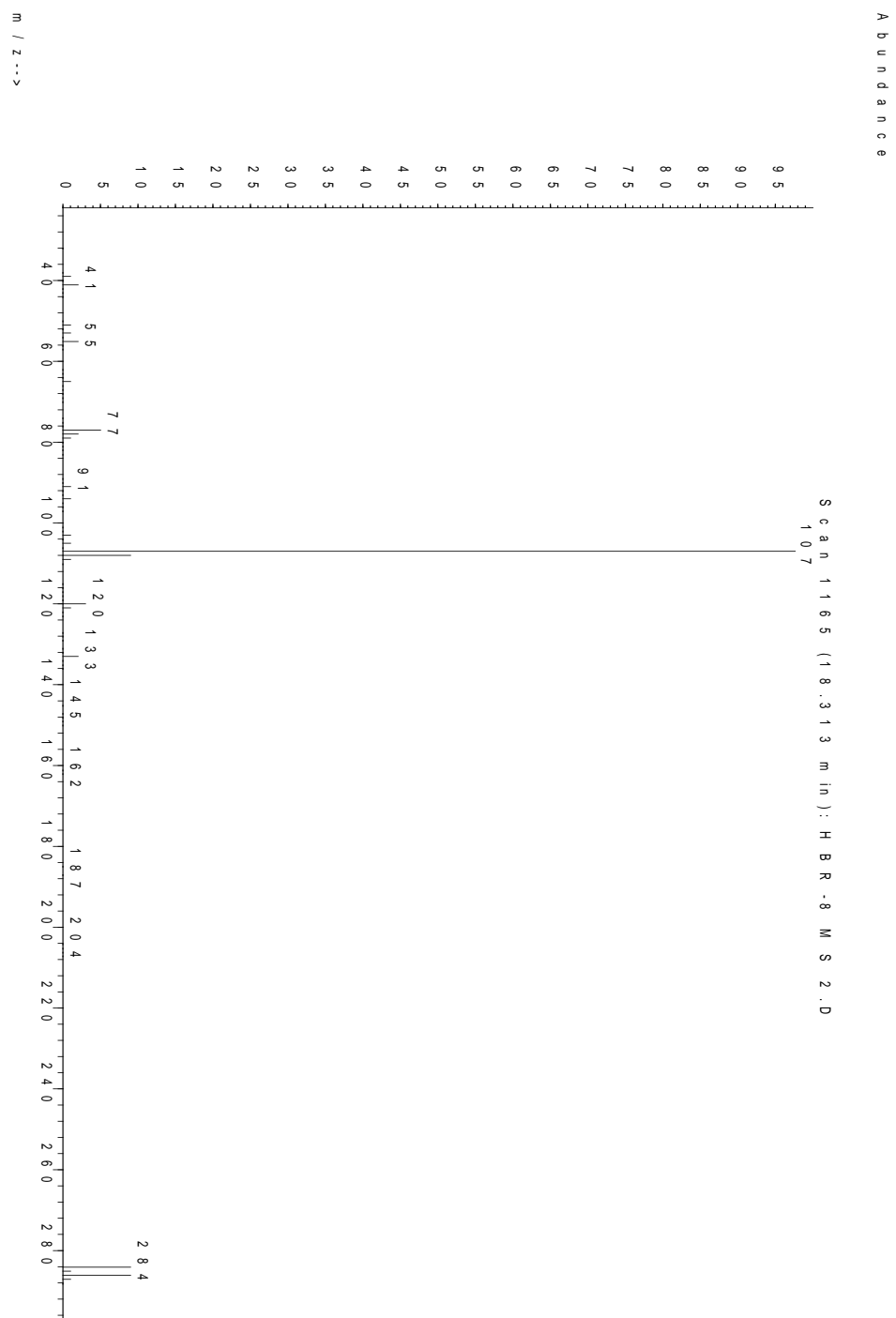


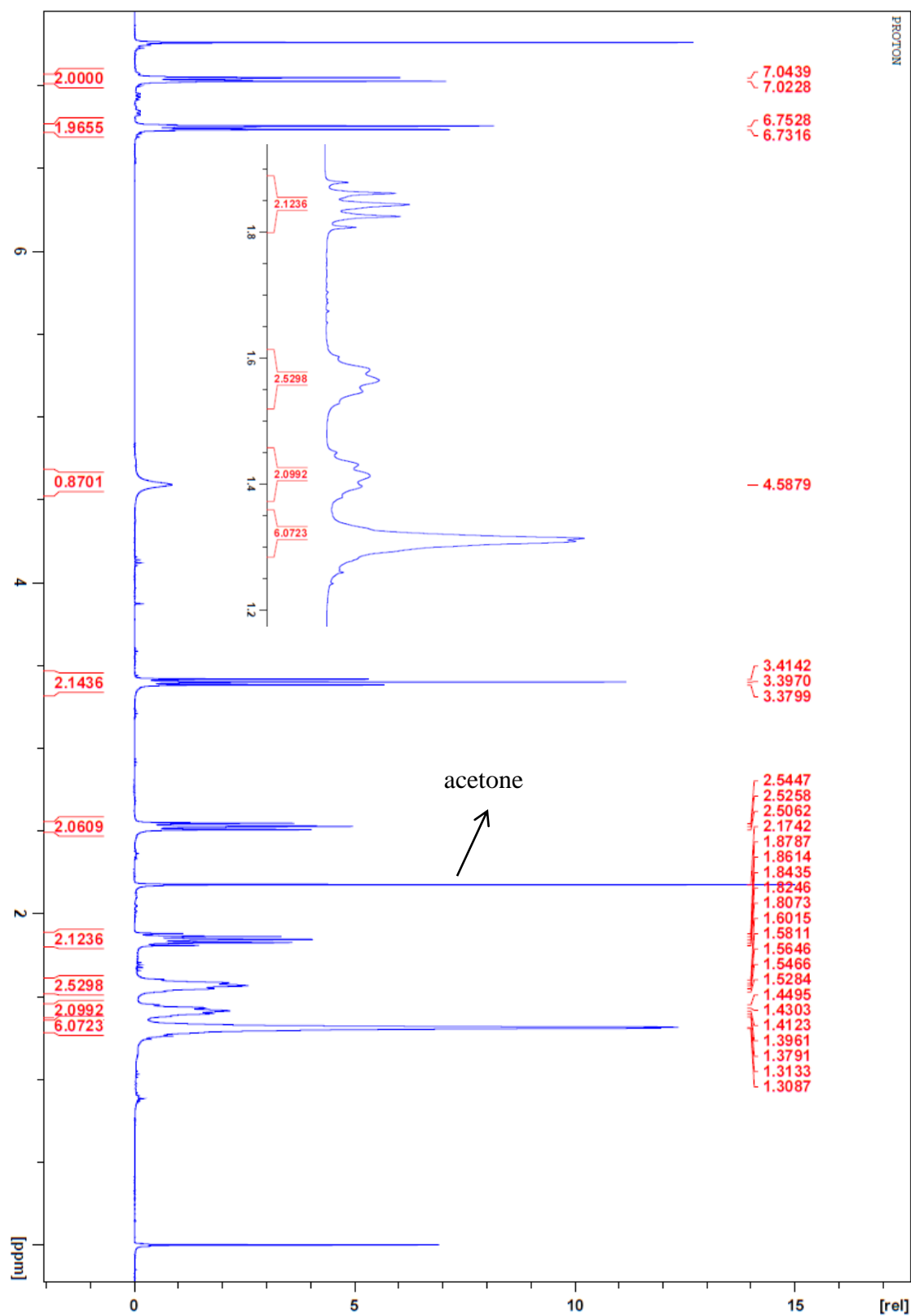
^{13}C NMR ($\text{CDCl}_3/0.03\%$ v/v TMS) of 8-bromo-1-(4-methoxyphenyl)-1-octanone

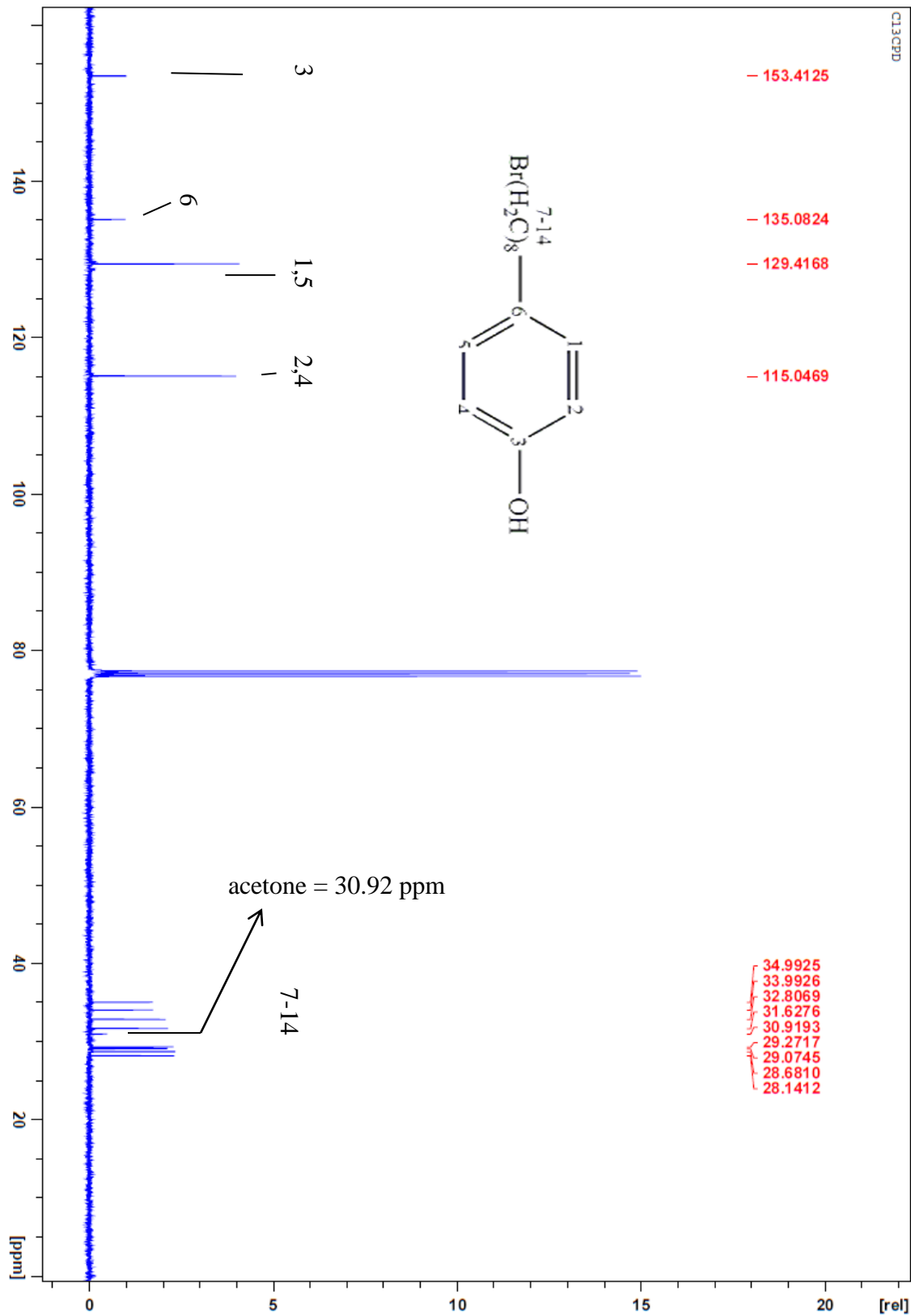
MS of 1-(8-bromooctyl)-4-methoxybenzene



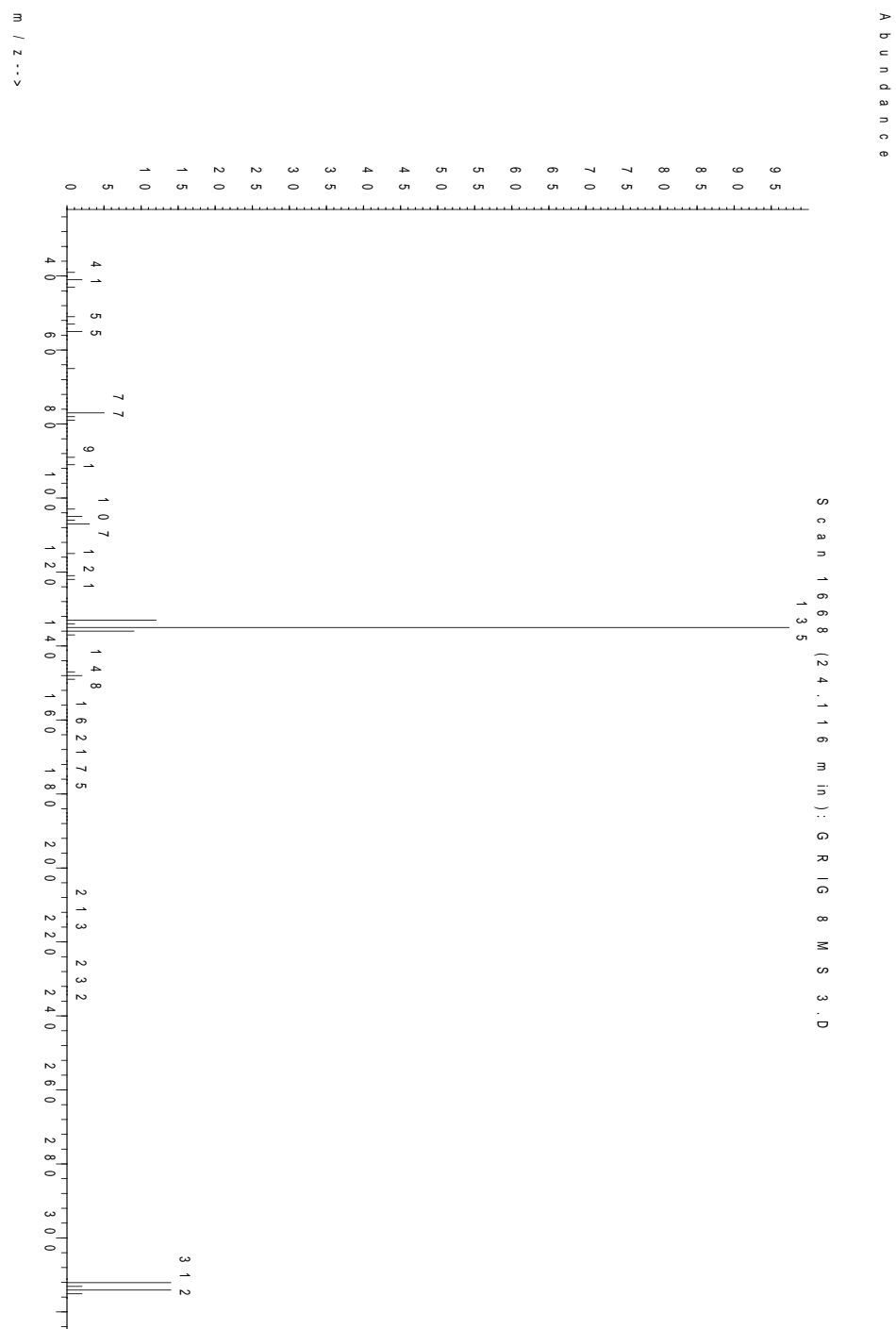
MS of 4-(8-bromooctyl)phenol

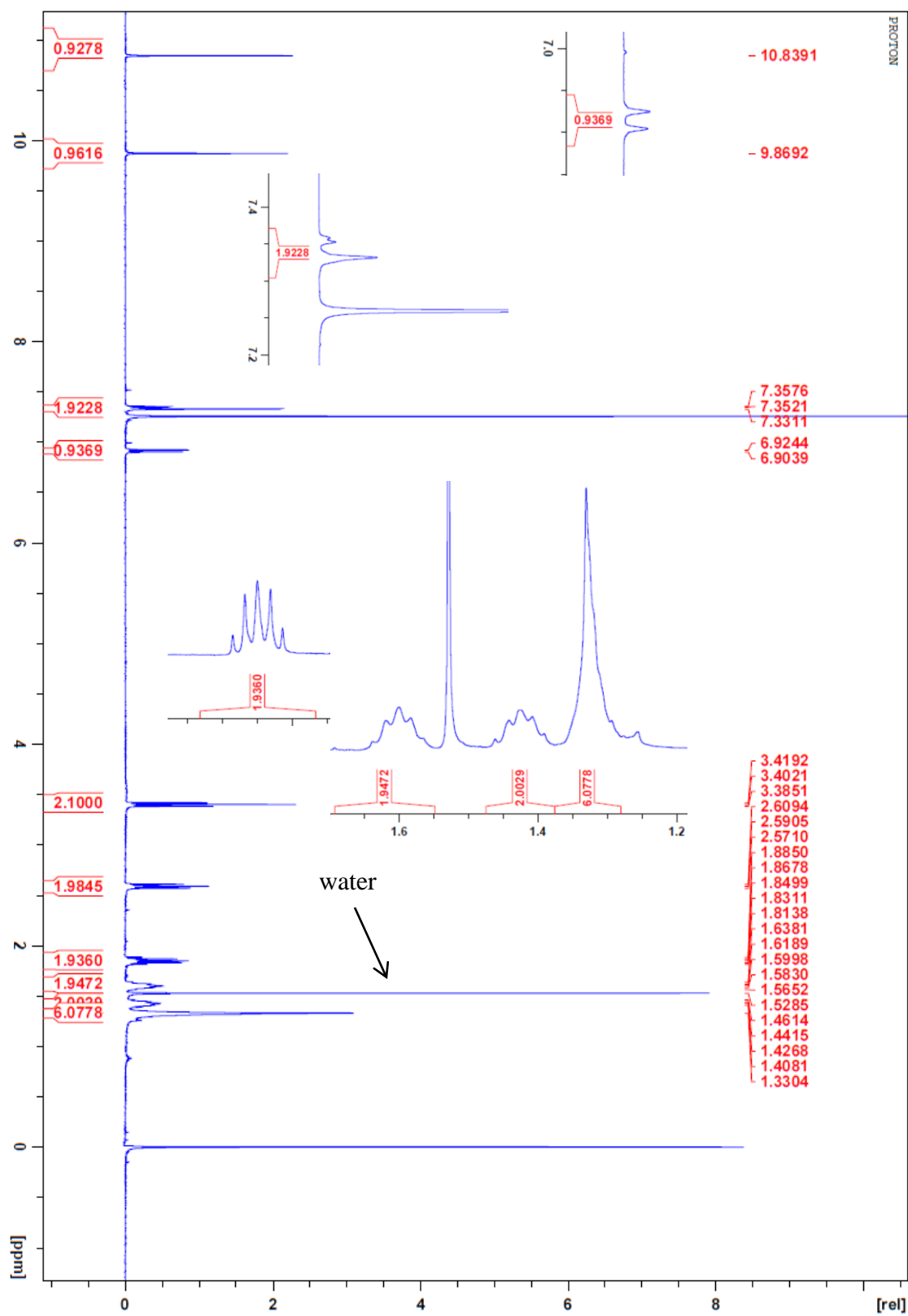


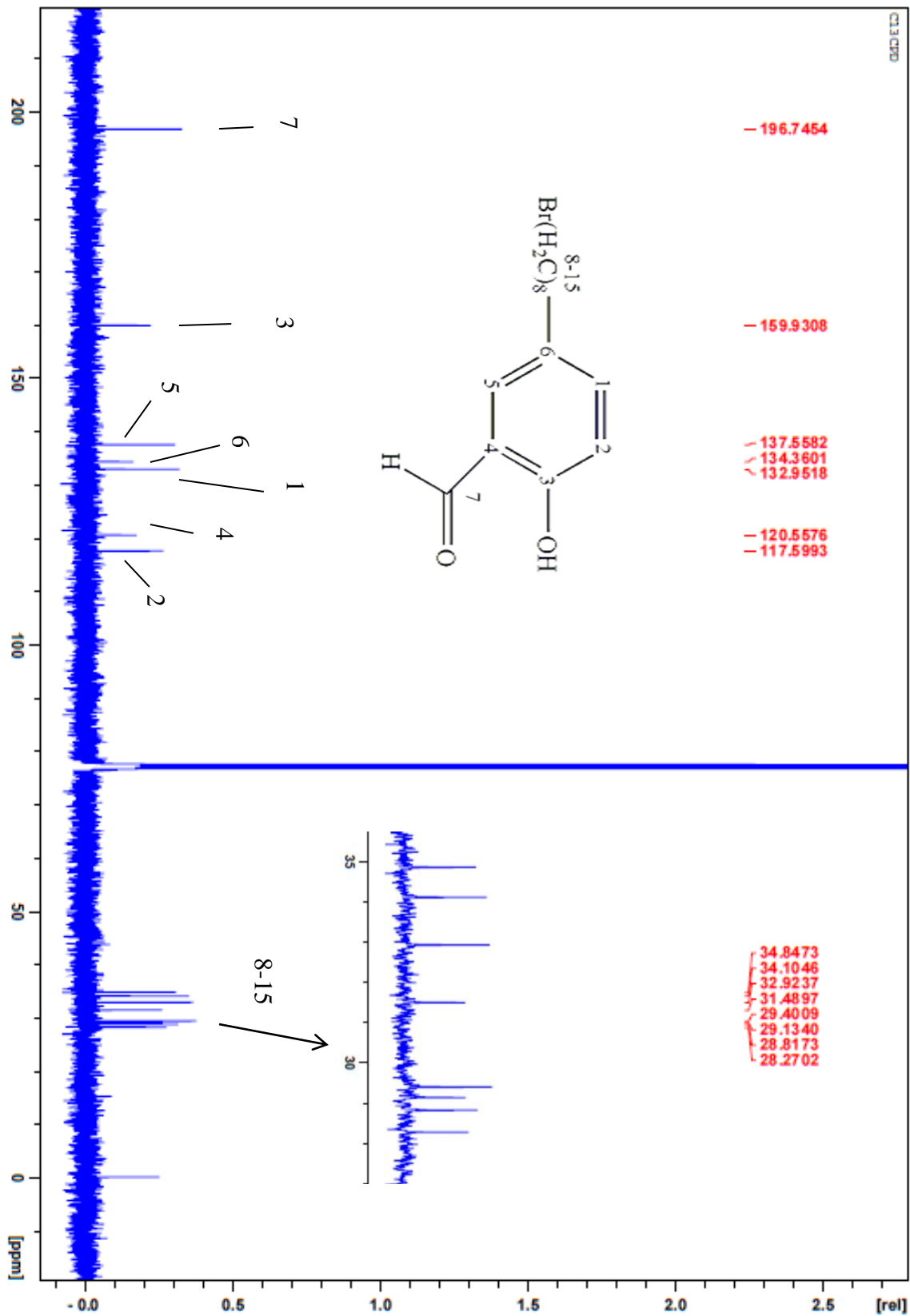
^1H NMR ($\text{CDCl}_3/0.03\%$ v/v TMS) of 4-(8-bromooctyl)phenol

^{13}C NMR ($\text{CDCl}_3/0.03\%$ v/v TMS) of 4-(8-bromooctyl)phenol

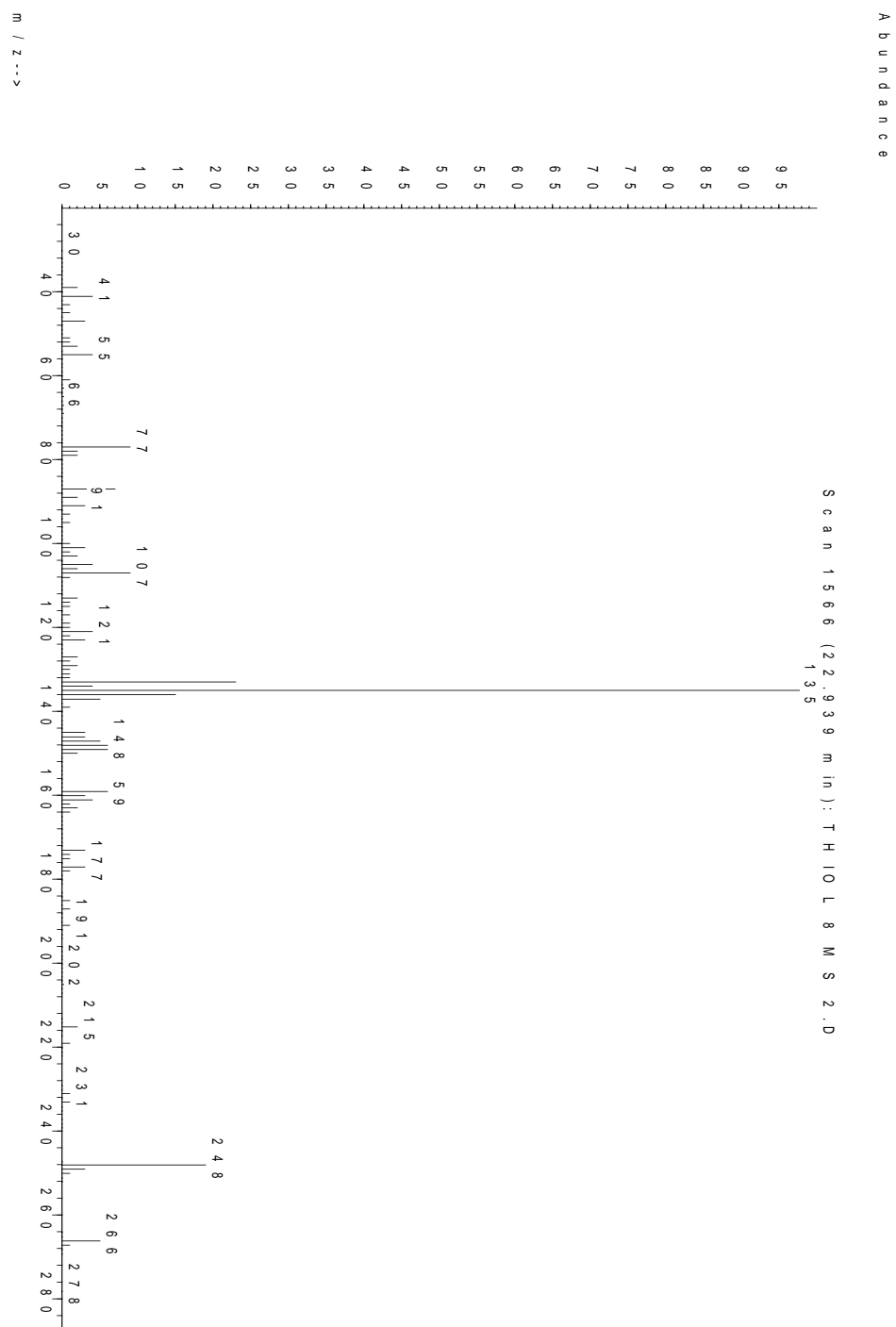
MS of 5-(8-bromooctyl)salicylaldehyde

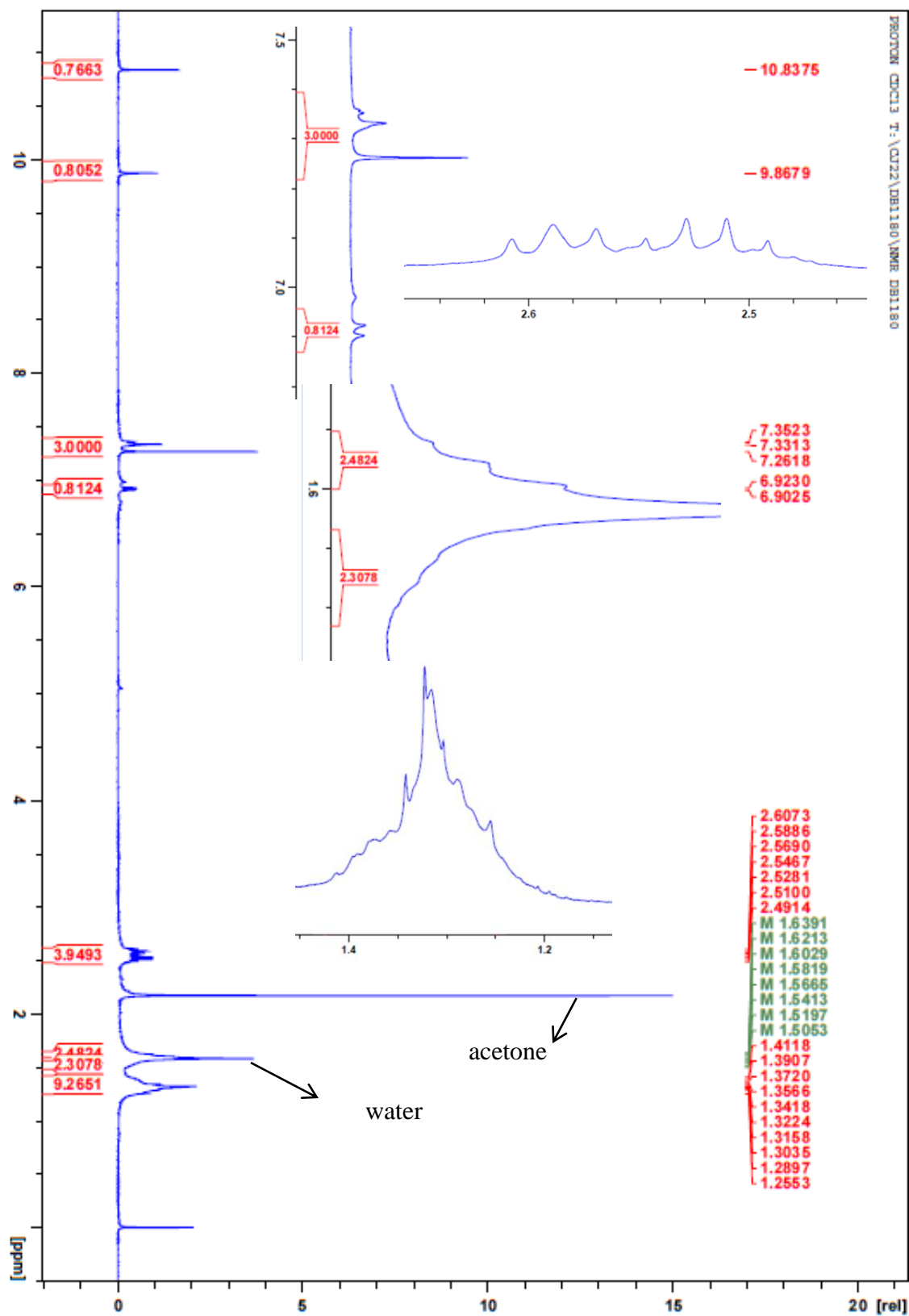


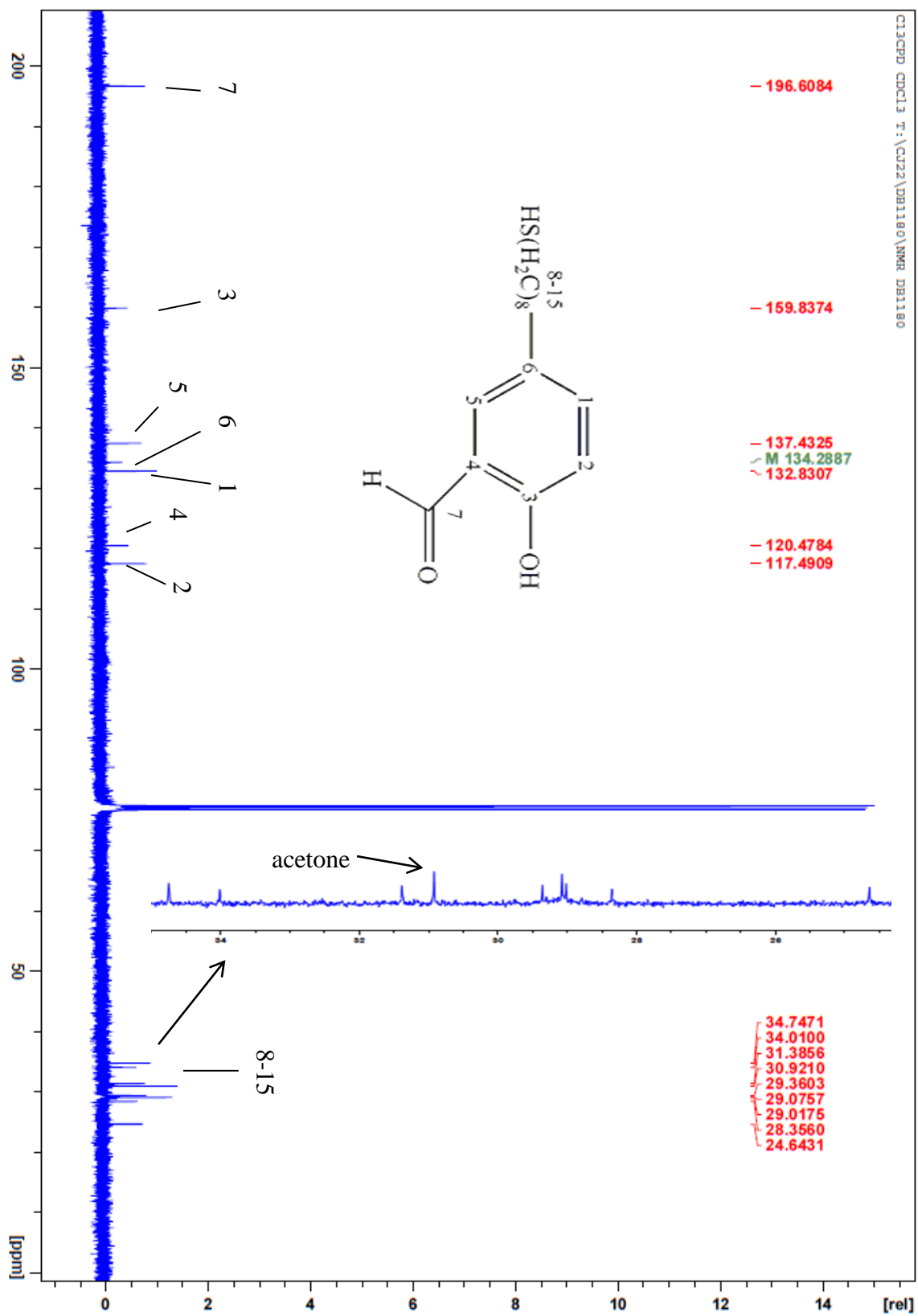
^1H NMR ($\text{CDCl}_3/0.03\%$ v/v TMS) of 5-(8-bromooctyl)salicylaldehyde

^{13}C NMR ($\text{CDCl}_3/0.03\%$ v/v TMS) of 5-(8-bromooctyl)salicylaldehyde

MS of 5-(8-sulfhydroctyl)salicylaldehyde



^1H NMR ($\text{CDCl}_3/0.03\%$ v/v TMS) of 5-(8-sulphydroctyl)salicylaldehyde

^{13}C NMR ($\text{CDCl}_3/0.03\%$ v/v TMS) of 5-(8-sulfhydroctyl)salicylaldehyde

REFERENCES

1. Nuzzo, R. G.; Allara, D. L. *J. Am. Chem. Soc.* **1983**, *105*, 4481.
2. Sehlotho, N.; Nyokong, T. *Electrochim. Acta* **2006**, *51*, 4463.
3. Schierbaum, K. D.; Weiss, T.; Thoden van Velzen, E. U.; Engbersen, J. F. J.; Reinhoudt, D. N.; Göpel, W. *Science* **1994**, *265*, 1413.
4. Hickman, J. J.; Ofer, D.; Laibinis, P. E.; Whitesides, G. M.; Wrighton, M. S. *Science* **1991**, *252*, 689.
5. Laibinis, P. E.; Whitesides, G. M. *J. Am. Chem. Soc.* **1992**, *114*, 9022.
6. Flink, S.; Boukamp, B. A.; van den Berg, A.; van Veggel, F. C. J. M.; Reinhoudt, D. N. *J. Am. Chem. Soc.* **1998**, *120*, 4652.
7. Laibinis, P. E.; Whitesides, G. M.; Allara, D. L.; Tao, Y. T.; Parikh, A. N.; Nuzzo, R. G. *J. Am. Chem. Soc.* **1991**, *113*, 7152.
8. Nuzzo, R. G.; Fusco, F. A.; Allara, D. L. *J. Am. Chem. Soc.* **1987**, *109*, 2358.
9. Nuzzo, R. G.; Dubois, L. H.; Allara, D. L. *J. Am. Chem. Soc.* **1990**, *112*, 558.
10. Lee, S.; Puck, A.; Graupe, M.; Colorado-Jr., R.; Shon, Y. S.; Lee, T. R.; Perry, S. S. *Langmuir* **2001**, *17*, 7364.
11. Bain, C. D.; Whitesides, G. M. *Science* **1988**, *240*, 62.
12. Clegg, R. S.; Reed, S. M.; Hutchinson, J. E. *J. Am. Chem. Soc.* **1998**, *120*, 2486.
13. Tsuji, N.; Nozawa, K.; Aramaki, K. *Corros. Sci.* **2000**, *42*, 1523.
14. Zamborini, F. P.; Crooks, R. M. *Langmuir* **1998**, *14*, 3279.
15. Eberspacher, T. A.; Collman, J. P.; Chidsey, C. E. D.; Donohue, D. L.; Van Ryswyk, H. *Langmuir* **2003**, *19*, 3814.

16. (a) Schiff, H. *Justus Liebigs Ann. Chem.* **1864**, 131, 118. (b) Schiff, H. *Ann. Chem. Suppl.* **1864**, 3, 343.
17. Fatibello-Filho, O.; Dockal, E. R.; Marcolino-Junior, L.H.; Teixeira M. F. S. *Analyt. Lett.* **2007**, 40, 1825.
18. (a) Schiff, H. *Ann. Chem.* **1869**, 150, 193. (b) Schiff, H. *Ann. Chem.* **1869**, 151, 186.
19. (a) Holm, R. H.; Everett-Jr., G.W.; Chakravorty, A. *Prog. Inorg. Chem.* **1966**, 7, 83 and ref. therein. (b) Hobday, M.D.; Smith, T.D. *Coord. Chem. Rev.* **1972-1973**, 9, 311 and refs. therein.
20. (a) Dalton, C. T.; Ryan, K. M.; Wall, V. M.; Bousquet, C.; Gilheany, D. G. *Top. Catal.* **1998**, 5, 75.
21. (a) Pfeiffer, P.; Breith, E.; Lübbe, E.; Tsumaki, T. *Justus Liebigs Ann. Chem.* **1933**, 503, 84. (b) Diehl, H.; Hach, C. C. *Inorg. Synth.* **1950**, 3, 196.
22. Ershad, S.; Sagathforoush, L. A.; Karim-nezhad, G.; Kangari, S.; *Int. J. Electrochem. Sci.* **2009**, 4, 846.
23. Leung, A. C. W.; MacLachlan, M. J. *J. Inorg. Organomet. Polymer. Mater.* **2007**, 17, 57.
24. (a) Zhang, W.; Loebach, J. L.; Wilson, S. R.; Jacobsen, E. N. *J. Am. Chem. Soc.* **1990**, 112, 2801. (b) Jacobsen, E. N.; Zhang, W.; Muci, A. R.; Ecker, J. R.; Deng, L. *J. Am. Chem. Soc.* **1991**, 113, 7063.
25. Alleman, K. S.; Samide, M. J.; Peters, D. G.; Mubarak, M. S. *Current Topics in Electrochemistry* **1998**, 6, 1 and references therein.
26. Ji, C.; Day, S. E.; Silvers, W. C. *J. Electroanal. Chem.* **2008**, 622, 15.
27. Fry, A. J.; Sirisoma, U. N. *J. Org. Chem.* **1993**, 58, 4919.
28. Vanalabhpatana, P.; Peters, D. G. *J. Electrochem. Soc.* **2005**, 152, E222.
29. Fang, D. M.; Peters, D. G.; Mubarak, M. S. *J. Electrochem. Soc.* **2001**, 148, E464.
30. Mubarak, M. S.; Barker IV, W. E.; Peters, D. G. *J. Electrochem. Soc.* **2007**, 154, F205.
31. Shahrokhian, S.; Karimi, M. *Electrochim. Acta* **2004**, 50, 77.
32. Teixeira, M. F. S. Dockal, E. R.; Cavalheiro, É. T. G. *Sensors and Actuators B* **2005**, 106, 619.

33. (a) Denisevich, P.; Abruña, H. D.; Leidner, C. R.; Meyer, T. J.; Murray, R. W. *Inorg. Chem.* **1982**, *21*, 2153. (b) Bruti, E. M.; Gianetto, M.; Mori, G.; Seeber, R. *Electroanal.* 1999, *11*, 565.
34. (a) Bedioui, F.; Labbe, E.; Gutierrez-Granados, S.; Devynck, J. J. *Electroanal. Chem.* **1991**, *301*, 267. (b) Vilas-Boas, M.; Freire, C.; de Castro, B.; Hillman, A. R.; *J. Phys. Chem. B.* **1998**, *102*, 8533. (c) Rodyagina, T. Y.; Gaman'kov, P. V.; Dmitrieva, E. A.; Chepurnaya, I. A.; Vasil'eva, S. V.; Timonov, A. M.; *Russ. J. Electrochem.* **2005**, *41*, 1101.
35. Horwitz, C. P.; Murray, R. W. *Mol. Cryst. Liq. Cryst.* **1988**, *160*, 389.
36. Goldsby, K. A.; Blaho, J. K.; Hoferkamp, L. A. *Polyhedron* **1989**, *8*, 113.
37. (a) Audebert, P.; Capdevielle, P.; Maumy, M. *New J. Chem.* **1991**, *15*, 235. (b) Tarábek, J.; Rapta, P.; Kalbáč, M.; Dunsch, L. *Anal. Chem.* **2004**, *76*, 5918. (c) Audebert, P.; Capdevielle, P.; Maumy, M. *New J. Chem.* **1992**, *16*, 697. (d) Audebert, P.; Capdevielle, P.; Maumy, M. *Synth. Met.* **1991**, *43*, 3049.
38. (a) Vasil'eva, S. V.; Chepurnaya, I. A.; Logvinov, S. A.; Gaman'kov, P. V.; Timonov, A. M. *Russ. J. Electrochem.* **2003**, *39*, 310. (b) Chepurnaya, I. A.; Gaman'kov, P. V.; Rodyagina, T. Y.; Vasil'eva, S. V.; Timonov, A. M. *Russ. J. Electrochem.* **2003**, *39*, 314.
39. Dadamos, T. R. L.; Teixeira, M. F. S. *Electrochim. Acta* **2009**, *54*, 4552.
40. (a) Dahm, C. E.; Peters, D. G. *Anal. Chem.* **1994**, *66*, 3117. (b) Dahm, C. E.; Peters, D. G. *J. Electroanal. Chem.* **1996**, *406*, 119. (c) Dahm, C. E.; Peters, D. G.; Simonet, J. J. *Electroanal. Chem.* **1996**, *410*, 163.
41. (a) Nielsen, M.; Gothelf, K. V. *J. Chem. Soc., Perkin Trans. 1* **2001**, *1*, 2440. (b) Nielsen, M.; Larsen, N. B.; Gothelf, K. V. *Langmuir* **2002**, *18*, 2795.
42. Ulman, A. *Chemical Reviews* **1996**, *96*, 1533.
43. (a) Walczak, M. M.; Chung, C.; Stole, S. M.; Widrig, C. A.; Porter, M. D. *J. Am. Chem. Soc.* **1991**, *113*, 2370. (b) Laibinis, P. E.; Fox, M. A.; Folkers, J. P.; Whitesides, G. M. *Langmuir* **1991**, *7*, 3167.
44. León, P. C.; Sürgers, C.; Löhneysen, H. v. *Phys. Rev. B* **2012**, *85*, 035434.
45. Maoz, R.; Sagiv, J. *Langmuir* **1987**, *3*, 1045.
46. Lee, T. R.; Laibinis, P. E.; Folkers, J. P.; Whitesides, G. M. *Pure & Appl. Chem.* **1991**, *63*, 821.

47. Bain, C. D.; Whitesides, G. M. *Angewandte Chemie. International Edition in English* **1989**, *28*, 506.
48. Naselli, J. F.; Rabolt, J. F.; Swalen, J. D. *J. Chem. Phys.* **1985**, *82*, 2136.
49. Bain, C. D.; Whitesides, G. M. *J. Am. Chem. Soc.* **1988**, *110*, 6560.
50. Imabayashi, S.; Iida, M.; Hobara, D.; Feng, Z. Q.; Niki, K.; Kakiuchi, T. *J. Electroanal. Chem.* **1997**, *428*, 33.
51. Widrig, C. A.; Chung, C.; Porter, M. D. *J. Electroanal. Chem.* **1991**, *310*, 335.
52. Esplandiú, M. J.; Hagenström, H.; Kolb, D. M. *Langmuir* **2001**, *17*, 828.
53. Kakiuchi, T.; Usui, H.; Hobara, D.; Yamamoto, M. *Langmuir* **2002**, *18*, 5231.
54. Borsari, M.; Cannio, M.; Gavioli, G. *Electroanal.* **2003**, *15*, 1192.
55. Porter, M. D.; Bright, T. B.; Allara, D. L.; Chidsey, C. E. D. *J. Am. Chem. Soc.* **1987**, *109*, 3559.
56. Peelen, D.; Smith, L. M. *Langmuir*, **2005**, *21*, 266.
57. Nogueira Diógenes, I. C.; Rodrigues de Sousa, J.; Moreira de Carvalho, I. M.; Arruda Temperini, M. L.; Tanaka, A. A.; de Sousa Moreira, I. *J. Chem. Soc., Dalton Trans.* **2003**, 2231.
58. Nogueira Diógenes, I. C.; Nart, F. C.; Arruda Temperini, M. L.; de Sousa Moreira, Í. *Inorg. Chem.* **2001**, *40*, 4884.
59. Lamp, B. D.; Hobara, D.; Porter, M. D.; Niki, K.; Cotton, T. M. *Langmuir* **1997**, *13*, 736.
60. Kalyuzhny, G.; Vaskevich, A.; Ashkenasy, G.; Shanzer, A.; Rubinstein, I. *J. Phys. Chem. B.* **2000**, *104*, 8238.
61. Sawaguchi, T.; Mizutani, F.; Yoshimoto, S.; Taniguchi, I. *Electrochim. Acta* **2000**, *45*, 2861.
62. Mashazi, P. N.; Ozoemena, K. I.; Maree, D. M.; Nyokong, T. *Electrochim. Acta* **2006**, *51*, 3489.
63. Lu, X.; Lv, B.; Xue, Z.; Li, M.; Zhang, L.; Kang, J. *Thin Solid Films* **2005**, *488*, 230.
64. Ozoemena, K. I.; Nyokong, T. *Microchem. J.* **2003**, *75*, 241.

65. Stolarczyk, K.; Bilewicz, R.; Siegfried, L.; Kaden, T. *Inorg. Chim. Acta* **2003**, *348*, 129.
66. Eberspacher, T. A.; Collman, J. P.; Chidsey, C. E. D.; Donohue, D. L.; Van Ryswyk, H. *Langmuir* **2003**, *19*, 3814.
67. Ciszek, J. W.; Keane, Z. K.; Cheng, L.; Stewart, M. P.; Yu, L. H.; Natelson, D.; Tour, J. M.; *J. Am. Chem. Soc.* **2006**, *128*, 3179.
68. Moav, T.; Hatzor, A.; Cohen, H.; Libman, J.; Rubinstein, I.; Shanzer, A. *Chem. Eur. J.* **1998**, *4*, 502.
69. Zhang, Z.; Imae, T. *Nano Lett.* **2001**, *1*, 241.
70. Soto, E.; MacDonald, J. C.; Cooper, C. G. F.; McGimpsey, W. G. *J. Am. Chem. Soc.* **2003**, *125*, 2838.
71. Ehler, T. T.; Malmberg, N.; Carron, K.; Sullivan, B. P.; Noe, L. J. *J. Phys. Chem. B.* **1997**, *101*, 3174.
72. Snopok, B. A.; Boltovets, P. N.; Tsymbal, L. V.; Lampeka, Ya. D., *Theor. Exp. Chem.* **2004**, *40*, 260.
73. Gobi, K. V.; Okajima, T.; Tokuda, K.; Ohsaka, T. *Langmuir* **1998**, *14*, 1108.
74. Beulen, M. W. J.; van Veggel F. C. J. M.; Reinhoudt, D. N. *Isr. J. Chem.* **2000**, *40*, 73.
75. Räsänen, M. T.; de Almeida, P.; Meinander, K.; Kemell, M.; Mutikainen, I.; Leskelä, M.; Repo, T. *Thin Solid Films* **2008**, *516*, 2948.
76. Poirier, G. E.; Pylant, E. D. *Science* **1996**, *272*, 1145.
77. Love, J. C.; Estroff, L. A.; Kriebel, J. K.; Nuzzo, R. G.; Whitesides G. M. *Chem. Rev.* **2005**, *105*, 1103.
78. Noh, J.; Hara, M. *Langmuir* **2002**, *18*, 1953.
79. Addato, M, A, F.; Rubert, A. A.; Benítez, G. A.; Fonticelli, M. H.; Carrasco, J.; Carro, P.; Salvarezza, R. C. *J. Phys. Chem. C.* **2011**, *115*, 17788.
80. Rowe, G. K.; Creager, S. E. *Langmuir* **1994**, *10*, 1186.
81. Schönherr, H.; Ringsdorf, H. *Langmuir* **1996**, *12*, 3891.

82. Pesika, N. S.; Stebe, K. J.; Searson, P. C. *Langmuir* **2006**, *22*, 3474.
83. Svensmark, B.; Hammerich, O. in *Organic Electrochemistry* (Eds: H. Lund, M. M. Baizer), Marcel Dekker, New York **1991**, ch. X, pp. 411-435, ch. XVII, pp. 659-698.
84. Ji, C.; Peters, D. G. *Tetrahedron Lett.* **2001**, *42*, 6065.
85. Ji, C.; Peters, D. G. *J. Chem. Educ.* **2006**, *83*, 290.
86. Creager, S. E.; Rowe, G. K. *J. Electroanal. Chem.* **1994**, *370*, 203.
87. Landini, D.; Montanari, F.; Rolla, F. *Synthesis* **1978**, 771.
88. Wang, R. X.; You, X. Z.; Meng, Q. J.; Mintz, E. A.; Bu, X. R. *Synth. Commun.* **1994**, *24*, 1757.
89. (a) Cossar, B. C.; Fournier, J. O.; Fields, D. L.; Reynolds, D. D. *J. Org. Chem.* **1962**, *27*, 93.; (b) Mikhed'kina, E. I.; Nedel'ko, P. V.; Prezhdo, V. V. *Russ. J. Org. Chem.* **2005**, *41*, 370.
90. Zuffanti, S. *J. Chem. Educ.* **1948**, *25*, 481.
91. Aurangzeb, N.; Hulme, C. E.; McAuliffe, C. A.; Pritchard, R. G.; Watkinson, M.; Bermejo, M. R.; Sousa, A. *J. Chem. Soc., Chem. Commun.* **1994**, 2193.
92. Totten, L.; Assaf-Anid, N. M. in *Dehalogenation*, (Eds. Häggblom, M. M.; Bossert, I. D.) Kluwer Academic Publishers, New York **2004**, Part III pp. 261-287.
93. Garnier, J.; Kennedy, A. R.; Berlouis, L. E. A.; Turner, A. T.; Murphy, J. A. *Beilstein J. Org. Chem.* **2010**, *6*, No. 73.
94. Kakiuchi, T.; Usui, H.; Hobara, D.; Yamamoto, M. *Langmuir* **2002**, *18*, 5231.
95. (a) Ding, S. J.; Chang, B. W.; Wu, C. C.; Lai, M. F.; Chang, H. C. *Anal. Chim. Acta* **2005**, *554*, 43. (b) Groat, K. A.; Creager, S. E. *Langmuir* **1993**, *9*, 3668. (c) Felgenhauer, T.; Rong, H. T.; Buck, M. *J. Electroanal. Chem.* **2003**, *550-551*, 309.
96. Zeynizadeh, B.; Iranpoor, N. *J. Chin. Chem. Soc.* **2003**, *50*, 849.
97. Azehara, H.; Yoshimoto, S.; Hokari, H.; Akiba, U.; Taniguchi, I.; Fujihira, M. *J. Electroanal. Chem.* **1999**, *473*, 68.
98. Yiannios, C. N.; Karabinos, J. V. *J. Org. Chem.* **1963**, *28*, 3246.

99. Naik, R.; Pasha, M. A. *Synthetic Commun.* **2007**, *37*, 1723.
100. Kuo, K. L.; Huang, C. C.; Lin, Y. C. *Dalton Trans.*, **2008**, *29*, 3889.
101. Houjou, H.; Ito, M.; Araki, K. *Inorg. Chem.* **2009**, *48*, 10703.
102. Kuhn, S. nmrshiftdb2, 2011. NMRShiftDB. <http://www.nmrshiftdb.org> or <http://nmrshiftdb.nmr.uni-koeln.de/> (accessed March 1, 2008 to March 1, 2012).
103. *SciFinder Scholar*; Chemical Abstracts Service: Columbus, OH; carbon-13 NMR and proton NMR; 57840616-CNMR; 57840616-HNMR; RN 57840-61-6; 23464451-CNMR; 23464451-HNMR; RN 23464-45-1; 64431794-CNMR; 64431794-HNMR; RN 64431-79-4; 372493657-CNMR; 372493657-HNMR; RN 372493-65-7; 372493679-CNMR; 372493679-HNMR; RN 372493-67-9; 224775353-CNMR; 224775353-HNMR; RN 224775-35-3; 164979082-CNMR; 164979082-HNMR; RN 164979-08-2; 95962768-CNMR; 95962768-HNMR; RN 95962-76-8; <https://scifinder.cas.org> (accessed March 1, 2008 to March 1, 2012); calculated using ACD/Labs Software, version 11.02; ACD/Labs 1994-2011.
104. Gottlieb, H. E.; Kotlyar, V.; Nudelman, A. *J. Org. Chem.* **1997**, *62*, 7512.
105. Fulmer, G. R.; Miller, A. J. M.; Sherden, N. H.; Gottlieb, H. E.; Nudelman, A. Stoltz, B. M.; Bercaw, J. E.; Goldberg, K. I. *Organometallics* **2010**, *29*, 2176.

VITA

Drew Kristopher Brown was born in Richmond, Texas, on July 11, 1985, the son of Lou Ann Brown and Robin Brown. After completing his work at Stephen F. Austin High School, Sugar Land, Texas, in 2004, he entered Texas State University-San Marcos. He received the degree of Bachelor of Science from Texas State in August 2008. In August 2008, he entered the Graduate College of Texas State.

Permanent Address: 2216 Kerr Trail

Cedar Park, Texas 78613

This thesis was typed by Drew Kristopher Brown.